Study of the mechanisms reponsible for the cohesion of sister chromosomes in bacteria

Jihane Challita

THÈSE DE DOCTORAT

NNT : 2022UPASL038

université PARIS-SACLAY

Study of the mechanisms responsible for the cohesion of sister chromosomes in bacteria

Etude des mécanismes responsables de la cohésion des chromatides soeurs dans la bactérie

Thèse de doctorat de l'université Paris-Saclay

École doctorale n° 577, Structure et dynamique des systèmes vivants (SDSV)
Spécialité de doctorat : Génétique
Graduate School : Sciences de la vie et santé. Référent : Faculté des sciences d'Orsay

Thèse préparée dans l'unité de recherche **Institut de Biologie Intégrative de la Cellule** (Université Paris-Saclay, CNRS) sous la direction de **François-Xavier BARRE**, Directeur de Recherche, le co-encadrement de **Elena ESPINOSA-ALFARO**, Ingénieure de Recherche

Thèse soutenue à Paris Saclay, le 10 juin 2022, par

Jihane CHALLITA

Composition du Jury

Stéphanie BURY-MONÉ Professeure, Université Paris-Saclay	Présidente
Sarah BIGOT Chargée de Recherche, HDR, CNRS, Université de Lyon 1	Rapporteur & Examinatrice
Jean-Yves BOUET Directeur de Recherche, CNRS, Université Toulouse 3	Rapporteur & Examinateur
Gaëlle DEMARRE Chercheuse R&D, Pherecydes Pharma, entreprise	Examinatrice
Olivier ESPELI Directeur de Recherche, Collège de France	Examinateur
François-Xavier BARRE Directeur de Recherche, I2BC, CNRS	Directeur de thèse

REMERCIEMENTS

J'aimerais tout d'abord remercier les membres du jury. Merci à Sarah Bigot et Jean-Yves Bouet pour avoir donné de leur temps pour lire et évaluer ma thèse. Je remercie également Stéphanie Bury-Moné, Gaëlle Demarre, et Olivier Espeli pour avoir accepté d'être examinateurs. La discussion qui a suivi la présentation de mon travail m'a paru très intéressante.

J'aimerais ensuite remercier mon directeur de thèse F.X. Barre ainsi que mon encadrante Elena Espinosa pour m'avoir fait confiance avec ce projet. Je vous remercie pour votre soutien pendant ces 3 ans et votre aide pendant les bons et mauvais moments. J'ai énormément appris à vos côtés.

Merci à Christophe qui était toujours à l'écoute et prêt à aider à tout moment. Tes conseils (sur des sujets scientifiques ou non) et ton humour m'ont particulièrement aidé tout au long de cette thèse. Merci aussi à Elisa pour les conseils ainsi que les discussions dans le bureau sur des faits divers qui changeaient toujours les idées quand il le fallait.

Merci à Anthony pour son soutien ainsi que tous les bons moments qu'on a pu partager : les pauses thé, les macdo d'après-meeting, les débats sur Marvel et les jeux vidéo… sans oublier les innombrables slides de microscopie, la liste est bien longue. J'ai eu de la chance de t'avoir en deuxième thésard de l'équipe.

Merci à James, Lucie, Orlando, Amélie, et Jean-Luc ainsi qu'aux anciens membres de l'équipe, notamment Evelyne et Justine. Pensée à vous pour tous les moments qu'on a partagé qui ont fait que ma thèse se soit aussi bien déroulée.

Je remercie également les équipes voisines, notamment Boccard et Yamaichi qui étaient toujours au rendez-vous pour des conseils de manip ainsi que des discussions qui nous ont fait du bien (pensée à Mounia, Mohammed, et Guillaume).

En outre, je tiens à remercier mes amis qui ont toujours été là pour moi. Jad, Pascale, Catherine, Angela, JP. Que ce soit par texto ou autour d'un verre, vous avez toujours su me rebooster. Merci à Cynthia pour ton soutien particulier et tous tes conseils depuis le master, tu m'as énormément aidé.
Je remercie tout particulièrement Charlotte qui a su m'épauler depuis le début, malgré les difficultés de la thèse. Merci pour ta compréhension ainsi que ton soutien inégalable.

Je tiens surtout à remercier ma famille et particulièrement mes parents pour m'avoir donné la chance de poursuivre mes études en France. Même de loin, vous avez toujours cru en moi et m'avez soutenu tout au long de cette aventure.

Titre : Étude des mécanismes responsables de la cohésion des chromatides sœurs dans la bactérie

Mots clés : *Vibrio cholerae*, maintenance de l'information génétique, séquençage massif, vidéo-microscopie de fluorescence, microfluidique

Résumé : La maintenance de l'information génétique est essentielle pendant la prolifération cellulaire. Chez les bactéries, la réplication et la ségrégation sont concomitantes. La réplication débute à l'origine de réplication bidirectionnelle du chromosome bactérien. Deux bras de réplications sont ensuite définis, et la réplication se termine dans la région diamétralement opposée à l'origine, le terminus. Alors que la réplication progresse, les chromatides sœurs nouvellement répliquées migrent vers des côtés opposés de la cellule. Cependant, des observations par microscopie suggèrent qu'il existe un délai entre la réplication et la ségrégation qui varie le long du chromosome. Ce délai entre la réplication et ségrégation des chromatides sœurs est appelé cohésion des chromatides sœurs. Pendant ma thèse, j'ai utilisé l'outil de haute-résolution qui permet une analyse de la cohésion du génome entier (Hi-SC2) pour étudier le profil de cohésion de l'organisme modèle *Vibrio cholerae*.

Il a été démontré chez *E. coli* que la cohésion responsable de la variation de la vitesse de ségrégation est modulée par Topoisomérase IV, une enzyme de décaténation majeure. L'un des partenaires identifiés de cette décaténase est le complexe SMC, MukBEF. Les cellules portant une délétion de mukB montrent une production de cellules anucléées, ainsi qu'une origine de réplication mal positionnée. La ségrégation des chromosomes est affectée, et la cohésion des chromatides sœurs est augmentée. L'interaction Topo IV-MukBEF est régulée par MatP qui chasserait MukBEF du terminus de réplication, facilitant ainsi l'association de MukBEF à l'origine de réplication. J'ai donc décidé d'étudier le rôle de MukB dans la formation des motifs de cohésion chez *V. cholerae*.

Grâce à des approches génétiques couplées à l'outil Hi-SC2, j'ai pu démontrer que la délétion de *mukB* mène à une augmentation de la cohésion sur le Chr1, plus précisément sur le bras gauche, assez loin de l'origine. Mes résultats suggèrent que MukB n'agit pas préférentiellement sur des régions spécifiques, mais que ces effets différents sur les deux chromosomes de cet organisme sont dus aux différences dans leurs origines de réplication et/ou leurs systèmes de partition. De précédentes observations dans notre laboratoire ont montré qu'une double délétion de MukB et ParAB1 cause un phénotype sévère, plus important que les délétions individuelles, j'ai donc étudié les conséquences de cette double délétion sur le profil de cohésion. Mes résultats montrent une augmentation additionnelle de la cohésion dans le Chr1 près de l'origine, suggérant ainsi que le système de partition agit sur la décohésion sur le domaine de l'origine pendant que MukB agit sur le reste du chromosome.

Il a été également montré que MatP retardait la ségrégation des chromatides soeurs du terminus de réplication du Chr1. J'ai utilisé le même outil qui m'a permis d'étudier le rôle de MatP dans la cohésion de cette région. J'ai pu montrer que MatP était responsable de cette cohésion uniquement au moment de la division cellulaire et non pas pendant la réplication contrairement à MukB. Mes résultats montrent également que la densité des *matS* présents dans le domaine ter de chaque chromosome qui influent sur la cohésion de ce même domaine.

Title: Study of the mechanisms responsible for the cohesion of sister chromosomes in bacteria

Keywords: *Vibrio cholerae*, maintenance of genetic information, next generation sequencing, fluorescence microscopy, microfluidics.

Abstract: During cell proliferation, the maintenance of genetic information is essential. In bacteria, replication and segregation are concomitant. Replication starts at the single, bidirectional origin of replication of bacterial chromosomes. Two replication arms are then defined, and replication ends in a region diametrically opposite to the origin, the terminus. As replication progresses, the newly replicated sister chromosomes migrate to opposite cell compartments. However, microscopic observations suggest that there is a delay between replication and segregation, and that this delay varies along the length of chromosomes. The delay between replication and segregation of the sister copies of a genomic position is referred to as sister chromatid cohesion. During my PhD, I used the high-resolution tool that allows for a genome-wide analysis of Sister Chromatid Cohesion (Hi-SC2) to study mechanisms implicated in the variations of cohesion along the length of the two chromosomes of *Vibrio cholerae*.

It has been shown in *E. coli* that the cohesion responsible for the variation of segregation speed is modulated by Topoisomerase IV, a major decatenating enzyme. One of the identified partners of this decatenase is an SMC complex, MukBEF. Cells carrying a mukB deletion show a production of anucleate cells, and a mispositioned origin of replication. Chromosome segregation is impaired, and therefore sister chromatid cohesion is increased overall. The Topo IV-MukBEF interaction is regulated by MatP, which seems to displace MukBEF from the terminus of replication, facilitating the association of the MukBEF complex with the origin of replication. *V. cholerae* carries homologues of MukBEF and MatP. I therefore decided to investigate the role of MukB, in the formation of the long-range patterns of cohesion in *V. cholerae.*

Using genetic approaches coupled with the Hi-SC2 assay, I demonstrated that the deletion of *mukB* leads to an increase in cohesion on Chr1, especially on its left replication arm, far from the origin. These results suggested that MukB does not preferentially act on specific regions and that the differential effect of the mukB deletion on Chr1 and Chr2 is probably linked to differences in their partition systems. Previous observations in the lab have in fact shown that a double deletion of MukB and ParAB1 leads to a strong phenotype, thus I investigated its effect on the cohesion profile. My results show an additional increase of cohesion in Chr1 near the *ori*, suggesting that the partitioning system acts on the decohesion of the *ori* domain while MukB acts on the chromosomal arms.

In addition, it has been shown that MatP kept the sister-copies of the ter domain of Chr1 together until cell division. I used the Hi-SC2 assay to study its role in the increased cohesion of this region. I showed that MatP was responsible for the cohesion of the ter1 domain at cell division not behind the replication fork, unlike MukB. My results have also shown that it is the density of the *matS* sites located on the ter domain of each chromosome that influence the level of cohesion of these domains.

SYNTHÈSE

La maintenance de l'information génétique est essentielle durant la prolifération cellulaire. Les chromatides sœurs nouvellement répliquées migrent vers des compartiments opposés de la cellule pour assurer la bonne ploïdie des cellules filles. Chez les eucaryotes, cette ségrégation n'a lieu qu'une fois la réplication terminée. Les chromatides sœurs restent associées le long des phases S et G2 grâce aux cohésines, un complexe de plusieurs protéines appelées Structural Maintenance Proteins (SMC), ainsi que leurs partenaires. Chez les bactéries cependant, la réplication et la ségrégation sont concomitantes. La réplication débute à l'unique origine de réplication bidirectionnelle des chromosomes bactériens. Deux bras de réplication sont alors définis, et la réplication se termine dans une région diamétralement opposée à l'origine : le terminus. Pendant la progression de la réplication, les chromosomes sœurs nouvellement répliqués migrent vers des compartiments opposés de la cellule. Cependant, des observations de microscopie à fluorescence suggèrent l'existence d'un délai entre la réplication et la ségrégation qui varie le long du chromosome. Le délai entre la réplication et la ségrégation de deux copies d'un locus est appelé la cohésion des chromatides sœurs. Cette cohésion a été étudiée pour certaines positions du chromosome d'*E. coli* en utilisant la fréquence de recombinaison des chromatides sœurs obtenue grâce au système Cre-*loxP* inséré en guise de rapporteur de contacts entre les chromatides sœurs (Lesterlin et. al, 2012).

Avant mon arrivée dans le laboratoire, ma co-encadrante Elena Espinosa a mise en place une technique à haute résolution nous permettant d'effectuer une analyse de la cohésion des chromatides sœurs à l'échelle du génome : Hi-SC2 (Espinosa et. al, 2020). Cette technique repose également sur le rapporteur Cre-*loxP* pour les contacts entre les chromatides sœurs. Le rapporteur est inséré dans un transposon. Des transpositions sont effectuées ensuite pour insérer le rapporteur à des positions différentes le long du génome avec une fréquence d'une insertion unique par cellule. Les cellules ciblées portent une copie inductible de la recombinase Cre. Des librairies de transposition contenant ~ 400 000 clones suffisent pour une couverture complète d'un génome bactérien de ~4 Mb. Nous utilisons du séquençage massif apparié afin de déterminer le statut de recombinaison du rapporteur ainsi que sa

position dans le génome. Nous pouvons ensuite extraire la fréquence de recombinaison le long du génome en divisant le nombre de reads recombinés d'un locus par le nombre total de reads du même locus. Plus la fréquence de recombinaison d'un locus est élevée, plus les chromatides sœurs sont restées en contact longtemps, et plus la cohésion du locus est élevée. J'ai utilisé cette technique pour étudier le profil de cohésion de notre organisme modèle, *Vibrio Cholerae*.

Le génome de *V. cholerae* est réparti sur deux chromosomes de natures différentes, Chr1 et Chr2. Chr1 dérive de l'ancêtre mono-chromosomal des *Vibrionacea*, alors que Chr2 dérive d'un méga-plasmide qui fut domestiqué pendant leur évolution. Chr1 et Chr2 portent un système de partition, parAB1 et parAB2 respectivement, qui participent à la ségrégation de leurs origines de réplication respectives. Leurs terminus sont organisés par la même protéine MatP, qui n'agit pas de la même façon sur les deux chromosomes. En effet, des observations microscopiques couplées à des approches génétiques ont montré que les chromatides sœurs du terminus de Chr1, *ter1*, sont maintenues ensembles au centre de la cellule jusqu'à la division cellulaire (Demarre et. al, 2014). En revanche, les chromatides sœurs du terminus de Chr2, *ter2*, sont ségrégées plus tôt que leurs homologues du Chr1 et sont maintenues à proximité du centre de la cellule jusqu'à la division cellulaire. En effet, l'absence de MatP se reflète par la perte de contacts entre les chromatides sœurs de *ter1*, ainsi qu'une perte de positionnement des chromatides sœurs de *ter2*. La technique Hi-SC2 a démontré que la vitesse de ségrégation des deux chromosomes n'était pas homogène, en accord avec les observations obtenues par microscopie à fluorescence. Il existe plusieurs territoires bien définis qui montrent une cohésion très élevée chez *V. cholerae* : les origines de réplication des deux chromosomes, *ori1* et *ori2*, les terminus de réplication des deux chromosomes, *ter1* et *ter2*, ainsi que l'île de pathogénicité VPI-1, située sur le bras gauche du Chr1. J'ai choisi d'étudier le long de ma thèse les différents mécanismes impliqués dans la cohésion des chromatides sœurs chez *V. cholerae*.

La technique Hi-SC2 nous permet de suivre la fréquence de recombinaison des chromatides sœurs le long du génome de *V. cholerae*. Nous pouvons ainsi comparer le profil de contacts de chromatides sœurs de différentes souches afin d'étudier différents facteurs impliqués dans le processus de cohésion. Cependant, nous devons au préalable nous assurer

que les différences observées lors de ces comparaisons sont dues aux mutations et non aux différentes variations intervenues le jour de l'application de la technique lors de la croissance cellulaire. Pour cela, j'ai mis en place un protocole reposant sur le turbidostat nous permettant de d'obtenir une croissance cellulaire à régime constant (steady-state) et d'éviter par la suite toute différence venant du changement dans le rythme de croissance des cellules. Cette amélioration nous a permis de comparer le profil de cohésion des chromatides sœurs de différentes souches de mutants en réduisant considérablement le risque d'artefacts. J'ai ainsi pu étudier l'influence de différents acteurs sur le profil de cohésion des chromatides sœurs de *V. cholerae*.

En premier lieu, j'ai étudié l'action de MatP sur la cohésion des chromatides sœurs de *ter1* et *ter2* de *V. cholerae*. Il a été montré chez *E. coli* par des techniques de ChIP-seq que MatP se fixe de manière spécifique sur les sites *matS* présents dans le *ter*. J'ai donc effectué les mêmes analyses chez *V. cholerae* afin de connaitre le profil de fixation de MatP dans cet organisme modèle. J'ai observé un profil similaire à celui d'*E. coli* avec une fixation spécifique de MatP sur les *matS* présents sur les deux chromosomes, dans les régions *ter1* et *ter2* respectivement. Il existe 38 sites *matS* répartis dans *ter1* et 22 sites *matS* répartis dans *ter2*. Le profil obtenu arborait uniquement deux larges pics de fixation de MatP, un par terminus, avec un niveau de fixation presque nul sur le reste du génome. En comparant ce profil de fixation avec le profil de cohésion des chromatides sœurs obtenu par Hi-SC2, j'ai pu observer une nette corrélation entre les pics de fixation de MatP sur *ter1* et *ter2* avec les pics élevés de contacts entre les chromatides sœurs de ces mêmes régions. Cette observation nous a permis d'émettre l'hypothèse selon laquelle MatP serait responsable de la cohésion des chromatides sœurs au moment de la réplication chez *V. cholerae*. Afin de la tester, j'ai appliqué la technique Hi-SC2 sur une souche Δ*matP*. Le profil obtenu était similaire au profil de la souche WT, à l'exception d'un niveau de contacts entre les chromatides sœurs légèrement diminué au niveau des deux terminus de réplication. Cette conséquence mineure de la délétion de MatP sur la cohésion des deux terminus a montré que la protéine n'était pas le facteur principal responsable de cette cohésion, et qu'elle n'y contribuait que faiblement. Cette observation réfute donc notre hypothèse et suggère l'implication d'autres facteurs jusque-là inconnus qui pourraient soit masquer l'activité de MatP, soit augmenter majoritairement la cohésion des deux terminus pendant la réplication avec une aide mineure de MatP.

Nous savions cependant que MatP maintenait les deux copies nouvellement répliquées de *ter1* lors de la division cellulaire. Nous avons donc décidé de suivre les contacts de chromatides sœurs des deux chromosomes au moment de la division cellulaire. Pour cela, nous avons utilisé la technique Hi-SC2 avec un rapporteur différent : le système de recombinaison Xer/*dif1*. A l'instar de Cre/*loxP* qui est capable d'agir indépendamment de tout autre facteur cellulaire, l'activité de Xer/*dif1* dépend de celle de la protéine FtsK. FtsK fait partie de la machinerie de la division cellulaire et n'est active qu'au moment de la constriction du septum. Cette particularité restreint donc l'activité de Xer/*dif1* aux sites cohésifs lors de la division cellulaire (Val et. al, 2008 ; Demarre et. al, 2014 ; Galli et al., 2017). L'application de Hi-SC2 avec ce rapporteur suivait les mêmes étapes qu'avec Cre/*loxP*, avec les sites *dif1* inséré dans un transposon puis dans des cellules grâce à une transposition suivant une fréquence d'une insertion unique par cellule. Le profil de la souche WT obtenu avec ce rapporteur est très différente de celui obtenu avec Cre/*loxP*, car on n'observe que deux pics de contacts entre les chromatides sœurs au moment de la division cellulaire : un pic élevé au niveau de *ter1* ainsi qu'un pic beaucoup plus faible au niveau de *ter2* ; le reste du génome arborant un niveau de contacts de chromatides sœurs nul. Ce profil attendu est en accord avec les observations de Demarre et. al en 2014 où les copies nouvellement répliquées de *ter1* étaient maintenues ensemble au milieu de la cellule au moment de la division cellulaire alors que les copies nouvellement répliquées de *ter2* étaient ségrégées plus tôt, malgré leurs positionnement à proximité du milieu de la cellule. Ce profil ne corrèle plus avec le profil de fixation de MatP obtenu par ChIP-seq, avec les pics de fréquence de contatcs entre les chromatides sœurs beaucoup plus fins que les pics de fixation de MatP. Ensuite, nous avons délété MatP et appliqué la technique Hi-SC2 avec le rapporteur Xer/*dif1* pour constater la conséquence de cette délétion sur les contacts entre les chromatides sœurs des deux terminus au moment de la division cellulaire. Nous avons observé une perte drastique de la fréquence de contacts entre les chromatides sœurs de *ter1* et *ter2* en absence de MatP en comparaison avec la souche WT, en accord avec les observations de microscopie à fluorescence publiées précédemment. Ces résultats confirment le rôle majeur de MatP dans la maintenance des contacts entre les chromatides sœurs des deux terminus lors de la division cellulaire et posent la question suivante : quelle est l'origine de la différence de comportement de *ter1* et *ter2* ?

Pour répondre à cette question, nous nous sommes penchés sur les sites *matS* des deux chromosomes. Les *matS* de *ter1* et *ter2* ont une séquence identique, éliminant ainsi l'hypothèse des différences génétiques. Cependant, *ter1* possède plus de sites *matS* que *ter2* avec une différence de 16 sites *matS* entre les deux. Nous avons donc déplacé 2 sites *matS* de *ter1* et les ont placés dans la région *ter2*, réduisant ainsi la différence à 14 sites *matS* entre les deux chromosomes. La comparaison du profil Hi-SC2 de cette souche avec la souche sauvage montre une augmentation considérable de la fréquence de contacts des chromatides sœurs au niveau de *ter2* par rapport à la souche WT. Cette augmentation démontre que la différence de comportement observée entre *ter1* et *ter2* provient de la différence en nombres de sites *matS* des deux chromosomes. Les résultats obtenus pour cette partie de mon projet de thèse montrent que MatP n'est pas le facteur principal responsable de la cohésion des chromatides sœurs de *ter1* et *ter2* pendant la réplication, mais était le facteur principal responsable des contacts entre les chromatides sœurs de *ter1* et *ter2* lors de la division cellulaire, avec le nombre des sites *matS* jouant un rôle important dans le niveau de contacts. Ces travaux posent plusieurs questions notamment : quels sont les acteurs responsables de la cohésion des chromatides sœurs de *ter1* et *ter2* pendant la réplication ? Comment MatP maintient-il les contacts entre les chromatides sœurs de *ter1* et *ter2* pendant la division cellulaire ? Des études supplémentaires sont nécessaires afin de pouvoir répondre à ces questions.

En second lieu, je me suis intéressée à la cohésion des chromatides sœurs au niveau des bras des deux chromosomes. Il a été démontré chez *E. coli* que la cohésion des chromatides sœurs responsable de la variation de la vitesse de ségrégation était modulée par la topoisomérase IV, qui est une enzyme de décaténation majeure (Wang et. al, 2008). L'un des partenaires de cette décaténase est une condensine : le complexe MukBEF (Nicolas et. al, 2014). La délétion de ce complexe a pour conséquence des défauts de ségrégation très sévères ainsi que la production de cellules anucléées. En l'absence de MukB, la ségrégation est affectée et la cohésion des chromatides sœurs est donc plus élevée. L'interaction Topo IV-MukBEF est régulée par MatP, et des observations récentes ont montré que MatP déplaçait MukB du terminus d'*E. coli*, facilitant ainsi l'association de MukB avec le reste du chromosome (Nolivos et. al, 2016 ; Makela & Sherratt, 2020). J'ai donc décidé d'étudier le rôle de MukB

dans la cohésion des chromatides sœurs des bras des chromosomes de *V. cholerae*. En effet dans cet organisme, nous pouvons déléter MukB sans répercussions sévères sur la ségrégation de Chr1 et Chr2. J'ai d'abord étudié le profil de fixation de MukB chez *V. cholerae* grâce au ChIP-seq. J'ai observé une fixation assez homogène le long du génome avec un léger enrichissement de MukB au niveau de l'origine de réplication par rapport au terminus. Cette observation corrèle avec l'expulsion de MukB du terminus d'*E. coli* par MatP.

J'ai ensuite appliqué la technique Hi-SC2 sur une souche Δ*mukB* en utilisant le rapporteur Cre/*loxP*. Le profil de cette souche montre une augmentation importante de la cohésion des chromatides sœurs sur le Chr1 avec un effet bien plus prononcé sur le bras gauche du Chr1 par rapport au bras droit de ce même chromosome. Dans le cas du Chr2, le profil de cohésion reste inchangé après la délétion de *mukB.* Ces résultats suggèrent une absence d'action visible de MukB sur le Chr2 ainsi qu'une action plus prononcée sur le bras gauche de Chr1. Afin d'approfondir cette différence de comportement des deux bras du Chr1, nous avons appliqué Hi-SC2 sur une souche Δ*mukB* ΔVPI-1, sachant que VPI-1 se situe sur le bras gauche du Chr1 et montre une augmentation particulière de cohésion en l'absence de MukB. Nous avons donc émis l'hypothèse que la présence de cette zone cohésive représentait un obstacle à la ségrégation et augmentait la cohésion du reste du bras gauche en l'absence de MukB. Les résultats obtenus montrent une diminution de la cohésion de la région de VPI-1 en l'absence de cette dernière par rapport à la souche Δ*mukB*, mais la cohésion du reste du bras gauche reste élevée, indiquant que VPI-1 n'était pas responsable de la différence de comportement des deux bras du Chr1. Nous nous sommes donc tournés vers la deuxième différence présente entre les deux bras : le système de partition.

Chaque chromosome de *V. cholerae* possède son propre système de partition : ParAB1 et ParAB2, qui se fixent de manière spécifique sur les sites *parS1* et *parS2* respectivement. Les sites *parS1* sont au nombre de trois et sont localisés sur le bras droit du Chr1, à grande proximité de l'origine de réplication de ce dernier. Cette localisation pourrait alors être à l'origine de la différence de comportement des deux bras du Chr1. ParAB1 pourrait ségréger principalement le bras droit du Chr1 grâce aux positions des sites *parS1*, et ségréger moins facilement le bras gauche du Chr1 par souci d'accès. En effet, la séquestration de l'origine par la protéine SeqA ayant lieu après l'initiation de la réplication pourrait entraver l'accès de

ParAB1 au bras gauche du Chr1. Cette hypothèse expliquerait la conséquence moins importante de la délétion de *mukB* sur le bras droit du Chr1, sachant que ParAB1 pouvait être principalement responsable de la décohésion de ce bras, avec ou sans MukB. Dans le cas du Chr2, les neufs sites parS2 sont distribués le long du Chr2, avec un enrichissement au niveau de l'origine de réplication de ce dernier. Nous pouvons appliquer le même raisonnement que pour le Chr1, et émettre l'hypothèse que la conséquence de la délétion de *mukB* est beaucoup moins ressentie sur le Chr2 en raison de l'omniprésence de ParAB2 qui ségrégerait l'entièreté du chromosome sans l'aide de MukB. Pour tester cette hypothèse, j'ai appliqué la technique Hi-SC2 sur une souche ΔVPI-1 Δ*mukB* Δ*parS1*. Je n'ai pas pu approfondir l'étude de la cohésion sur le Chr2 étant donné qu'à l'instar de ParAB1, ParAB2 est essentiel pour la cellule. En effet, la délétion de ParAB1 n'entraine pas de défauts de ségrégations graves du Chr1. Cependant, un phénotype majeur est observé lors de la délétion simultanée de MukB et des trois sites *parS1*, en accord avec notre hypothèse actuelle. Le profil de cohésion de la souche ΔVPI-1 Δ*mukB* Δ*parS1* montre une augmentation significative de la cohésion des chromatides sœurs du bras droit du Chr1 par rapport à la souche ΔVPI-1 Δ*mukB*. La cohésion des chromatides sœurs du bras gauche du Chr1 reste également élevée. Ces résultats confirment notre hypothèse d'une action similaire mais non redondante de MukB et ParAB1 sur la décohésion du Chr1. Ils suggèrent également l'existence d'un système de décohésion de secours mis en place par la cellule dans le cas d'une défaillance au niveau de MukB ou ParAB1. Des études supplémentaires sont nécessaires pour approfondir ce mécanisme et valider ou non cette hypothèse. Une étude du Chr2 par Hi-SC2 est également impérative afin d'éclaircir le(s) mécanisme(s) de décohésion de ce chromosome, notamment avec des souches sans système de partition.

Mes travaux ont mis en lumière les rôles respectifs de MukB et ParAB1 dans la décohésion du Chr1 pendant la réplication. Ces trois facteurs, qui sont avant tout des facteurs de ségrégation, seraient donc impliqués dans la décohésion du chromosome bactérien. Cette observation soulève la question suivante : qu'est-ce vraiment la ségrégation du chromosome bactérien ? Chez les eucaryotes, les étapes de ségrégation et de décaténation sont distinctes. Les chromosomes sont répliqués et les chromatides sœurs sont séparées grâce à la décaténation mais restent jointes au niveau du centromère par les cohésines. Quant à la ségrégation, elle a lieu bien plus tard dans le cycle cellulaire à l'aide du fuseau mitotique. En

revanche, la réplication et la ségrégation sont concomitantes chez les bactéries. Les chromatides sœurs sont séparées au fur et à mesure qu'elles sont répliquées grâce à différents facteurs notamment MukB et le système de partition. Cette séparation a longtemps été nommée ségrégation par homologie avec les eucaryotes. Cependant, il se peut qu'elle soit plus proche de l'étape de décaténation eucaryote que de la ségrégation. En effet, les chromatides sœurs sont séparées par décaténation et migrent immédiatement vers des compartiments opposés de la cellule, à l'instar de la ségrégation eucaryotes qui a lieu par étapes. Cela suggèrerait que le mécanisme baptisé ségrégation bactérienne serait en effet une simple séparation par décaténation et non une ségrégation à proprement parler. Quant à la cohésion des chromatides sœurs, son rôle d'un point de vue biologique reste flou. Elle peut être modulée par différents facteurs : MukB, le système de partition, et Topo IV ce qui suggèrerait un rôle de protection de l'organisation du chromosome en entravant la séparation précoce des chromatides sœurs après le passage de la fourche de réplication.

Table of Contents

Introduction ***17***

1. The bacterial cell cycle **17**

1.1. Genetic organization in bacteria 17

1.2. The replication of bacterial chromosomes 20

1.2.1. Replication initiation 22

1.2.2. Replication elongation in bacteria 23

1.2.3. Replication termination in bacteria 24

2. Chromosome segregation: what are the driving forces **28**

2.1. General introduction 28

2.1.1. Segregation in eukaryotes 28

2.1.2. Segregation in bacteria 29

2.2. Bacterial chromosome organization and its role in segregation 31

2.2.1. Nucleoid-Associated Proteins (NAPs) 31

2.3. The partition system 34

2.3.1. General introduction 34

2.3.2. Structure of the partitioning system 35

2.3.3. Mechanisms of action of the partitioning system 38

2.4. MatP: an important structuring factor 40

2.5. The bacterial SMC complexes and SMC-like condensins 41

2.5.1. The discovery of MukBEF 41

2.5.2. Structural Maintenance of Chromosomes (SMC) 43

2.5.3. Structure of the different SMC and SMC-like complexes 44

2.5.4. Role of SMC and SMC-like complexes in bacteria 45

2.6. Segregation of the *ter* domain with XerC, XerD, and FtsK 49

2.7. Segregation and chromosomal arrangement in *V. cholerae*: a summary 50

3. Cell division in bacteria **52**

3.1. FtsZ: one of cell division's main proteins 52

4. Sister chromatid cohesion in bacteria **55**

4.1. DNA Catenation 55

4.1.1. Supercoiling and catenation 55

4.1.2. The role of topoisomerases in decatenation 55

4.1.3. Topoisomerase IV: roles and mechanisms 56

4.1.4. Consequences of gyrase mutations on the chromosome 58

4.2. Sister-chromatid contacts 60

4.2.1. Sister-chromatid cohesion 60

4.3. High-throughput whole genome analysis of Sister Chromatid Contacts (Hi-SC2) 61

4.3.1. A recombination assay to follow sister-chromatid interactions 61

4.3.2. Hi-SC2: the mechanisms behind the assay 62

4.3.3. Hi-SC2: a new and improved view of Sister Chromatid Contacts 64

Objectives ***66***

Results ***67***

Chapter 1: Cohesion in the ter domain: the extent of MatP's involvement **67**

1. Cohesion at the *ter* domain behind the replication fork 68

1.1. Replication termination is not responsible for cohesion at the *ter* domain 68

1.2. Correlation between the local concentration of MatP and the Hi-SC2 profile at *ter1* and *ter2* 70

1.3. MatP is not the major factor in the cohesion at *ter* domains during replication 74

2. Cohesion at the *ter* domain at cell division 75
2.1. Cohesion between sister copies of the extreme *terminus* of replication of Chr1 and Chr2 during cell division 75
2.2. The genetic composition of *ter1* specifies the elevated frequency of *dif1* cassette excision ..76
2.3. MatP is responsible for sister-chromatid contacts of the *ter* domains at cell division 77
2.4. The difference in the behavior of the *ter* domains is due to differences in the density of the *matS* sites....78

Chapter 2: The role of segregation factors in decohesion along the chromosome.... 82
1. The binding pattern of MukB in *V. cholerae* 82
2. MukB in *V. cholerae* plays a role in chromosome decohesion 84
2.1. The role of MukB in a WT context 84
2.2. Confirmation of the results in a Δ*VPI-1* context....85
2. MukB and the partition system both play a role in chromosome decohesion 87
2.1. The role of ParABS in chromosome decohesion 87
2.2. The effect of a double mutation on chromosome cohesion....88
2.3. Confirmation of the results with different microscopy tags 89
3. The effect of MukB on Chr2 is masked 90
4. The length of the arms of Chr1 and Chr2 do not play a role in masking the effect of MukB ...91

Chapter 3: Supplementary data 93
Transposon insertion plots for Hi-SC2 experiments....93

Discussion and Perspectives 95
1. Potential actors of cohesion in the ter domain: the role of MatP 95
2. Potential actors of cohesion in the *ori* domain 97
3. The contribution of MukB and the partition system to cohesion behind the replication fork 97
4. Small local variations of cohesion....99
5. Segregation versus decohesion – the role of cohesion in bacteria....100

Materials and Methods 101
1. Bacterial strains and growth conditions 101
2. High-resolution whole-genome assay of Sister-Chromatid Contacts (Hi-SC2)....102
3. ChIP-seq assays 106
4. RNA-seq assays 108
5. Microscopy assays 109
6. Cell count monitoring 109

Annexes 110

Bibliography....116

Introduction

1. The bacterial cell cycle

1.1. Genetic organization in bacteria

During the last decades, our knowledge of the bacterial cell cycle and its characteristics has drastically improved. Our vision has evolved from the original, disorganized, view of the bacterial cell into a model of chromosomes, ribosomes, and other proteins fitting together in an orderly fashion. The circular nature of the *Escherichia coli* chromosome and the F plasmid was demonstrated in 1961 by elaborate genetics (Jacob F., Wollman E., 1961). It was later reported that there was a single large replication unit in *E. coli*, suggesting that it carried a single chromosome (Cairns, 1963). Together, these discoveries led to the idea that bacterial genomes consist of a single circular chromosome occasionally accompanied by smaller, non-essential circular plasmid(s) (Cairns, 1963). However, the *E. coli* model masked the diversity of bacteria: the discovery of a linear plasmid in *Streptomyces* demonstrated that bacterial DNA molecules are not always circular (Hayakawa et al., 1979). A "megaplasmid" was found two years later in *Rhizobium meliloti* (Rosenberg et al., 1981) and it was established in 1989 that *Rhodobacter sphaeroides* harbored two chromosomes (Suwanto & Kaplan, 1989). The development of whole genome sequencing techniques allowed for an extended investigation of bacterial genomes and the subsequent discovery that multipartite genomes are not as rare as we once thought, with a rate of approximately 10% of all known bacterial species harboring a second chromosome (Harrison et al., 2010).

Whereas the different chromosomes of eukaryotic cells have similar properties, a clear distinction can be made between the replicons of bacteria with a multipartite genome: the larger of the replicon is related to the single chromosome of other bacteria, but the other replicons are akin to mega-plasmids. Harrison and their team therefore proposed a new name for those DNA molecules: chromids. A chromid represents an intermediate between a chromosome and a plasmid as, unlike the latter, it carries at least one essential core gene for cell viability (Harrison et al., 2010). Its replication system, however, resembles that of plasmids and megaplasmids, although it may hold additional regulatory controls (Val et al.,

2014). The classification of a replicon in one of the five groups: chromosome, second chromosome, chromid, megaplasmid, and plasmid can be found in **Figure 1** in the form of a flow chart. The sorting can be made depending on the presence of essential genes, the origin of the replicon (the presence of the replicon, not to be confused with its origin of replication), and its size.

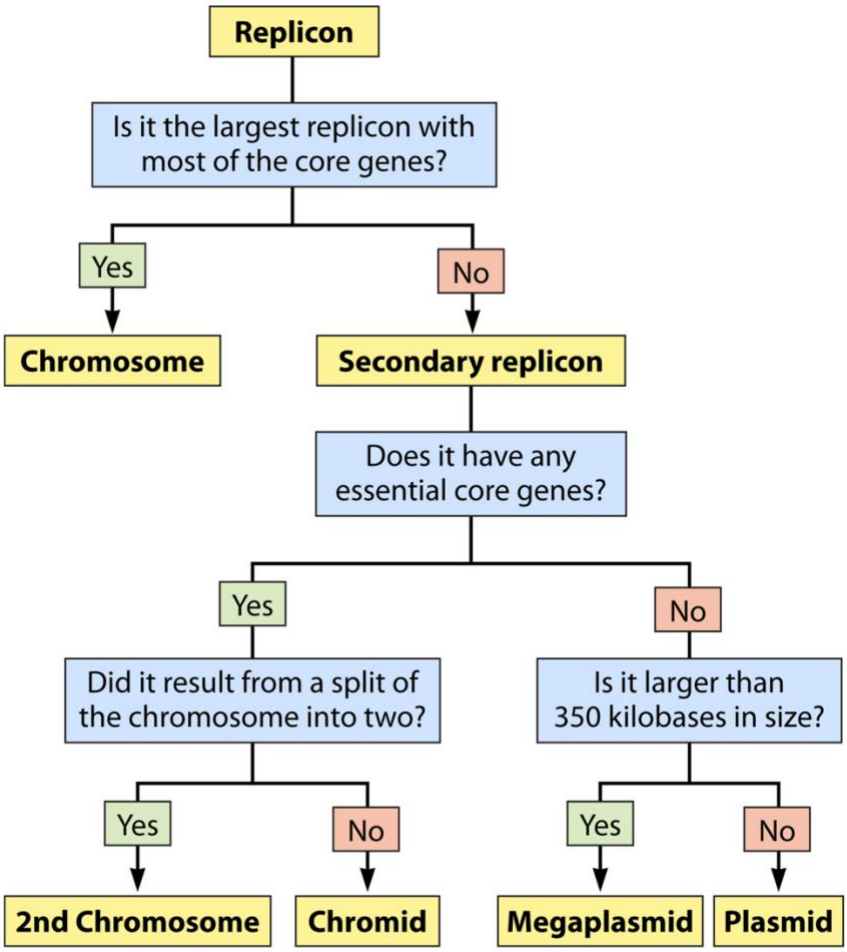

Figure 1: A flow chart representing the steps involved in the classification of bacterial replicons in one of the five categories: chromosome, second chromosome, chromid, megaplasmid, and plasmid. Taken from (diCenzo & Finan, 2017).

Vibrio cholerae, the model organism of the present study, carries a chromosome and a chromid. Its chromosome hereafter referred to as Chr1 is ~3 Mb long while its chromid hereafter referred to as Chr2 is ~1 Mb long (Heidelberg et al., 2000). It is proposed that Chr2 was derived from the domestication of a plasmid in the ancestor of the current Vibrionaceae families, following the transfer of essential genes from the main chromosome to the replicon (Kirkup et al., 2010). Both chromosomes have their own distinct replication initiation set-up,

and are fortified with multiple prophages and genomic islands (Pant et al., 2020). *Vibrio cholerae* is a highly motile, comma-shaped, gram-negative rod bacterium with a single polar flagellum. It is part of the Vibrionaceae family, which is the closest order to Enterobacteria, thus making it a cousin to *E. coli* and a very interesting model organism **(Figure 2)**. Like other Vibrios, its natural environment is salty or briny waters. However, *V. cholerae* is the agent of the disease of the same name: cholera. The pathogenic strains harbor specialized adherence factors to attach to host microvilli surfaces, often the small intestine. Once attached, it produces a cholera enterotoxin into the intestinal epithelial cell. Cholera toxin causes an adenylate cyclase dysregulation, leading to an excess in cAMP and subsequent hypersecretion of chloride and bicarbonate followed by water (Ojeda Rodriguez & Kahwaji, 2022). Although *V. cholerae* has almost 200 serogroups, only O1 and O139 have been linked to epidemic diseases as the O-antigen is the primary element allowing cells to attach to epithelial cells (Albert, 1996).

Several other additions play an important role in *V. cholerae*'s pathogenicity. A colonization factor, the toxin co-regulated pilus (TCP) is encoded within a region called the Vibrio Pathogenicity Island (VPI), a ~41 kb sequence on Chr1 that is characterized, amongst other things, by a significantly different GC content from the rest of the chromosome. The major pathogenicity determinant, the cholera toxin (CT), is encoded in the genome of a lysogenic phage CTXΦ. CTX only infects cells producing TCP, which is its receptor on the bacterial surface. CTXΦ inserts in a site-specific manner near the terminus of one, the other or both Vibrio chromosomes (Heidelberg et al., 2000). In order to integrate, CTXΦ uses two host-encoded highly conserved tyrosine recombinases, XerC and XerD, which serve to resolve dimers of circular chromosomes (Lesterlin et al., 2004; Val et al., 2005).

Another interesting characteristic of the pathogen is the presence of an extremely large genetic memory of adaptive functions on Chr2: the superintegron. This structure contains a large set of intergenic repeated sequences named *V. cholerae* repeats (VCR), that flank sets of extremely variable genes; it is one of the largest integrons known to date (Mazel et al., 1998). VCRs are the recombination sites in mobile genetic elements called integron cassettes, that recruit new genes in order to acquire new adaptive functions (Collis et al., 1993). Superintegrons have been found in the chromosomes of several major human pathogens

such as *Pseudomonas aeruginosa* (Boucher et al., 2007) and it is now known that they have driven bacterial evolution for thousands of years (Mazel, 2006). Among others, it encodes genes with various functions such as virulence, DNA modification, toxin-antitoxin systems, and phage-related functions conferring an evolutionary advantage to the organisms that carry it *via* its extremely variable array of genes (Rapa & Labbate, 2013).

This thesis investigates the bacterial chromosome and its cycle, which will be detailed in the following sections starting with replication, segregation, and finally cell division with an emphasis on *V. cholerae*.

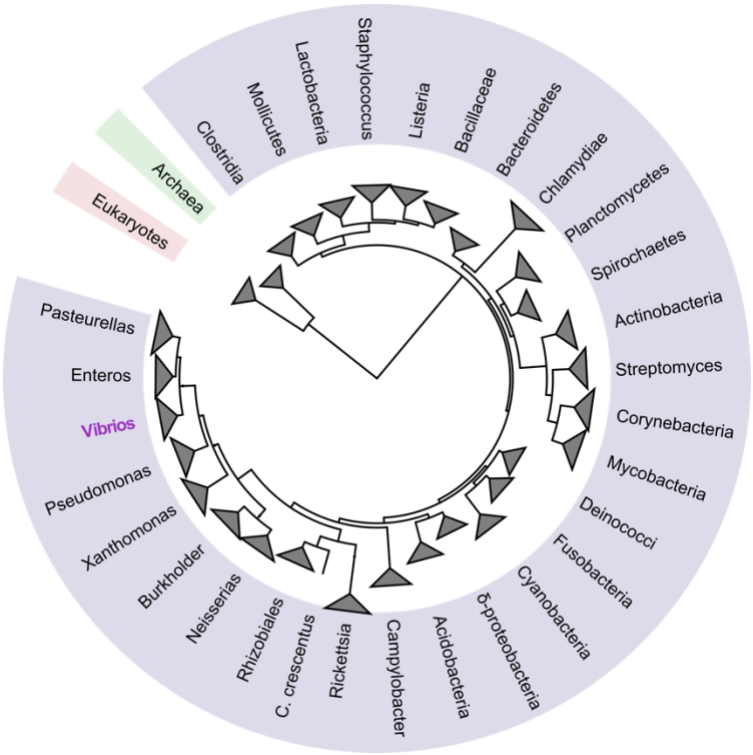

Figure 2: The simplified phylogenetic tree of the bacterial domain of life. The Vibrionaceae order is highlighted in purple. Grey lines and triangles depict the ancestral relationships between the different families. Vibrios and Enteros are close relatives as they derive from the same ancestor.

1.2. The replication of bacterial chromosomes

There are some important differences between bacterial and eukaryotic chromosomes (Kaguni, 2011). DNA replication begins at particular regions of the chromosome called "origin". Bacterial chromosomes are usually circular and have a single bidirectional origin of replication, hereafter referred to as *ori,* that gives birth to two replication arms. The replication fork progresses along those two arms, and replication ends in the terminus of

replication, hereafter referred to as *ter*, that is diametrically opposed to the origin (**Figure 3A**) (Reyes-Lamothe et al., 2008). In contrast, eukaryotic chromosomes are linear, and usually carry several origins each (O'Donnell et al., 2013). Multiple origins are in fact a necessity for eukaryotes as their genomes are much larger than bacteria, and their replication forks move about 20 times more slowly than the bacterial replication forks (O'Donnell et al., 2013). Replication initiation in eukaryotes leads to two divergent replication forks at each origin, thus producing several replicons. With the progression of the replication forks, the newly replicated replicons yield two daughter chromosomes called sister chromatids that remain together for the entirety of their replication (**Figure 3B**).

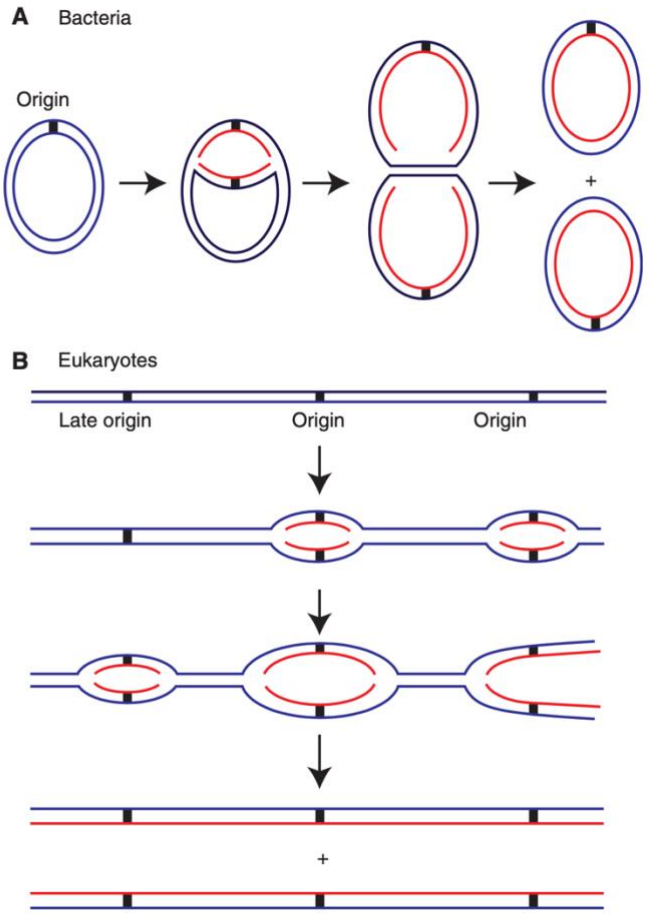

Figure 3: Scheme representing replication initiation in bacteria and eukaryotes. The blue lines represent the sister chromatids serving as a template, while the red lines represent the newly replicated sister chromatids. **(A)** Most bacteria have circular chromosomes with a single bidirectional origin of replication which yields two replication forks that progress in opposite directions. **(B)** Eukaryotes have long linear chromosomes with multiple origins of replications. Bidirectional replication is initiated at each of these origins. Taken from (O'Donnell et al., 2013).

1.2.1. Replication initiation

Bidirectional replication initiation requires the recruitment of several proteins in a tightly regulated manner. Most of what we know has been learned from studies conducted in *E. coli*. For instance, the main actors involved in this process are the DnaA, DnaB, and DnaC trio; together, they establish the replication fork machinery at *oriC* (Kaguni, 2014). In terms of function, DnaA binds to ATP as well as specific sequences in *oriC* called DnaA boxes. It also interacts with a number of other proteins and self-oligomerizes (Leonard & Grimwade, 2011). DnaB is a member of the superfamily 4 of DNA helicases and is the major replicative helicase of *E. coli*. It serves to unwind of the parental DNA helix *via* ATP binding and hydrolysis. Lastly, DnaC is a chaperone protein that assists DnaB in its loading onto the chromosome (Baker et al., 1986).

DNA replication is initiated through the loading of DnaB at the origin of replication. To this effect, DnaA, often considered the initiator protein, mediates DNA melting and the recruitment of the helicase as well as its loader on the chromosome (Duderstadt & Berger, 2008). Multiple copies of DnaA oligomerize in an ATP-dependent manner, thus forming a helical structure that will subsequently bind to DNA. The consensus binding sequence for DnaA is a highly conserved asymmetric nine nucleotides long motif called the DnaA box, that is present multiple times per *oriC* (Wolański et al., 2015). There are two types of DnaA boxes in bacteria, the strong-binding and the weak-binding boxes. In *E.coli*, *oriC* contains three strong-binding DnaA boxes flanking two sets of four weak-binding DnaA boxes, although they are not all essential for DnaA activity (Rozgaja et al., 2011, Stepankiw et al., 2009). DnaA occupies the strong-binding boxes throughout the cell cycle, in both of its nucleotide-binding states, thus suppressing any intrinsic capacity of the helix to unwind prematurely (Sakiyama et al., 2017). In contrast, DnaA binds to the weak-binding boxes when simultaneously bound to ATP, which varies during the cell cycle. This fluctuation defines the occupancy of weak binding sites, thus regulating DnaA's high initiating activity (Kawakami et al., 2005). The increase in DnaA's ATPase activity is also modulated after replication initiation to avoid immediately reinitiating replication. Accessory proteins such as SeqA modulate the binding of DnaA to the weak-binding boxes, hence fine-tuning the initiation time. To that effect, SeqA

prevents rebinding of DnaA to the weak boxes by binding to hemimethylated GATC sites for about ten minutes after origin firing (Nievera et al., 2006).

There are several differences between *V. cholerae* and *E. coli* in terms of replication initiation. As mentioned earlier, each chromosome has its own distinct replication initiation mechanism with different factors involved. The origin of replication of Chr1 resembles the canonical *E. coli* chromosomal origin of replication (*oriC*). Just like *oriC*, *ori1* contains binding sites for DnaA, the main initiator of replication that promotes the unwinding of the origins (Katayama et al., 2010). Chr1 also harbors an IHF binding site as well as several GATC sites for methylation by DNA adenine methyltransferase (Dam), which regulates the timing of re-initiation to once per cell cycle along with SeqA (Koch et al., 2010). In contrast, the origin of replication of Chr2 is similar to the replication origin of plasmids. The replication of Chr2 is triggered by RctB, a *Vibrio*-specific factor. RctB requires methylation of the GATC sites for binding (Venkova-Canova et al., 2012). It is important to note that Chr1 and Chr2 do not initiate replication at the same time, with Chr2 starting to replicate with a certain delay. This delay is due to a non-coding locus on Chr1, *crtS*, that will be detailed later in this thesis.

Another difference between *V. cholerae* and *E. coli* is the loading agent of the helicase DnaB. It has been found that most bacterial genomes including *V. cholerae* lack the *dnaC* gene, and harbor instead *dciA*: a gene of ancestral bacterial origin that encodes a protein essential to the loading of DnaB and the early steps of replication initiation (Brézellec et al., 2016). The role of DciA was investigated and it was demonstrated that it stimulates the loading of DnaB onto DNA by a factor of 3 to 4. It was also shown that the conformation of the DnaB x DciA complex is modified upon binding to DNA, causing the release of DciA and a correct functioning of the helicase (Marsin et al., 2021).

1.2.2. Replication elongation in bacteria

All bacterial processes are tightly regulated, and DNA replication is no exception. Not only does it need to initiate at a specific time during the cell cycle, it also progresses at an appropriate rate during the elongation stage. It has been shown that this rate varies depending on the bacterium and its growth rate (Kornberg & Baker, 2005, Allman et al., 1991). DNA replication is carried out by a multiprotein machinery called the replisome

(Beattie & Reyes-Lamothe, 2015). Directional unwinding of the double-stranded DNA by DnaB results in two template strands that will be replicated simultaneously. It is important to note that these strands have opposing polarities, one being oriented from 5'->3' and the other from 3'->5'. This implies that the new DNA strands are synthesized at different speeds (Beattie & Reyes-Lamothe, 2015). The 3'->5' strand, named the "leading" strand is synthetized continuously while the 5'->3' strand, named the "lagging" strand is synthetized discontinuously as a series of short Okazaki fragments of 1-2 kilobase pairs. The replisome is quite conserved across bacteria despite some differences in composition, most of the subunits remain the same among different organisms (Robinson et al., 2012). But what happens when an organism has a multipartite genome? A good example is *V. cholerae* that has developed a system to monitor the replication termination timing of its primary chromosome and its chromid.

1.2.3. Replication termination in bacteria

The replication termination process requires a tight coordination as two replication forks progress simultaneously towards the *ter* at very high speed. Some organisms including *E. coli* harbor a Replication Fork Trap (RFT) system dedicated to maintaining a correct ending of the chromosome's replication and preventing any overlap between the two replication forks (Hill & Marians, 1990). In other words, the RFT system sets up roadblocks on either side of the *ter* region, thus stopping one replication fork if it overstepped on its partner's sister chromatid. The two replication forks fuse instead within the *ter* region, diametrically opposed to the *oriC* domain. The details of this mechanism are still largely unknown, as its inactivation has no obvious consequence on the mutated cells (Duggin et al., 2008). However, stronger phenotypes emerge in *E. coli* when its inactivation is paired with the deletion of the *tus* gene, which encodes a DNA-binding protein that blocks replication forks when bound to *ter* sites (Roecklein et al., 1991). These results are consistent with the idea that over-replication occurs in the absence of functional fork traps. The RFT system, also known in *E. coli* as the *ter/tus* system, is not highly conserved among the bacterial realm as it is absent in many organisms such as *V. cholerae*, whose chromosomal organization ensures a correct termination of replication (Galli et al., 2019).

A very interesting aspect of *V. cholerae* is that the timing of replication initiation of both chromosomes is coordinated for them to terminate their replication at the same time, despite their size difference (Baek & Chattoraj, 2014). Replication of Chr2 is triggered by RctB, a *Vibrio*-specific factor. RctB requires methylation of the GATC sites for binding (Venkova-Canova et al., 2012). To do so, Chr2 'senses' the replication status of Chr1 to time the initiation of its replication using a non-coding locus on Chr1, *crtS* (Chr2 replication triggering site) (Val et al., 2016, Baek & Chattoraj, 2014). A deletion of *crtS* leads to a strong fitness defects and a large proportion of filamentous cells because of a defect in *ori2* replication initiation. Val et al. replaced *ori2* by *ori1* thus rendering Chr2 independent from RctB and subsequently removed *crtS*. No strong phenotype was observed demonstrating that *crtS* is essential for a correct replication initiation of Chr2.

These intriguing results lead to a deeper investigation of *crtS* and its conservation in the *Vibrionaceae* family. It has been found that the position of *crtS* varies depending on the size difference between Chr1 and Chr2 to have the replication termination of both to happen simultaneously (**Figure 4**). The bigger Chr1 is compared to Chr2, the further *crtS* will be from *ori1* (Kemter et al., 2018). This mechanism is especially important to maintain a coordinated and faithful segregation of the chromosomes for cell division to safely occur.

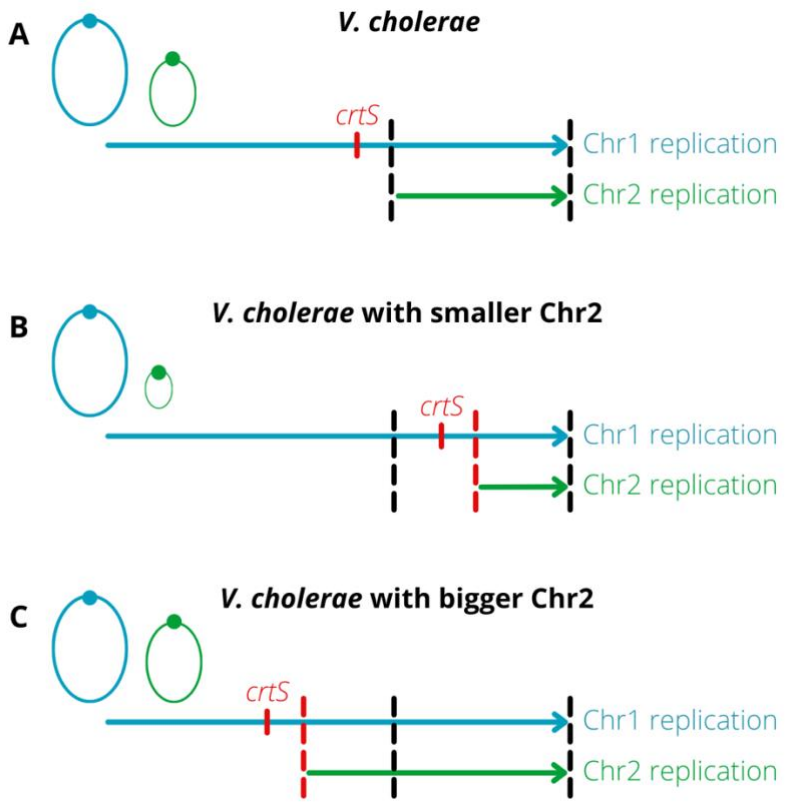

Figure 4: Scheme of replication patterns in *V. cholerae*. The circles represent the chromosomes: blue for the primary chromosome (Chr1) and green for the secondar chromosome (Chr2), and the arrows represent the length and timing of replication. Black dashed lines represent the start and end of replication of Chr2, while the red dashed line represents the expected start of replication of Chr2. With a much smaller Chr2, the *crtS* locus would replicate later whereas it would replicate earlier if Chr2 was bigger. This figure was loosely adapted from (Kemter et al., 2018).

Galli et al. used an MFA method to monitor the fork convergence point (fcp) in *V. cholerae* in order to follow the progression of replication on both chromosomes (Galli et al., 2019). As expected, the profiles obtained for both Chr1 and Chr2 are V-shaped, consistent with the fact that replication starts at *oriC1* and *oriC2* and makes its way along the chromosome arms to *ter1* and *ter2* respectively. Replication of Chr2 only started when *crtS* was replicated, thus allowing both chromosomes to terminate replication simultaneously **(Figure 5)**. The second key step in the bacterial cell cycle is the segregation of the newly replicated sister chromatids, which is discussed in the next section of this thesis.

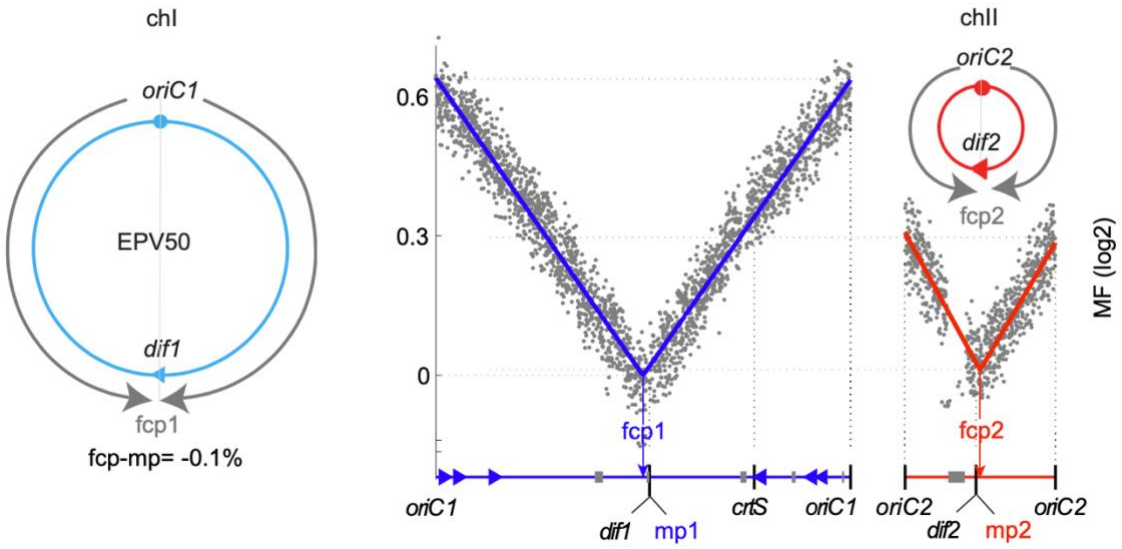

Figure 5: MFA of the WT strain of *V. cholerae* (EPV50). Marker frequencies (grey dots) are represented in Log2 as a function of the genome position. The *oriC1* or *oriC2* of Chr1 or Chr2, respectively, are indicated at each extremity. Position of *dif1*, *dif2*, *crtS*, the different mp (origins mid-point) are indicated. The lowest point on Chr1 was set to "1" in such a way that log2(1) = "0" and all data were normalized to this point. The curve fitting the marker frequency data are indicated by either a blue or a red line for Chr1 and Chr2, respectively. They define the forks convergence points (fcp), indicated under the data. On the left side of the marker frequency data, a scheme representing the program of replication of Chr1 is indicated on the circular map of the strain. The program of replication of Chr2 is represented above the MFA of Chr2. The plain grey line corresponds to the direction of fork progression. The distance between fcp and its mp (noted fcp-mp) is indicated in % of the replicon fraction, oriented from the first origin encounters in the clockwise direction. Taken from (Galli et al., 2019).

2. Chromosome segregation: what are the driving forces

2.1. General introduction

2.1.1. Segregation in eukaryotes

In eukaryotes, distinct key steps separated in time replication in the S phase, condensation state of M-phase Prophase, segregation (Anaphase), cell division, and de-condensation (G1). In the case of eukaryotes, each of these phenomena happens in its own time, after the previous step has finished (Saitoh et al., 1997). The chromosomes are segregated after replication by the mitotic spindle that makes all chromosomes and each individual loci on those chromosomes segregate simultaneously relatively quickly.

But what exactly is the mitotic spindle and how does it segregate eukaryotic chromosomes? The mitotic spindle is a self-organized dynamic macromolecular structure that is constructed from microtubules, microtubule-associated proteins, and motor proteins (Prosser & Pelletier, 2017). The assembly of this spindle requires the involvement of multiple pathways such as centrosome, chromatin, and microtubule mediated nucleation pathways that each have their role to play. Once finished, this assembly results in an antiparallel, bipolar microtubule array consisting of three different categories of microtubules: kinetochore (K-MTs), astral (A-MTs), and non-kinetochore (nK-MTs); with the plus ends radiating towards the equator and the minus ends radiating towards the centrosomes (**Figure 6**) (Dumont & Mitchison, 2009). K-MTs are responsible for the attachment of chromosomes to the spindle poles using the kinetochore, a specialized protein structure that is assembled on the surface of each centromere. The attachment of several K-MTs results in the stabilization of each kinetochore into a kinetochore fiber, which mediates chromosome movement. A-MTs are crucial for spindle positioning, as they radiate from the spindle poles and interact with the cell cortex. nK-MTs on the other hand, originate from opposite poles and help separate them, thus providing stability to the spindle *via* their extensive sliding (Grill & Hyman, 2005, McNally, 2013).

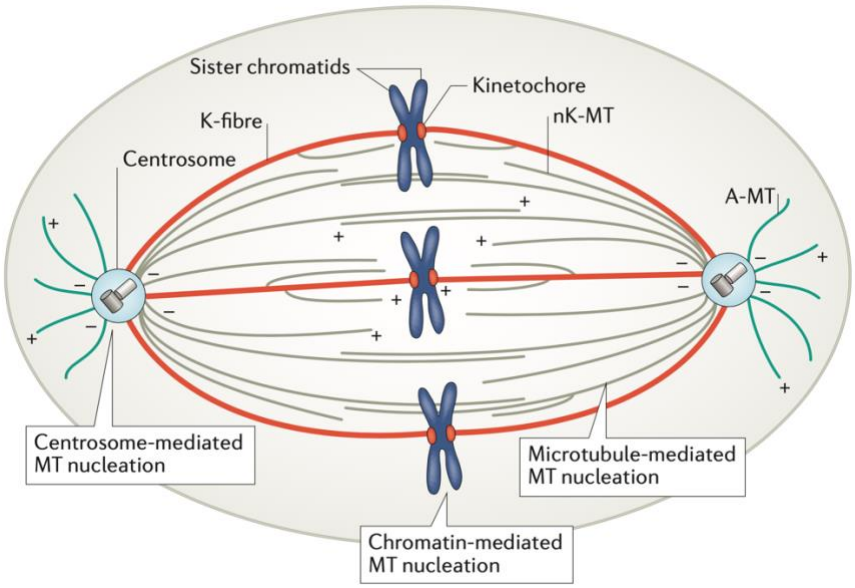

Figure 6: A scheme representing the mitotic spindle and the sister chromatids. The mitotic spindle is comprised of three different types of microtubules: Kinetochore (K-MT), Astral (A-MT), and non-kinetochore (nK-MT). The chromosomes are attached to the microtubules *via* kinetochore fibers (K-fibre), here in red, that are composed of 20-30 K-MTs. Three different pathways drive the nucleation of microtubules in order to form the spindle: the centrosome, the chromatin, and the microtubule itself. These microtubules have a plus end that radiates towards the equator, and a minus end that radiates towards the centrosomes, resulting in an antiparallel array. This figure was taken from (Prosser & Pelletier, 2017).

As for the segregation of chromosomes, the sister chromatids are transported to opposite spindle poles as the kinetochore fibers shorten. A model termed “feeder and chipper” proposes that the depolymerization of kinetochore microtubules requires a motor that feeds them to an immobilized kinesine depolymerase that would “chip away” at the microtubule ends, thus shortening them in a continuous manner. This depolymerization would take place at both ends of the microtubules, therefore allowing the steady movement of the chromatids toward the poles during anaphase (Gadde & Heald, 2004).

2.1.2. Segregation in bacteria

In contrast, segregation is continuous in prokaryotes and is concurrent with replication. This discovery came after numerous hypotheses and early models that were gradually refuted as investigations progressed. The first model termed “origin attachment model” was proposed in 1963 and lasted for more than three decades (Jacob et al., 1963). It suggested that the two newly replicated origins were tethered to the cell envelope close to mid-cell and

were separated by cell growth. It was later demonstrated that cell growth in rod-shaped bacteria was not restricted to mid-cell but rather occurred throughout the cell, thus refuting this hypothesis (Fiebig et al., 2006).

Subsequent studies tracking the *ori* have shown that newly replicated loci rapidly move to their specific destination to opposite poles of the cell and they do so right after their replication. In *E. coli*, the duplicated *oriC* are separated at mid-cell and are then accurately positioned at one quarter and three quarters of the cell respectively (Junier et al., 2014). This is true for most bacteria including *V. cholerae*, where the partition system was shown to segregate the origins of replication (David et al., 2014). As the two replisomes progress on their respective replication arms, newly-replicated are moved towards opposite cell parts (Viollier et al., 2004).

Several models were proposed implicating DNA replication in the segregation of the replication arms. One of those models was termed “replication factory” and suggested that the replisomes were stationed at mid-cell, thus forming a factory that pulls DNA inwards for replication before pushing the replicated DNA outwards (Lemon & Grossman, 1998). However, later studies in *E. coli* and *Caulobacter crescentus* have shown mobile replisomes that track independently along the chromosome (Bates & Kleckner, 2005, Jensen, 2001), thus suggesting that while the replisome along with DNA replication could help chromosome segregation, it did not provide the main force necessary to segregate the sister chromosome by itself.

The molecular mechanisms responsible for bacterial chromosome segregation are only starting to emerge. It is now known that they involve both specific protein components as well as non-protein, and mechanical-based mechanisms, which will all be detailed in the following sections. The four domains of the chromosome (*ori*, *ter*, left, and right arms) were also found to occupy their own fixed places in the cell instead of being mixed, and it translated into a striking symmetry of the two daughter nucleoids (Wang et al., 2006). Therefore, our vision of bacterial segregation gradually evolved from a slow and primitive phenomenon to a fast and highly regulated event. Research, both previous and ongoing, shows that bacteria are far more complex than we originally thought, and we still have a long way to go to understand their chromosomal mechanisms.

2.2. Bacterial chromosome organization and its role in segregation

The fact that replication and segregation happen concomitantly in bacteria adds a new challenge for segregation, as the chromosomes need to be organized in a specific way to allow for the various cellular processes to occur. The *E. coli* chromosome for instance, is organized in four macrodomains and two less-structured regions (Valens et al., 2004). The four macrodomains are: *ori, ter,* right arm, and left arm. The two less-structured regions flank the Ori, one on each side. The development of new techniques these last few years has allowed us to expand our knowledge on the subject and to reveal the different mechanisms used by the cell to efficiently organize their chromosomes for proper replication and segregation. In this thesis, we will discuss a few of these mechanisms: Nucleoid-Associated Proteins (NAPs), as well as DNA supercoiling and MatP which will be detailed later on.

2.2.1. Nucleoid-Associated Proteins (NAPs)

One mechanism responsible for compacting the chromosome is a group of proteins referred to as nucleoid-associated proteins (NAPs) (Luijsterburg et al., 2006). These proteins share a lot of similarities with eukaryotic histone proteins such as basicity, abundance, DNA binding properties, and low molecular weight; and they play a role in several DNA-related processes, i.e.: recombination, DNA repair, replication, as well as transcription. Main examples of NAPs include HU (heat-unstable protein) and H-NS (histone-like nucleoid structuring protein) (Hołówka & Zakrzewska-Czerwińska, 2020). While HU induces bends in the DNA, H-NS can bridge two DNA strands. These activities induce both structural and topological changes in the chromosome to ensure a correct compaction inside the cell, and their variety implies that different NAPs are expressed during different phases of the cell cycle. NAPs like HU are more produced in stationary phase as they can efficiently compact the chromosome (Sato et al., 2013) while H-NS is constantly expressed at a low-level throughout the cell cycle, allowing it to regulate the expression of certain genes under specific conditions (Shahul Hameed et al., 2019).

a. Heat-Unstable protein: HU

There are two HU proteins: alpha and beta. HU-alpha is consistently expressed while HU-beta is only expressed during stationary phase. The HU protein is one of the most abundant and conserved NAP in bacteria, specifically during exponential phase (Azam & Ishihama, 1999). HU's interactions with DNA are variable as it is an important protein for DNA compaction, replication, transcription, recombination, and shape modulation in many bacteria (Broyles & Pettijohn, 1986, Roy et al., 2005, Oberto et al., 2009). While HU can bind all DNA in a non-sequence-specific manner, it does show a high affinity for abnormal structures such as gaps, nicks, and four-way junctions that are generated following DNA damage as well as AT-rich sequences (Kamashev, 2000). Interestingly, it can also help prevent DNA damage by binding to the nucleic acid chain and therefore protecting it from agents like intracellular nucleases. HU-protein interactions have also been found as it has been shown to form HU dimers, as well as take part in the formation of the pre-replication complex of IHF/DnaA/*oriC*. In this case, HU can either activate or suppress the complex depending upon its concentration (Ryan et al., 2002).

In terms of function, HU is able to induce negative supercoiling when in the presence of topoisomerase I, and thus influence gene expression (Rouvière-Yaniv et al., 1979). It also controls the DNA-multiprotein complex formation, the "repressosome", that regulates transcription initiation of the *gal* operon in *E. coli*. Although HU has no sequence specificity, it seems to play an important role in the formation of transcription regulatory complexes.

b. Histone-like Nucleoid Structuring protein: H-NS

H-NS is best studied as a repressor of gene expression in several Gram-negative bacteria such as *E. coli* and *V. cholerae* (Dorman, 2004). It is an abundant protein that binds preferentially to AT rich regions and curved DNA and has the ability to constrain supercoils *in vitro* (Tupper et al., 1994). This makes it an interesting protein as it does not have a consensus sequence like IHF does, it has instead a conserved structure, which is typically associated with that of promoters. The best way to describe H-NS is a gene silencer, as it downregulates countless promoters and can also inhibit recombination (O'gara & Dorman, 2000). In fact, RNA-seq assays have shown that H-NS regulates the expression of a significant fraction of *V. cholerae*'s genome in a growth phase-dependent manner. It down-regulates multiple genes

encoding chemotaxis proteins, the RTX toxin, and the RTX toxin transport system. It has also been shown to silence genes encoding virulence regulators such as ToxR, as well as known cytotoxic factors that are differentially expressed in *V. cholerae* biotypes including the pathogenicity islands VPI-1 and VPI-2 and the CTXΦ (Ayala et al., 2017; H. Wang et al., 2015). As for horizontal gene transfer, it has been demonstrated that it prevents the transcription of the horizontally acquired genes in both enterobacteria and Vibrionaceae (Fitzgerald et al., 2020; Kahramanoglou et al., 2011).

Concerning its own regulation, H-NS's activity does not seem to be modified by the common mechanisms as it is not subject to protease-mediated degradation, and as far as we know, it does not seem to bind a ligand that might alter its activity. It can however form heteromeric complexes with paralogous proteins like StpA as well as members of the more distinct Hha protein family, which could represent a mechanism for H-NS modulation in Enterobacteriaceae (Fitzgerald et al., 2020; Madrid et al., 2007).

H-NS is mostly known for its transcriptional regulatory activity although it is not its only role. It also contributes, along with other NAPs, to nucleoid organization. The exact proteins involved differ depending on the organism but in *E. coli* and enterobacteria, these proteins include NAPs such as HU and H-NS as well as a specific group of proteins that coevolved with Dam methylase, for instance the condensin complex MukBEF (Brezellec et al., 2006). 3C experiments have been conducted to further investigate H-NS's involvement in chromosome organization and the local binding of H-NS was found to prevent a large fraction of its target from interacting with their neighboring loci (Lioy et al., 2018). The short-range contacts increased in many cases in absence of H-NS, which further validate the model in which H-NS silences extensive regions of the bacterial chromosome by binding nucleating high-affinity sites (Lang et al., 2007). Recent investigations have shown that H-NS increases sister-chromatid cohesion within specific regions of the genome of *V. cholerae* such as VPI-1 and the O-Antigen, both involved in the bacterium's virulence level (Espinosa, Paly, et al., 2020).

2.3. The partition system

2.3.1. General introduction

A lot remains unsolved when it comes to chromosome segregation in bacteria. The discovery of partitioning systems in the 1980s was a breakthrough in the subject (Ogura & Hiraga, 1983). They were found to be essential for stable low-copy plasmid maintenance and play an important role in the segregation of the origins of replications. Orthologues of the plasmid-encoded *par* genes were later identified on bacterial chromosomes (Ogasawara & Yoshikawa, 1992). It is important to note that these systems are highly conserved, as they are present in over 65% of the sequenced bacterial genomes (Livny et al., 2007). It is impressive to know that two thirds of bacteria carry nearly identical *par* genes given the wide diversity of the bacterial realm. Species like *C. crescentus*, *B. subtilis*, and *V. cholerae* all have partitioning systems, while others like *E. coli* and its close relatives do not (Gerdes et al., 2000).

It has been observed however that the deletion of these systems does not have the same effects on all the organisms (see Table 1), as it is shown to be essential in some but not in others (Kawalek et al., 2020). The phenotypes observed range from anucleate cells to mild perturbations in chromosome segregation, along with reduced growth rate and elongated cells. As expected, the strongest phenotypes belong to the species in which the *par* genes are essential. For example, the absence of ParB in *Caulobacter crescentus* leads to severe segregation defects, long polyploid cells, and a large portion of anucleate cells. In the case of bacteria where *par* genes are non-essential, we observe a wide array of phenotypes that are more or less obvious depending on the species. In *B. subtilis*, we observe a defect in sporulation as well as elongated cells, which seems to be a recurrent phenotype, and 1-2% of the cells studied were anucleate. Some organisms have a variable percentage of anucleated cells depending on the temperature or the growth media. *Streptococcus pneumoniae* showcases 0.8% of anucleate cells at 30°C, which increases at 3.5% when the cells are grown at 37°C. We see no apparent growth defect aside from this percentage, as well as mild perturbation in segregation. It is important to note that this organism does not harbor a *parA* gene, unlike the rest of the organisms listed here. *Pseudomonas aeruginosa* however, shows 2-4% of anucleate cells when grown in rich growth media (LB) and 7% of anucleate cells when

grown in minimal growth media (M9). *V. cholerae* stands out with its primary and secondary chromosomes. It has been demonstrated that *par* genes are non-essential on Chr1 but are essential on Chr2. The absence of ParB1 shows no segregation defect, but we do observe an increased frequency of replication initiation as well as disturbed *oriC* positioning at the cell poles. The absence of ParB2, however, has drastic consequences on the cells as aberrant, unviable Chr2-deficient cells are produced (Yamaichi, et al, 2007).

Species	*par* genes	Anucleate cells in *parB* mutant	Other phenotypes
Bacillus subtilis	Non-essential	1-2%	Defect in sporulation, elongated cells
Streptococcus pneumoniae	Non-essential no *parA*	0.8% at 30°C 3.5% at 37°C	No apparent growth defects, mild perturbation in segregation
Caulobacter crescentus	Essential	Indispensable	Severe segregation defects, long polyploid cells
Pseudomonas aeruginosa	Non-essential	2-4% in LB 7% in M9	Reduced growth rate, affected motility, 10% > in cell size
Vibrio cholerae	Non-essential: Chr1 Essential: Chr2	No change in ParB1 mutant	No segregation defect in Chr1, increased frequency of replication initiation, disturbed *oriC* positioning at cell poles

Table 1: Characterization of chromosomally encoded *par* systems, adapted from Kawalek et al., 2020.

2.3.2. Structure of the partitioning system

The partitioning system's impact may differ from one organism to another, but its components typically remain the same. The ParABS systems are composed of two proteins, ParA and ParB, as well as a centromere-like cis-acting DNA element: *parS*. ParA is an ATP-ase that binds to non-specific DNA (nsDNA) in an ATP-dependent manner by forming a dimer and localizes to the nucleoid (Bouet et al., 2007; Hester & Lutkenhaus, 2007). ParB on the other hand, is a sequence-specific DNA-binding protein that specifically binds to the *parS* sequences, thus forming a dimer as well. ParB binds to *parS* in a helix-turn-helix motif (Schumacher et al., 2010) and can bind to sequences adjacent to the *parS* sites with very little

sequence specificity (Taylor et al., 2015). This phenomenon is known as ParB spreading, and seems to be essential for the correct functioning of the ParABS system as mutations blocking spreading were shown to cause partition deficiency (Breier & Grossman, 2007). Recent studies have suggested that ParB proteins have CTPase activity implying that the ParB spreading process depends on CTP hydrolysis (Jalal et al., 2020). Now that a quick overview of the partitioning system has been done, it is time to dive deeper into the details. It is important to know that a chromosome's partitioning system is different than that of a plasmid. I will be breaking down those differences in the subsections below.

a. Partitioning systems in plasmids

As mentioned earlier, the partitioning system was discovered in low-copy number plasmids. High-copy number plasmids rely on a mechanism called passive diffusion, which will not be discussed in this thesis. The segregation of plasmids involves the transportation of the copies in opposite directions to ensure that every daughter cell receives at least one copy of the plasmid (Onogi et al., 2002). Partitioning systems of plasmids are typically comprised of three components: at least one copy of a partition site called the centromere, a centromere-binding protein (CBP), and either an ATPase or a GTPase, termed NTPase (Bouet & Funnell, 2019). In order to transport plasmid DNA, the CBP will bind to the plasmid centromere(s) and interact with the NTPase. There are three different types of partition systems that have been identified so far, defined by the type of NTPase that promotes plasmid localization (Gerdes et al., 2002). Type I partition systems encode a Walkter-type ATPase which promotes segregation by forming dynamic patters on the bacterial nucleoid. They are the most prevalent type in sequenced plasmid genomes and have been the most extensively studied for *Enterobacteriaceae*. Type II partition systems harbor an actin-like ATPase which polymerizes into dynamic filaments and effectively pushes plasmids apart. Type III systems have a similar mechanism as they encode for a tubulin-like GTPase that uses a dynamic polymerization method to efficiently segregate plasmids. This type has not been found in *Enterobacteriaceae* so far but has been identified in plasmids of some *Bacillus* species as well as some bacteriophages. It is important to note that partition systems are not mutually exclusive, as a number of plasmids were found to contain two different partition systems, but generally one of each type. In some cases, both types were shown to contribute to plasmid stability (Ebersbach & Gerdes, 2001).

b. Partitioning systems in chromosomes

Unlike plasmid partitioning systems, chromosomally encoded Par systems are exclusively of type I. The chromosomal *parS* sequences that have been identified so far on chromosomes contain an inverted repeat sequence similar to the *parS* site that was originally identified in *B. subtillis* (Lin & Grossman, 1998). Another difference from plasmids since the *parS* sequences on plasmids lack similarity, but commonly consist of an inverted and/or direct repeat (Hayes & Barillà, 2006). *parS1* sites are highly conserved among diverse species while the *parS2* sequences are significantly different depending on the bacterial family (Livny et al., 2007). In the case of *V. cholerae*, Chr1 and Chr2 each has its own segregation dynamics but they both have *parAB* genes near their replication origins. Interestingly, the ParA and ParB proteins encoded by the *par* locus on Chr1 (ParAB1) are similar to other chromosomal proteins, whereas the ones encoded by the *par* locus on Chr2 (ParAB2) resemble those of plasmids and phages (Yamaichi & Niki, 2000). A study published in 2007 identified several *parS* sites on the genome of *V. cholerae*: three sites on Chr1 (*parS1*) and ten sites on Chr2 (*parS2*) that differed from the sequence of *parS1* (Yamaichi et al., 2007). The *parS1* sites were found close to *oriC1*, as were most of the *parS2* sites to *oriC2* (**Figure 7**). Surprisingly, a *parS2* site was found to be located on Chr1, suggesting that it might have a role in the segregation of the ter domain of Chr1. It is important to note that a polar organizing factor termed HubP directs the action of the partitioning machinery in *V. cholerae*, although its absence significantly disrupts the proper cellular positioning of proteins such as ParA1 and a ParA homolog, ParC, on Chr1 while no detectable change was observed on Chr2 (Yamaichi et al., 2012).

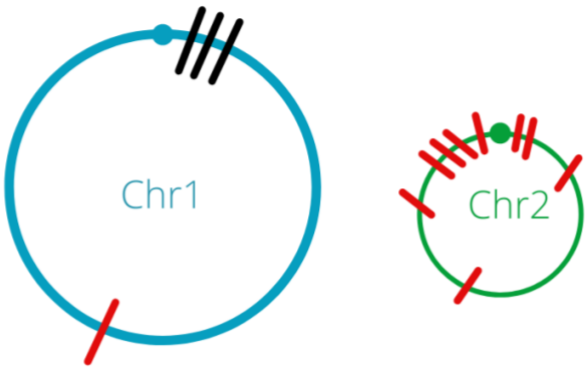

Figure 7: A scheme representing the distribution of the *parS* sites on the genome of *V. cholerae*. Chr1 is represented in blue while Chr2 is represented in green. The three *parS1* sites of Chr1 are represented by black lines and the ten *parS2* sites (nine on Chr2 and one on Chr1) are represented by red lines. Adapted from Yamaichi et al., 2007.

2.3.3. Mechanisms of action of the partitioning system

Now that the composition of the ParABS system has been established, we will dive into its mechanics. ParA binds to the N-terminal region of ParB with high specificity, and the two centromere binding motifs form an extended centromere binding domain (Sanchez et al., 2013), with the involvement of most, if not all, of the 16 base pairs of *parS* sites (Pillet et al., 2011). When bound to ParB, ParA activates its ATPase, and releases ParB from the *parS* sequence it has been bound to, thus activating the partitioning machinery (**Figure 8**) (Taylor et al., 2021). The stimulation of the ATPase activity by ParB is essential for this stage (Ah-Seng et al. 2013).

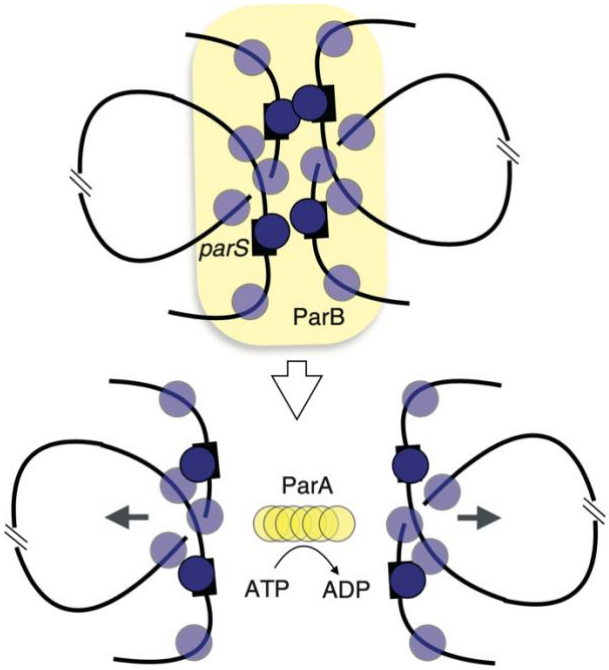

Figure 8: Scheme representing the segregation of the *ori* by the ParABS. Chromosomes are represented by black lines. Blue circles indicate proteins with pairing activities and yellow circles represent proteins with release activities. The top panel shows 4 *parS* sites, two on each sister chromosome, paired inside a cluster of ParB proteins. ParB dimers bind both specific *parS* sites (black bars) as well as neighboring non-specific sequences (light blue circles). The bottom panel represents ParA releasing the ParB-dependent pairing *via* ATP hydrolysis. Adapted from Bouet et al., 2014.

The behaviors of *parA* and *parB* mutants have shown that ParA is necessary to segregate pairs or groups of plasmids (Fung, 2001). In addition, ParA forms patterns within the nucleoid mass due to dynamic interactions with ParB when it is bound to *parS*. These patterns are necessary for the segregation of chromosomes as well as plasmids (Le Gall et al., 2016). As *parS* sequences are usually located near the *ori*, the partitioning system is one of the main actors involved in the segregation of newly replicated origins of replication. According to several studies, the ParA motor uses the nucleoid along with its non-specific DNA (nsDNA) to pull the replicated origins to opposite cell poles (Vecchiarelli et al., 2010).

In addition to their primary role in segregation, the Par proteins have evolved other functions such as mediating replication initiation or loading of Structural Maintenance of Chromosomes complexes (SMCs). The recruitment of SMC complexes to the origin by ParB is involved in segregation during fast-growth by constraining *ori*-proximal regions, thus drawing

the origin domain in on itself and away from its newly replicated sister in an effort to overcome origin cohesion (Wang et al., 2014). It is important to note that even though ParA is not essential for the formation of ParB-DNA complexes, it can influence or modulate them (Ah-Seng et al., 2013). SMC recruitment helps the segregation of chromosome arms that is detailed in the following sections. The *ter* regions require the same level of investigation, as their segregation marks the end of one step of the bacterial cell cycle, and the start of another. Many different actors are involved in this process including MatP, which will be the focus of the next section.

2.4. MatP: an important structuring factor

MatP was discovered *via* bioinformatics analysis and genetic screening, and was found to have macrodomain-specific DNA-binding profile (Mercier et al., 2008). It is conserved in both *Enterobacteriaceae* and *Vibrionaceae*, binds exclusively to the *ter* macrodomain, and was shown to be its main organizer (Durand et al., 2012). In fact, in the absence of MatP, segregation of the *ter* macrodomain occurs early in the cell cycle. No cohesion step is observed between the two replicated *ter* macrodomains, DNA is less compacted, and the mobility of markers located in the macrodomain is increased (Lioy et al., 2018; Mercier et al., 2008). MatP binds exclusively to the *matS*, a short motif of 13 bp repeated 23 times in an 800 kb domain located in the *ter* region of the *E. coli* chromosome and this localization is conserved among enterobacteria and *Vibrionaceae*.

MatP plays several roles in the second half of the bacterial cell cycle and interacts with different actors and processes. Its interaction with a specific component of the divisome machinery results in MatP maintaining the newly replicated *ter* copies at mid-cell (Espéli et al., 2012). *V. cholerae*'s chromosome and chromid segregate their *ter* domains in different ways. While the newly replicated copies of *ter1* remain together and mid-cell for a very large portion of the cell division stage, sister *ter2* copies segregate in the two cell halves before the initiation of septation (Demarre et al., 2014). The two sister copies of *ter1* remaining together is the consequence of MatP's action, as they separate early in the cell cycle in its absence. However, they remain in the vicinity of the cell center (Demarre et al., 2014).

MatP also plays a role in the selection of the division site and the licensing of the divisome assembly *via* physical interaction with the divisome (Männik et al., 2016). It is also linked to the SMC-like complex MukBEF, the topoisomerase Topo IV, and the cell division translocase FtsK. Each of these interactions will be explained in the following sections as we continue to talk about the different steps of the cell cycle and their actors.

2.5. The bacterial SMC complexes and SMC-like condensins

2.5.1. The discovery of MukBEF

In 1991, a mutant defective in a new gene named *mukB* was discovered through observations of spontaneous, normal sized, anucleate cells at low temperature (Niki et al., 1991). The *mukB* gene encodes for a large protein of the same name, with distinct domains that were characterized later on. Niki et al observed that the *mukB* mutants though not lethal at low temperature, showcased aberrant chromosome partitioning. At high temperature, the same mutants were unable to form colonies and many nucleoids were distributed irregularly along elongated cells, concluding that MukB is required for the partitioning of chromosomes in *E. coli* (Niki et al., 1991).

This discovery led to years of studying what eventually became the MukBEF complex, with the discovery of two subunits: MukE and MukF. All three subunits of the protein are encoded in the same operon, together with the unrelated gene *smtA*: *smtA-mukF-mukE-mukB* (Yamanaka et al., 1996). MukB is at the heart of the MukBEF complex with two globular domains, N- and C-terminal, connected by two long α-helices with a hinge region in between **(Figure 9)** (Melby et al., 1998). The two domains fold into a singular globular head domain with the ATP binding site located on its surface. When in solution, MukB dimerizes *via* the hinge domain to form a distinctive V-shaped molecule and the DNA binding site is located on the positively charged hinge-proximal side of the head domain and spreads over its sides (Woo et al., 2009). The other two units form a stable complex together and dynamically associate with MukB. Although MukEF does not show any DNA binding activities, it modulates MukB-DNA interactions (Cui et al., 2008). MukF acts as a kleisin that interacts with MukB heads and links MukE to the complex **(Figure 9)** (Woo et al., 2009).

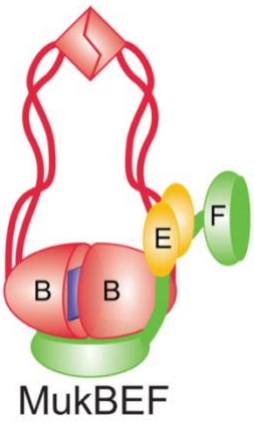

Figure 9: Organization of MukBEF. An ATP-mediated dimerization of the MukB (here in red) heads creates a high affinity DNA binding site. The head can accommodate a single C-terminal binding of MukF (here in green). The N-terminal domain of MukF could accommodate further dimerization. MukE (here in yellow) is linked to the complex by MukF and is located directly atop the MukB heads. Adapted from (Rybenkov et al., 2014).

When it comes to its function, MukBEF has been demonstrated to bind linear and circular DNA equally, and fluorescence microscopy has shown that its primary substrate is double-stranded DNA (She et al., 2013). MukB was proven to induce DNA condensation when overproduced in living cells (Wang et al., 2006), which implies the existence of DNA bridging events as such condensation cannot be explained by DNA binding alone. This binding however, is highly cooperative, as MukB binds the DNA according to the zipper mechanism which resembles DNA annealing, when the slow nucleation step is followed by a fast propagation of the protein cluster (Cui et al., 2008). This mechanism renders the DNA significantly resilient to applied forces including chromosome segregation. MukB is thus expected to bind unspecific regions of DNA that do not participate in other cellular activities, and relocate when necessary (i.e., when a need arises for the bound DNA to participate in a cellular event) (Rybenkov et al., 2015). A fluorescence microscopy study has shown a difference of function between the three subunits. While MukB is responsible for DNA organization, MukE ensures that it is targeting specific cellular addresses, and MukF links the two of them together and potentially coordinates their activities by modulating ATP turnover (She et al., 2013). Functional interactions between MukBEF and DNA topoisomerases, especially Topo IV, have been reported (Vos et al., 2013) and will be detailed later in this thesis.

2.5.2. Structural Maintenance of Chromosomes (SMC)

Structural Maintenance of Chromosomes proteins were first discovered in 1993 when Strunnikov et al were screening for genes that cause a loss of artificial mini chromosomes when they are knocked out in yeast (Strunnikov et al., 1993). They were surprised to find that this new protein did not resemble any other known mechanochemical domain and knew that SMC1 as they called it represented a new class. They found however that it shared similar homologies with the *E. coli* protein MukB. While they had no clear knowledge of what this new protein did, they could speculate about its function since it was known that MukB was involved in nucleoid segregation, and that the deletion of *smc1* impedes segregation of the chromosomes (Niki et al., 1991; Strunnikov et al., 1993).

Their work started a wave of investigations into the SMC field, in both prokaryotes and eukaryotes, and several aspects of this protein family have since been elucidated. One of the first questions raised was whether the SMC proteins were conserved among different species. Phylogenetic analysis has shown that these proteins are indeed conserved as they form a largely diverse family tree with several subgroups (Melby et al., 1998). In Eukaryotes, there are three types of SMC complexes: the cohesin complex (SMC1 and SMC3), and the two condensin complexes (SMC2 and SMC4, SMC5 and SMC6). In bacteria, there are SMC proteins and SMC-like proteins such as MukB.

After in-depth genetic sequencing, it was found that proteins like MukB are highly different from SMC proteins sequence-wise despite having similar three-dimensional structures as shown in **Figure 9**. They are all structured in three specific parts: a head ATPase domain formed by both the N- and C- termini, followed by a long intramolecular coiled-coil that ends with the third domain, the hinge (Cobbe & Heck, 2004). They are typically in dimers, bridged together by a kleisin and a second non-SMC subunit, forming what is called the SMC complex (Nolivos & Sherratt, 2014) (**Figure 10**).

At first glance, these three complexes look almost identical however small but significant differences can be found if one looks close enough.

2.5.3. Structure of the different SMC and SMC-like complexes

The SMC complexes differ depending on the species. For instance, *E. coli* lacks an SMC complex but has the SMC-like complex: MukBEF. In the presence of ATP, MukF interacts with the cap region of MukB via its C-terminal domain, while its central region interacts with a homodimer of MukE. On the other hand, after ATP hydrolysis, two MukE dimers and a single MukF dimer bind a dimer of MukB (**Figure 10A**) (Nolivos & Sherratt, 2014). However, other bacteria such as *Bacillus subtilis* have a SMC complex composed of an ScpA kleisin whose C-terminal domain interacts with the cap region of one Smc head, while its N-terminal domain binds the neck region of the other Smc monomer. In addition, a central ScpA domain wraps around a dimer of ScpB, a segregation and condensation protein. ATP binding and head engagement prevent a second ScpA binding (**Figure 10B**) (Nolivos & Sherratt, 2014). In eukaryotes, the SMC cohesin complex is composed of a heterodimer of Smc1 and Smc3, a kleisin called Scc1 binding them both and a cloud of non-SMC subunits (**Figure 10C**) (Nolivos & Sherratt, 2014). In the absence of ATP, the C-terminal domain of Scc1 binds to the head domain of Smc1 while its N-terminal domain binds to the head domain of Smc3. In presence of ATP, the SMC complex takes on a closed conformation, with the head domains of both Smc1 and Smc3 interacting.

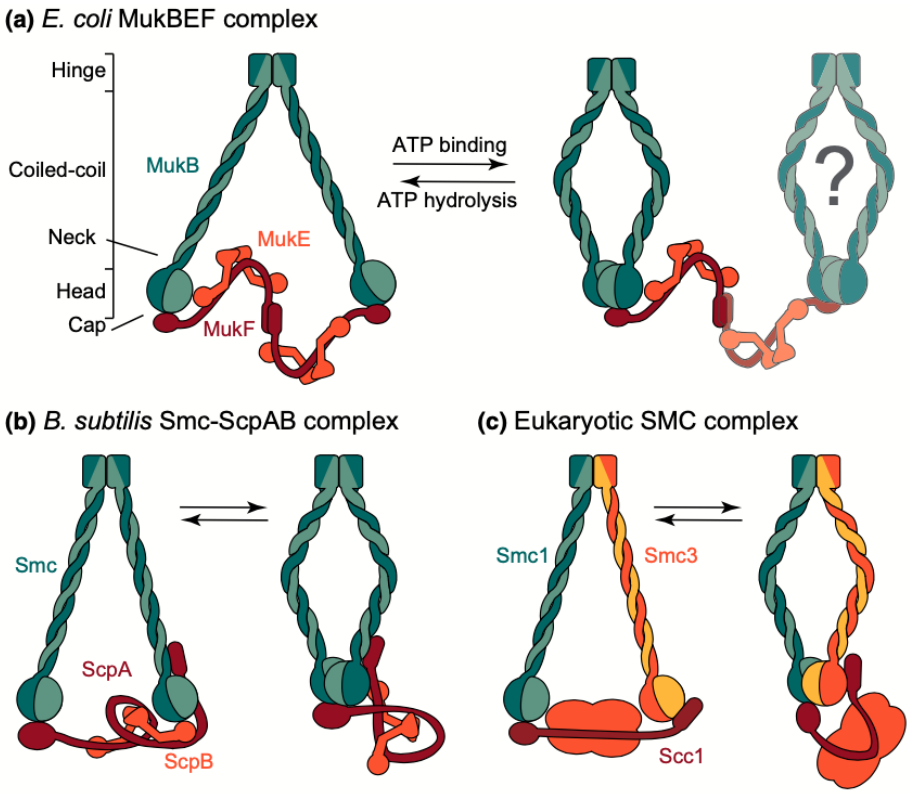

Figure 10: Structures of SMC and SMC-like complexes, adapted from (Nolivos & Sherratt, 2014). **(A)** shows the *E. coli* MukBEF complex, with its conformation before (left) and after (right) ATP binding. **(B)** shows the Smc-ScpAB complex in *B. subtilis*, with the same ATP binding/hydrolysis conformations as the top panel. **(C)** shows the eukaryotic SMC complex, with both conformations before and after ATP binding on the left and right respectively.

2.5.4. Role of SMC and SMC-like complexes in bacteria

Several models have emerged over the course of the last decade when it came to the SMC's involvement in chromosome segregation in bacteria. From fixed replisomes near the cell center (Jacob et al., 1963) to observations of moving replisomes along opposite chromosome arms (Jensen, 2001), we have come a long way concerning segregation models. Different prokaryotic organisms have been studied, uncovering different operating mechanisms for SMCs.

a. *Bacillus subtilis*

The major SMC protein in *B. subtilis* is the BsSMC condensin, and it was found to be linked to the compaction of the bacterial chromosome (Kleine Borgmann et al., 2013). The recruitment of this condensin is mediated by the partitioning system protein ParB, and this

recruitment is essential in fast growing bacteria as it was shown to reduce DNA entanglement (Wang et al., 2015). Early studies demonstrated that the BsSMC proteins were capable of entrapping DNA within their structure (Wilhelm et al., 2015). We had to wait a few years for high-throughput chromosome conformation capture (Hi-C) techniques to shine a light on the interactions between the two actors of segregation: the partitioning system and the SMC complexes. Hi-C allows us to follow chromosome folding by measuring the rate of interactions between genome loci that are close spatially speaking but may be located far from each other on the genome (Wang et al., 2015, 2017). This study has shown that once ParB has loaded the SMC proteins onto the genome, the SMCs slide along the length of a single chromosome, from *oriC* to *ter*, while holding on to both chromosome arms and subsequently aligning regions on opposing arms.

They reached this conclusion following Hi-C experiments on a strain lacking ParAB and compared the contact map with that of a wild-type (WT) strain (**Figure 11**). The contact map of the WT strain shows extensive short-range interactions along both chromosome arms (the primary diagonal) as well as robust interactions between the two arms (the secondary diagonal). In the *parAB* mutant however, the long-range interactions between the two chromosome arms were completely lost, while the short-range interactions were largely unchanged; each arm now forms independent interaction domains. These results align with data from fluorescent microscopy where GFP-tagged SMCs are seen to localize at *parS* sequences before spreading out along the genome. Multiple copies of SMCs seem to consecutively bind to *parS* and slide away from it. Recent studies have shown that in addition to sliding along the genome, BsSMCs unload near the *ter* domain (Karaboja et al., 2021). Piecing these results together unravels a model for segregation where SMCs are loaded onto each replicating chromosomal arm with the help of the partitioning system and slide along the genome, therefore helping the segregation of each replicated arm.

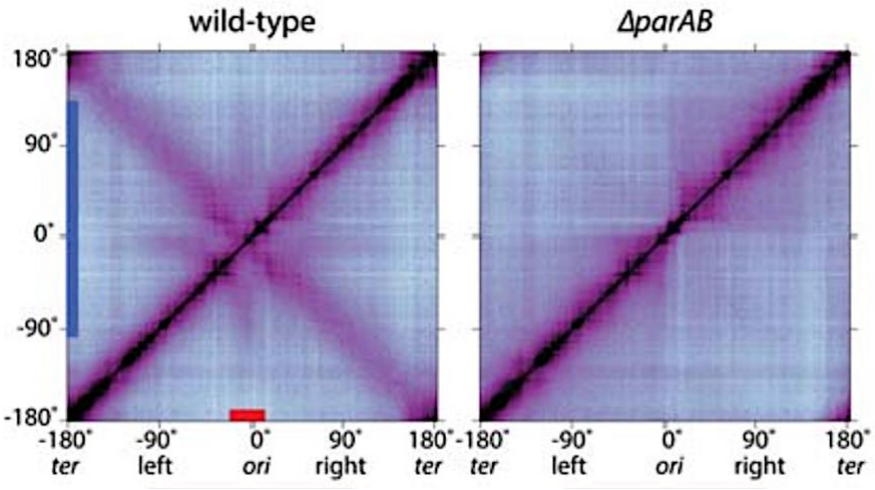

Figure 11: Hi-C contact maps of a WT strain (left) and a *parAB* mutant strain. The matrices display contact frequencies for pairs of 10-kb bins across the genome. The axes indicate the gnome positioning of each bin in degrees, and the genome was oriented along the axes with the *ori* in the center and the left and right arms on either side. A ~300 kb region spanning from the origin (red bar on the X axis) and a broad region on the left and right arms (blue bar on the Y axis) are highlighted to show the long-range interactions.

b. *Caulobacter crescentus*

The SMC complex plays an important role in many organisms and *C. crescentus* is no exception. As stated before, several approaches were used over the years to investigate the SMC complexes, one of them being the Hi-C assays. The very first application of Hi-C to bacteria was directed at the genome of *C. crescentus* and revealed a well-defined organization of its chromosome (Le et al., 2013). They performed Hi-C assays on cells lacking the *smc* gene and found a clear drop in the frequency of inter-chromosomal interactions in comparison to the WT strain. In contrast, the frequency of intra-chromosomal interactions remained unaffected in the mutant strain. These results were later supported by the Hi-C assays on *B. subtilis* strains, pointing towards a common role for SMC proteins in bacteria. As mentioned above, multiple copies of SMCs seem to consecutively bind to *parS* and slide away from it in *B. subtilis*, and this behavior was also characterized in *C. crescentus* (Tran et al., 2017).

c. *Escherichia coli*

In the case of *E. coli,* the major SMC-like protein is the tripartite MukBEF complex that is composed of two copies of each MukB, MukE, and MukF. Similar studies to *B. subtilis* and *C. crescentus* were conducted in this organism as Hi-C experiments were performed to learn

more about the role of MukBEF in chromosome organization. The results show a loss of long-ranged intra-chromosomal contacts *in vivo* upon the deletion of MukBEF, suggesting that the complex organizes large chromosome loops of hundreds of kilobases in the nucleoid (Lioy et al., 2018). Another interesting result from the same study showed that MatP seems to prevent MukBEF-induced long-range contacts in the *ter* macrodomain. This observation comes in agreement with the findings of MukB interacting with MatP at the *matS* sites (Nolivos et al., 2016). Recent studies have backed this model with 3D Structured Illumination Microscopy (SIM) that allows for the observation of fluorescent samples at resolutions that are below the limit of any optical microscope. This extremely precise imaging has shown that when upregulated, MukBEF proteins form a horse-shoe-like backbone structure, thus co-aligning with the chromosome structure of DNA loops (**Figure 12**) (Mäkelä & Sherratt, 2020). This structure did not form at the *ter* region in the presence of MatP, but a deletion of the latter resulted in the MukBEF ring closing through *ter*, leading to a global re-orientation as well as a re-positioning of the chromosome.

As for its binding pattern, MukBEF does not bind on *parS* sites near the *oriC* domain, and the search for its loading mechanism is still ongoing today. One of the models that are being discussed suggests that it is MatP that creates a gradient of MukBEF along the chromosome by driving it away from the ter (Nolivos et al., 2016). Another model suggests that MukBEF is preferentially loaded near the *oriC* at mid-cell and is moved away from the center due to cell elongation, therefore segregating the duplicated origins (Hofmann et al., 2019). Even though this aspect of MukBEF's action remains a mystery, the consequence of its deletion is not. The absence of MukBEF in *E. coli* results in guillotining of the nucleoid and thus an anucleation of the cells (Niki et al., 1991)

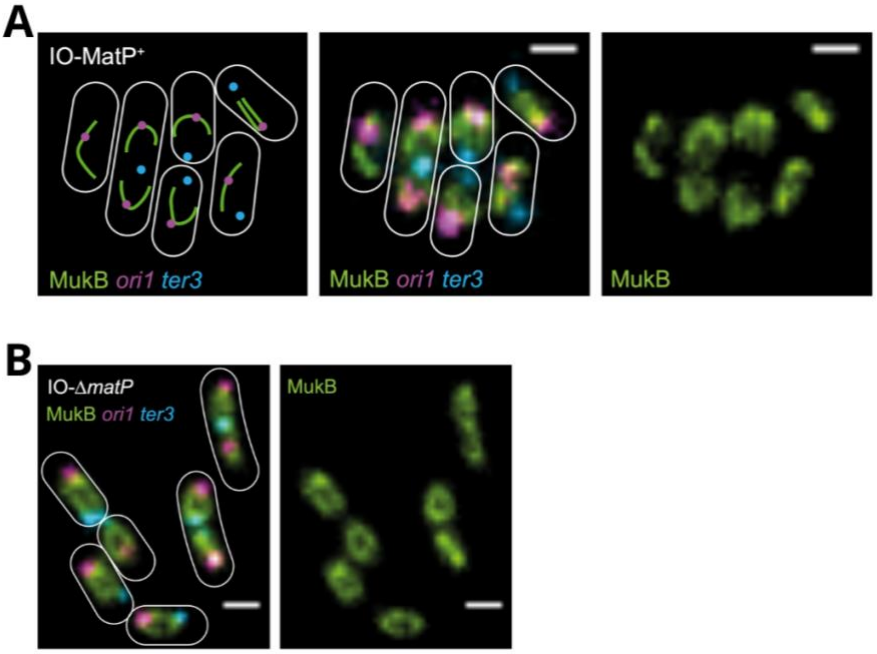

Figure 12: Fluorescent images with cell borders of **(A)** *E. coli* cells with increased occupancy MukBEF (IO) of cells with labelled MukB, *ori1*, and *ter3*. A scheme of the images is found on the left. **(B)** *E. coli* IO-Δ*matP* cells with labelled MukB, *ori1*, and *ter3*. Scale bars: 1 μm. Taken from (Mäkelä & Sherratt, 2020).

d. *Vibrio cholerae*

When it comes to SMC and SMC-like complexes, *V. cholerae* has MukBEF to count on for chromosome condensation. It is important to note that the main difference between *E. coli* and *B. subtilis* or *V. cholerae* is that while the last two have a partitioning system, *E. coli* does not. The severe phenotype present in *E. coli* when *mukB* is deleted is not observed in every MukBEF or SMC harboring organism as previous unpublished analysis in our laboratory suggests it is absent in *V. cholerae*, which furthers the question of MukBEF's relationship to segregation. Little is known about MukB in *V. cholerae*, which furthered our interest in the subject.

2.6. Segregation of the *ter* domain with XerC, XerD, and FtsK

Most bacterial chromosomes face an additional complication during the cell cycle due to their circular nature, chromosome dimers. In fact, newly replicated sister chromatids can generate dimers during homologous recombination events, thus threatening chromosome segregation (McClintock, 1932). These recombination events are resolved by two tyrosine recombinases, XerC and XerD, adding a crossover at a specific site within the *ter* region

termed *dif* (Midonet & Barre, 2014). This mechanism is conserved in most bacteria, and it is present in *V. cholerae* as well as *E. coli*. A cell division protein, FtsK, is also involved in this process. By binding and hydrolyzing ATP, FtsK is able to pump DNA between the daughter cell compartments after the assembly of the divisome but before the final scission (Demarre et al., 2013). Polar DNA motifs, FtsK-Orienting Polar Sequences (KOPS), then orient the loading of FtsK on the DNA, thus setting the direction of translocation (Bigot et al., 2005, 2006). The translocation typically starts at *ori* and heads towards *dif*. As a result, FtsK brings together the two *dif* sites of a chromosome dimer at mid-cell. It later activates the Xer recombination *via* a direct interaction with XerD for chromosome dimer resolution with a Holliday Junction as an essential reaction intermediate (Midonet & Barre, 2014).

2.7. Segregation and chromosomal arrangement in *V. cholerae*: a summary

Below is a scheme summarizing Chr1 and Chr2 arrangement and segregation in *V. cholerae*, in the left and right panel respectively (**Figure 13**) (Espinosa et al., 2017). In the case of Chr1, newborn cells have their origin of replication *oriC1* anchored by HubP and the ParAB1 system to the old pole while *ter1* is kept near the new pole by MatP. During the cell cycle, HubP starts transitioning towards the old pole, quickly followed by ParAB1 as well as one sister copy of the newly replicated *oriC1*. The two copies of *oriC1* are segregated to opposite cell halves, and the *ter1* region bound by MatP moves to mid-cell where they remain together until the end of the cell cycle. As for Chr2, it occupies the younger half of the cell. *oriC2* is maintained at mid-cell by the ParAB2 system and *ter2* remains close to the new pole thanks to MatP. After replication, the *oriC2* sister copies are segregated at quarter positions by the ParAB2 system while the *ter2* sister copies are restricted around the division site by MatP.

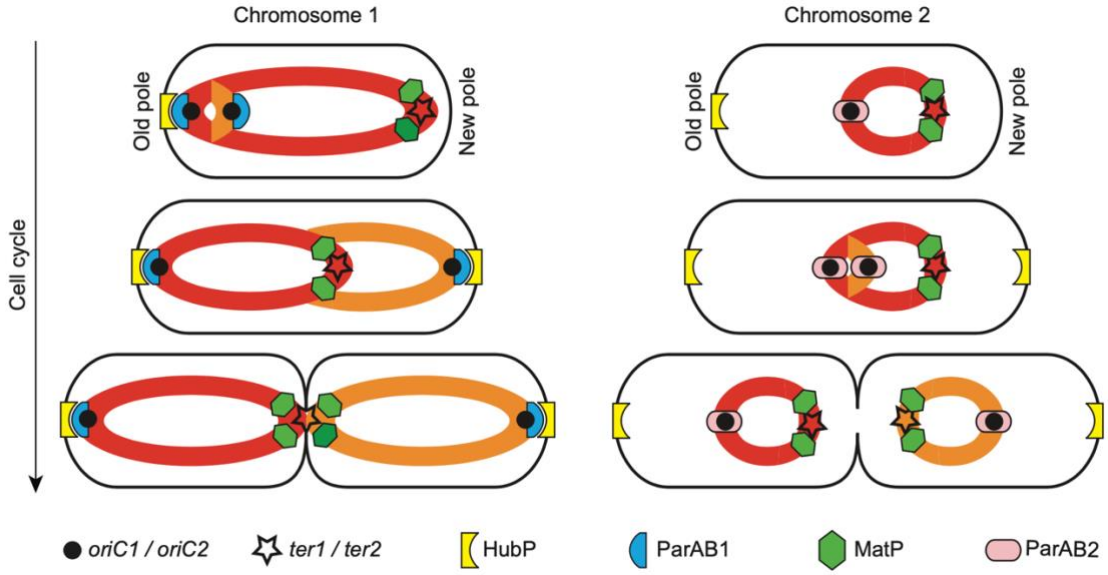

Figure 13: Schematic representations of Chr1 and Chr2 segregation and arrangement in *V. cholerae.* The origins of replication are represented by a black circle while the termini of replication are represented by stars. The template chromosome and the newly replicated chromosome are represented by red and orange circles respectively. HubP is represented in yellow at the cell poles along with ParAB1, represented in blue. ParAB2 however, is represented by pink cylinders and remains next to *oriC2*. MatP is represented by green hexagons and remains at the *ter* domains of both chromosomes. Taken from (Espinosa et al., 2017)

3. Cell division in bacteria

Now that we went through chromosome segregation, it is time to talk about cell division. It is not an easy task for the bacterial cell as it must identify the mid-cell site, differentiate it from the rest of the cell, and form the septum in order to divide (den Blaauwen, 2013). Similarly to the rest of the cellular mechanisms, the complexity of bacterial cell division was underestimated when it was first observed. The first investigations into the matter quickly proved that things were far more complicated than the standard "the bacterium is cut in half, and two daughter bacteria are born", and scientists learned that there are three main steps to achieve correct cell division: mark the division site, recruit the division machinery (divisome), and activate cell wall synthesis to form the septum and drive constriction (Mahone & Goley, 2020). Cell wall hydrolysis and membrane fusion are also required for the physical separation of the two daughter cells.

3.1. FtsZ: one of cell division's main proteins

One cannot talk about cell division without mentioning FtsZ, one of the main actors of cell division. The *ftsZ* gene was found in 1980 in *E. coli* (Lutkenhaus et al., 1980) as a filamenting temperature sensitive mutant and has been actively studied ever since. Bi & Lutkenhaus published a decade after its discovery that FtsZ self-assembles into a ring-like structure (a Z-ring) at the future site of division, which depends on the binding and hydrolysis of the GTP nucleotide (Bi & Lutkenhaus, 1991). We know now that FtsZ is critical for the process of cell division in many organisms such as *E. coli, V. cholerae,* and *B. subtilis* and is highly conserved among prokaryotes (Vaughan et al., 2004). FtsZ homologues can be found as well in several eukaryotic species and are involved in multiple cell division processes including chloroplasts and mitochondria (Gilson & Beech, 2001). FtsZ has three conserved domains: a polymerizing GTPase domain, a C-terminal conserved peptide (CTC) that binds to membrane anchors, and a disordered C-terminal linker (CTL) that connects the first two domains together (Vaughan et al., 2004).

FtsZ may be one of the main actors of cell division, but it cannot orchestrate this important step by itself. Division site selection is incredibly precise and Z-ring positioning is controlled by very distinct mechanisms that will not be discussed in large detail in this thesis. For correct cell division, over 35 different divisome proteins have to be recruited to the Z-ring, interact with FtsZ, tether the ring to the membrane, and regulate its dynamics (Du & Lutkenhaus, 2017). Once the divisome machinery is in place, proteins such as peptidoglycan synthesis enzymes arrive at the division site, allowing for the formation of the septum and finally cytokinesis. There are two FtsZ-polymerization inhibitory systems that initiate cell division at mid-cell, Min and nucleoid occlusion (NO) (J. Lutkenhaus, 2007).

In *E. coli*, Min is composed of three proteins: MinC, MinD, and MinE. The three of them have different roles as MinC is responsible for blocking Z-ring formation, MinD is the activator of MinC, and MinE is the topological regulator of MinCD (J. Lutkenhaus, 2007). The regulated oscillation of MinCDE between the two cell poles leads to the specific inhibition of the polymerization at the cell poles. NO on the other hand, couples the timing and assembly of the Z-ring to the replication/segregation cycle. To achieve this, the nucleoid serves as a scaffold for the positioning of SlmA, a DNA binding protein that inhibits FtsZ polymerization (Cho et al., 2011). SlmA binding sites (SBS) are asymmetrically distributed along the genome of *E. coli* and are essentially absent from the *ter* region. This results in cell division only initiating at the very end of the segregation cycle when the two sister copies of *ter*, devoid of SBS, are the only regions left at mid-cell (Tonthat et al., 2011).

V. cholerae carries orthologs of both MinCDE and SlmA, and MinD was shown to oscillate between the two cell poles in this organism as reported for *E. coli* (Galli et al., 2016). SBS sites were also identified on both Chr1 and Chr2 and their distribution was demonstrated to drive the choreography of the cell division proteins as well as the timing of assembly of the divisome. One main difference between the two organisms is the absence of any apparent phenotype after Min-inactivation in *V. cholerae*, as opposed to the cellular arrangement perturbations observed in *E. coli* (Galli et al., 2016). A reasonable hypothesis to explain this difference is the presence of the partitioning system in *V. cholerae*, and it becoming the primary cell division regulation mechanism in the bacteria, thus superseding the Min system (Galli et al., 2016).

Another important note is the presence of a familiar protein MatP. Other than being involved in chromosome segregation, MatP is also involved in cell division (Crozat et al., 2019). It indeed directly connects *via* physical interaction to ZapB and ZapA, who are both part of the divisome machinery (Männik et al., 2016). ZapA, a widely conserved protein among bacteria, is a cell division inhibitor that interferes with the formation of the Z-ring *via* a direct interaction with FtsZ (Gueiros-Filho & Losick, 2002). As for ZapB, it is a novel cell division factor that stimulates the assembly of the Z-ring as well as cell division (Ebersbach et al., 2008). Together, these three proteins form a complex that anchors the ter region to the Z-ring, thus orchestrating divisome positioning with chromosome segregation (Espéli et al., 2012).

4. Sister chromatid cohesion in bacteria

4.1. DNA Catenation

4.1.1. Supercoiling and catenation

Before diving into the depth of sister chromatid cohesion and its mechanisms, let's start with the basics: catenation. In its relaxed state, a bacterial chromosome does not constitute a circle with both chromatids perfectly parallel to one another. It is indeed supercoiled, with the two sister chromatids forming a helix post replication. DNA supercoiling frequently occurs along the genome as a consequence of replication, at a rate of 50-400 negatively supercoiled DNA loops averaging about 10 kb each in size (Johnson et al., 2014). The DNA loops are topologically independent, and the presence of these independent domains significantly contributes to the chromosome's compactness (Leng et al., 2011).

This helix can either be relaxed with fewer turns (negative supercoiling) thus separating the two strands or wound up with several turns (positive supercoiling) and stabilizing the helix (Witz & Stasiak, 2010). It is important to note that negative supercoiling plays a major role in transcription and replication, as the separation of the strands relaxes the torsional stress caused by this supercoiling and consumes less of the energy produced by the ATP hydrolysis on the hands of the DNA gyrase (Kreuzer & Cozzarelli, 1980). Supercoiling and catenation are not mutually exclusive as both can coexist on the chromosome. Catenation is the phenomenon in which two circular DNA molecules are linked together in a chain-like process. When two DNA strands are catenated, replication can still occur but segregation however, cannot. The bacterial cell wishing to divide calls for another mechanism: decatenation *via* specific enzymes, the DNA topoisomerases.

4.1.2. The role of topoisomerases in decatenation

Topoisomerases are enzymes that can reduce supercoiling by forming either single stranded or double stranded breaks in the targeted DNA strands. They are highly conserved as they are required in eukaryotes and at least two topoisomerases can be found in every bacterial genome. These enzymes are diverse as well since several families have been discovered throughout the years. They are classified based on evolutionary relationships,

sorting the topoisomerases into five families each deriving from a distinct ancestral enzyme (Forterre & Gadelle, 2009). Type I families are monomeric topoisomerases and harbor three unrelated families: IA, IB, and IC, while type II families are dimeric and are comprised of two families: IIA and IIB. Several topoisomerases were found throughout the years and numbered according to their discovery. In a happy coincidence, all odd numbers fall under the category of type I isomerases while all even numbers are type II isomerases. The distribution is as follows:

Type I: Topo I, III, V

Type II: Topo II, IV, VI

As for their conservation, there is no general rule. Some of them are widely distributed among the three domains of life while others are present in one domain (Forterre & Gadelle, 2009).

Eukaryotes	Bacteria	Archea
Topo IA TopoIB Gyrase Topo IIA Topo IIB	Topo III TopoIB Gyrase Reverse Gyrase Topo IV Topo IIB	Topo IIII TopoIC Reverse Gyrase Topo IIA Topo IIB

Figure 14: Distribution of the various topoisomerases throughout the three domains of life: Eukaryotes, Bacteria, and Archaea, according to (Forterre & Gadelle, 2009).

4.1.3. Topoisomerase IV: roles and mechanisms

As stated earlier, topo IV is a type II topoisomerase that contributes to the condensation and segregation of most bacteria. It is formed by two dimers of the ParC and ParE subunits and has been demonstrated as the major decatenase in *E. coli* (Zechiedrich et al., 1997). Topo IV activity depends on the topology of its DNA substrate, as it is strongest on positively supercoiled DNA and shows a preference for relaxing L-braids (Crisona et al., 2000). The

regulation of its activity was proposed to be an important factor for modulating chromosome segregation as Topo IV alteration was shown to lead to an alteration of sister chromatid separation patterns (Lesterlin et al., 2012). Indeed, Topo IV is essential for correct chromosome segregation and the effects of the alteration of its activity have been studied for a long time now. Its inactivation was shown to lead to an increase in short-range contacts produced by pre-catenanes (intertwining of replicated sister-chromatids behind the fork) as well as new long-range contacts between *dif* and the rest of the chromosome (Conin et al., 2022). On the other hand, its overexpression was shown to reduce cohesion time substantially, with cohesion being two sister loci staying together after replication (Wang et al., 2008).

This activity can be regulated by different factors including MukB and SeqA that each interact with Topo IV in a different way. MukB for instance, binds to the C-terminus domain of the ParC subunit of Topo IV and enhances both its relaxation and decatenation activities as well as favors the formation of Topo IV clusters near the *ori* (Li et al., 2010; Nicolas et al., 2014; Vos et al., 2013). A study conducted by Y. Li also shows that a MukB mutation hindering its capacity to bind ParC fails to rescue a *mukB*- strain, suggesting that this interaction is essential for the activity of MukBEF in *E. coli* (Li et al., 2010).

SeqA on the other hand, was also found to interact with the ParC subunit of Topo IV but stimulates its supercoiled DNA relaxation activity as well as its conversion of catenanes to monomers (Kang et al., 2003). This interaction was later shown to stabilize cohesion *via* the antagonization of Topo IV-mediated sister resolution at the hands of SeqA (Joshi et al., 2013). An excess in SeqA however inhibited the activity of all topoisomerases. Ten Topo IV enriched regions have recently been identified through ChIP-seq assays although no consensus sequence has been found, suggesting a sequence-independent binding type for Topo IV (El Sayyed et al., 2016). An interesting discovery from the same study was that H-NS rich regions were significantly less enriched for nonspecific Topo IV binding than the rest of the chromosome, suggesting a strong negative correlation between the two. Taken together, these characteristics suggest that in addition to its individual role in chromosome organization, Topo IV could be involved in different crucial processes *via* its interactions with different cellular actors.

4.1.4. Consequences of gyrase mutations on the chromosome

Topo IV is a main actor of chromosome condensation, but it does not work alone as the alteration of factors including DNA gyrase and MukB leads to an alteration of Topo IV's activity as well. The gyrase is a type II topoisomerase and shares a lot of structural similarities with Topo IV as they are both hetero-tetramers formed by two subunits: ParC/ParE in the case of Topo IV and GyrB/GyrA for the gyrase (Mizuuchi et al., 1978). Their roles differ however as Topo IV preferentially works behind the fork to remove pre-catenanes while the gyrase is inefficient in decatenation. Instead, it is located in front of the replication fork and works to remove positive supercoils (Stracy et al., 2019).

This difference stems from gyrase's operating method: the wrapping mechanism. In contrast to the canonical mechanism used by the rest of the type II topoisomerases including Topo IV, where DNA is passed through a transient, double stranded break of another DNA molecule in an ATP-dependent manner; the wrapping mechanism consists of the C-terminal domain of GyrA wrapping DNA, thus inducing a positive crossover between the G- and T-segments and mimicking a positive supercoil (**Figure 15**) (Basu et al., 2016; Roca & Wang, 1992). An important implication of this wrapping mechanism is the gyrase working in a unidirectional manner, thus only being able to remove positive supercoils (Brown & Cozzarelli, 1979). Another implication is the ability of gyrase to introduce negative supercoils and subsequently remove positive supercoils, thus allowing it to be the only known topoisomerase to be able to introduce negative supercoils onto the DNA (Sissi & Palumbo, 2010).

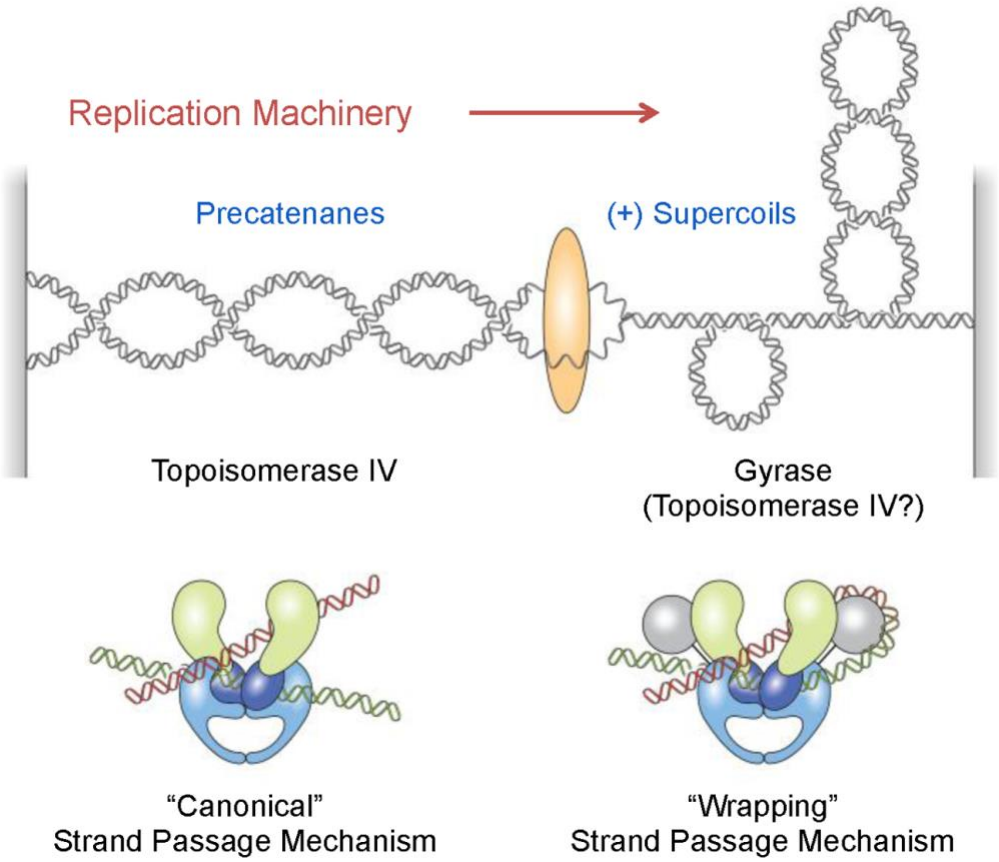

Figure 15: The cellular functions and DNA strand passage mechanisms of both Topo IV and Gyrase. Topo IV represented on the left primarily acts to resolve pre-catenanes behind the fork and unlink the newly replicated chromosomes using a canonical strand passage mechanism. Gyrase uses a wrapping strand passage mechanism to remove positively supercoil DNA ahead of the replication fork. Taken from (Ashley et al., 2017)

Several crucial cellular processes are affected by chromosomal supercoiling such as replication, transcription, and recombination. It was demonstrated that genes in the transcriptome of *E. coli* and *S. pneumoniae* were sensitive to alterations in response to gyrase inhibition (Ferrandiz et al., 2010; Peter et al., 2004). Gyrase is an essential enzyme required for the viability of bacterial cells as it is a negative regulator of replication initiation in several organisms. A study conducted in *B. subtilis* found that gyrase inhibition leads to an over-initiation of replication as the gyrase inhibits DnaA's association with *oriC*, and excessive positive supercoils ahead of the replication fork are no longer removed (Samadpour & Merrikh, 2018).

4.2. Sister-chromatid contacts

4.2.1. Sister-chromatid cohesion

Sister chromatid cohesion is the phenomenon that holds newly replicated sister chromatids together and therefore delays their segregation by several minutes. This process is essential in eukaryotes for both correct segregation and DNA repair as it makes sure that the chromosomes remain tightly aligned until the onset of mitosis (Figure 16) (Nasmyth & Haering, 2009). Cohesion is regulated by the SMC complexes that were discussed above (i.e., Smc1 and Smc3) (Haering et al., 2002).

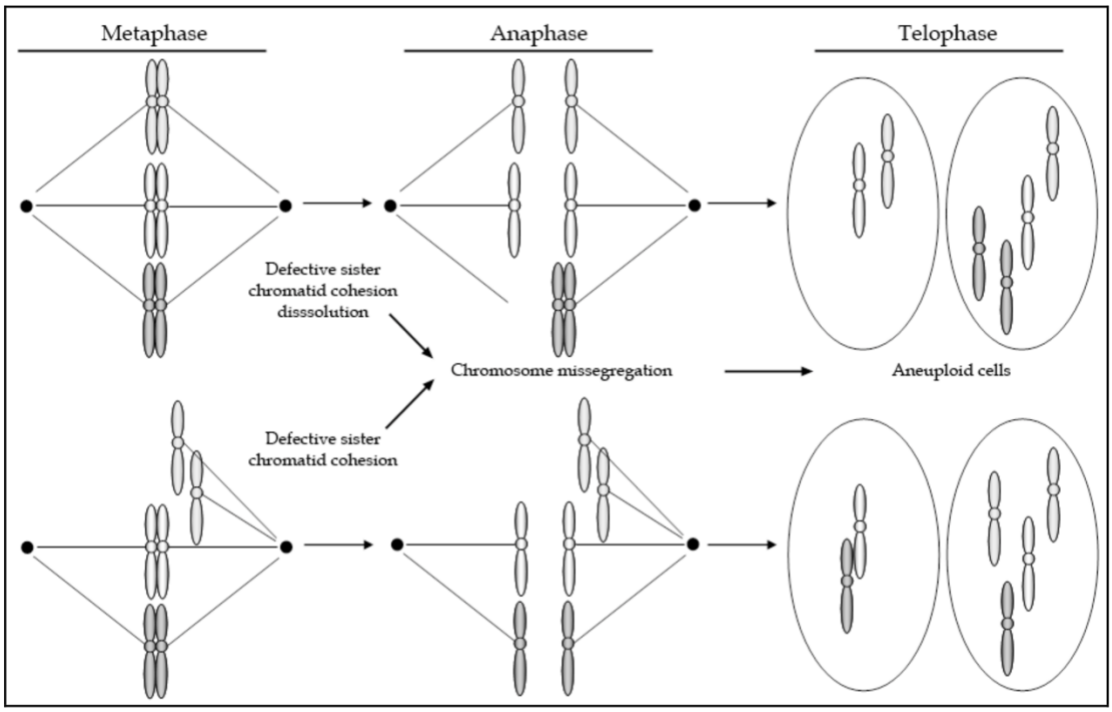

Figure 16: A schematic representation of defective sister chromatid cohesion during metaphase leading to missegregation during anaphase, and therefore aneuploidy in eukaryotic cells during telophase. Taken from (Watrin & Prigent, 2012).

We still have a lot to learn when it comes to cohesion in prokaryotic cells and even though the subject has been studied for several years now, a lot of its mechanics remain obscure. The exact role of sister-chromatid contacts is still unknown even though it is established that it has functional implications such as ensuring the availability of the sister chromatid to repair newly synthesized damaged DNA near the replication fork (Watrin et al., 2006). It has been demonstrated that topological entanglement is implicated in facilitating sister chromatid

cohesion in all three domains of life: bacteria, archaea, and eukaryotes through pre-catenanes (the sister chromatids are intertwined during the replication process), catenanes (the sister chromatids are intertwined outside of the replication process), or hemi-catenanes (the sister chromatids are linked by single-strand interwinding) (Espeli & Marians, 2004). These links are undone by type II topoisomerases, mainly the bacterial topoisomerase Topo IV. It has been shown that the deletion of Topo IV prevents the correct chromosome segregation in *E. coli* though the cells appear to finish replication, therefore implying that its action is needed for sister chromatid separation throughout the replication process, rather than at replication termination only (Wang et al., 2008). The same study has shown as well that the inactivation of Topo IV has little influence on the progression of the replication fork, although the segregation of *ori1* is severely impaired. It is important to note however that Topo IV cannot account to the entirety of sister-chromatid cohesion on its own, and that other factors are most probably involved. One main candidate for the short-term cohesion remaining is the *E. coli* SMC-like complex MukBEF.

4.3. High-throughput whole genome analysis of Sister Chromatid Contacts (Hi-SC2)

4.3.1. A recombination assay to follow sister-chromatid interactions

As the interest for this phenomenon grew, teams rushed to find a way to follow the sister-chromatid contacts rather closely. In 2008, Adachi et al conducted a series of microscopy and flow cytometry assays to investigate cohesion at *oriC* in *E. coli* cells and found that the *oriC* as well as the *ter* sister copies were cohesive (Adachi et al., 2008). In 2011, comprehensive assays done by Joshi et al showed that at two unique regions, sister chromatids remain closely juxtaposed much longer than other loci, thus comprising late-splitting intersister snaps (Joshi et al., 2011). These sister chromatids then separate synchronously as part of the overall nucleoid reorganization. This study comprised of microscopy assays helped bring to light several aspects of the sister-chromatid contacts as it focused on six different loci: three near the *oriC* domain and three near the *ter* domain, suggesting that the delay between the replication of a locus and its segregation depends on the locus itself. A year later, Lesterlin et al managed to reveal those interactions using a site-specific recombination assay (Lesterlin et al., 2012). Their assay is based on the Cre/*loxP* site-specific recombination system of the

bacteriophage P1. They interrupted the *lacZ* gene with two *loxP* sites separated by 21 base pairs only, this short distance did not allow them to recombine with each other as the minimal distance required is reportedly 82 base pairs (Hoess & Abremski, 1985). Therefore, the only way for the reconstitution of an active *lacZ* gene is an intermolecular recombination of two *loxP* sites on different sister chromatids that were located spatially close to one another. They found that these recombination events did not occur after the full replication and segregation of the chromosomes, implying that this phenomenon was strictly dependent on the replication of the locus. While this method has held its own for many years, the techniques that the scientific community has at hand have drastically improved and we can now follow the sister-chromatid contacts along the genome at a higher resolution *via* an assay called High-throughput whole genome analysis of Sister Chromatid Contacts, hereafter referred to as Hi-SC2.

4.3.2. Hi-SC2: the mechanisms behind the assay

As suggested by the name, the Hi-SC2 assay allows us to follow sister chromatid contacts along the genome at a very high resolution. Developed by our laboratory based on both Tn-seq approaches and site-specific recombination assays, it uses transposons to insert site-specific recombination sites at random evenly distributed positions on the chromosome in a library of cells harboring the cognate recombinase gene under a tight inducible promoter, and follow their recombination after induction of the expression of the recombinase (Espinosa et al., 2020). Two distinct site-specific recombination systems were used: (Cre/*loxP*) and (XerCD/*dif1*).

A. <u>The Cre/*loxP* recombination system</u>

Cre does not depend on any host factor to recombine *loxP* sites. Therefore, the Cre/*loxP* system can serve to monitor the frequency of contacts between sister loci as soon as they are replicated. In brief, the Cre recombinase gene was introduced in the genome of *V. cholerae* under the control of the arabinose promoter P_{BAD} to only induce the recombinase at the time of the experiment (Ding & Tan, 2017). Two *loxP* sites separated by 21 base pairs were inserted into a Mariner transposon flanked by the inverted repeats of the transposon (*Himar*). The short distance between the two *loxP* sites prohibited any intramolecular recombination event **(Figure 17A)**. The transposon was randomly inserted in the designated strains with a single

insertion per genome and with an insertion rate high enough to cover the length of the genome in an even distribution. When induced with arabinose, intermolecular recombination can occur when the sites present on two chromatid sisters are within reach from one another long enough for the recombination to take place **(Figure 17B)**. This results in a chromatid sister with one *loxP* site and another with three *loxP* sites, which are subsequently converted into one site due to intramolecular recombination. The DNA is then harvested, and libraries are constructed as described in the materials and methods of this thesis, and the samples are sequenced using paired-end sequencing to monitor the recombination status of each DNA fragment as well as its position on the genome **(Figure 17C)**. The data can be plotted as per **Figure 17D** with the excision frequency of the reporter of choice at a specific locus plotted against the genomic position of the locus.

B. <u>The XerCD/*dif1* recombination system</u>

The XerC/D/*dif* siste-specific recombination system was used in the same way as the Cre/*loxP* site-specific recombination system. The main difference between XerCD and Cre recombination is that the activity of XerCD is regulated by a cell division protein, FtsK. FtsK is an essential part of the cell division machinery. In addition, it assembles into an hexameric DNA pump in the division septum, which translocates chromosomal DNA from one cell compartment in an oriented manner. Translocation is oriented by repeated motifs that point for the origin of replication to the terminus: the KOPS (Bigot et al., 2005, 2006). FtsK is only active during septum constriction, therefore limiting the action of XerC/D to the *dif* sites (Demarre et al., 2014; Val et al., 2008; Galli et al., 2017). As it was for Cre, we used strains in which the XerC/XerD genes were placed under the control of the arabinose promoter P_{BAD} to only induce the recombinase at the time of the experiment. The *dif1*-cassettes consisted of two *dif1* sites separated by 27 base pairs. This distance was short enough to prevent intramolecular recombination events (Demarre et al., 2014).

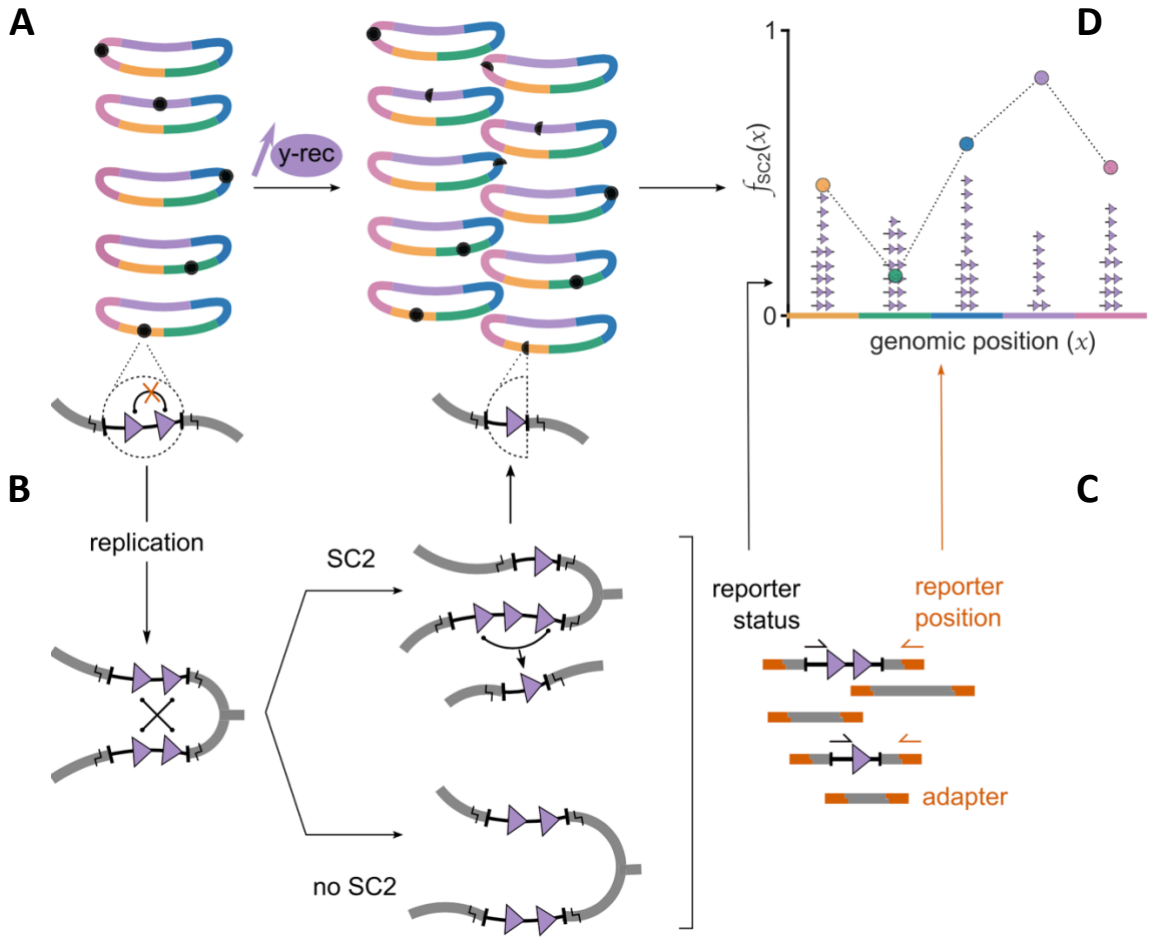

Figure 17: The design of the Hi-SC2 assay. The *loxP* sites are represented by purple triangles. **(A)** Two loxP sites are inserted in a single position on the genome *via* a transposon, the inserted *loxP-loxP* cassette is represented by a black circle. The purple arrow and "y-rec" symbolize the recombinase being induced using arabinose. The recombined cassette is represented by a black half-circle. Intramolecular recombination cannot occur due to the short distance separating them. **(B)** Recombination events occur when two *loxP-loxP* cassettes are close enough due to sister-chromatid contacts (SC2), not when the sister-chromatids are too far apart (no SC2). **(C)** Adapters, here in orange, are ligated to both sides of samples during the construction of the libraries and allow for paired-end sequencing to follow on the reporter status (SC2 or no SC2) on one hand, and the reporter position on the genome on the other hand. **(D)** An example of how the Hi-SC2 data is plotted with the frequency of excision of the reporter as a function of its genomic position. The number of recombined reads obtained from the paired-end sequencing per locus is plotted to follow the rate of sister-chromatid contacts along the genome. Taken from (Espinosa et al., 2020).

4.3.3. Hi-SC2: a new and improved view of Sister Chromatid Contacts

The Hi-SC2 assays were performed on the model organism *Vibrio cholerae,* and the results were very interesting. What they observed was a profile with a varying recombination frequency, supporting the previous model that states that sister chromatid cohesion is not

constant along the genome (Joshi et al., 2011). They found different types of cohesion patterns (**Figure 18**).

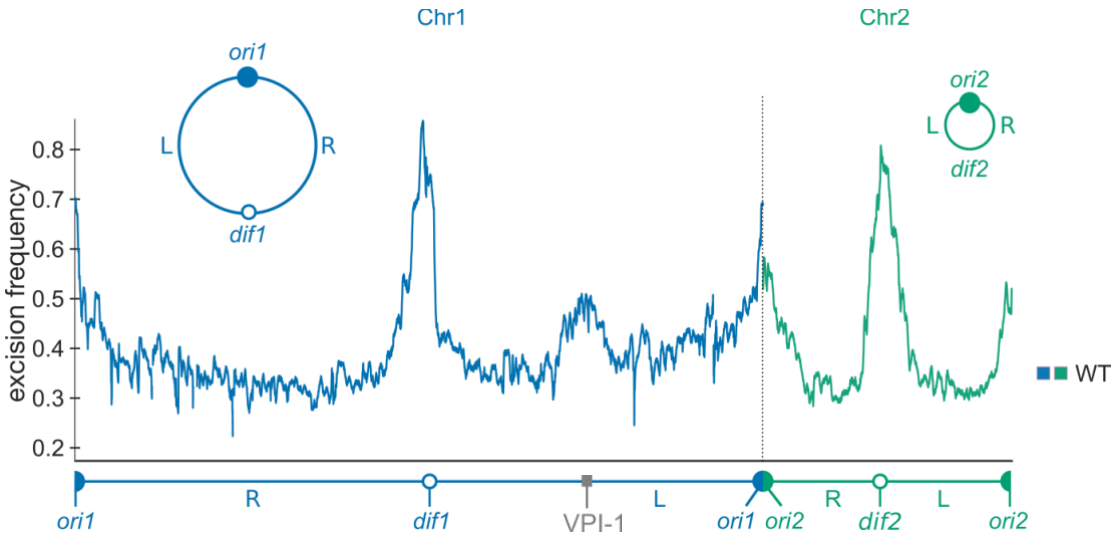

Figure 18: Hi-SC2 profile of a *V. cholerae* WT strain. Chromosome one is represented in blue, while chromosome two is represented in green. The excision frequency of the *loxP* sites is plotted according to their position on the genome. Below the X axis is a linear map of each chromosome with the *oriC* and *dif* domains (1 and 2 for each chromosome). R and L indicate the right and left arm of the chromosomes. The two chromosomes are separated by a dotted line, and a schematic representation of each chromosome is displayed as well. The excision frequency of the loxP cassettes is plotted at a 10-kbp window, which permits to see both types of cohesion patterns. Adapted from (Espinosa et al., 2020).

The profile obtained clearly shows a high amount of *loxP* excision frequency along both origins and termini of replication, as well as a bump on the left arm of chromosome 1, that corresponds to the pathogenicity island VPI-1. These results suggest that sister-chromatid cohesion is significantly higher around *oriC* and *ter*, implying that cohesion takes place at the beginning and the end of the replication process. As mentioned earlier in this thesis, VPI-1 is silenced by the NAP H-NS and a deletion of the protein led to a decrease in the surrounding area of VPI-1 (Espinosa et al., 2020). The Hi-SC2 method uncovered a new function of H-NS as an active player in cohesion in HGT regions, thus allowing us to explore sister-chromatid cohesion and its potential candidates in great detail.

Objectives

We have established that sister-chromatid cohesion varies along the chromosome in a non-homogeneous manner, as several patterns can be observed. These patterns are reflected by peaks and drops in the Hi-SC2 profile of the strains: we observe in fact a peak of cohesion around the origin and the termini of replication, as well as on the pathogenicity island of chromosome I: VPI-1.

As discussed earlier, it has been shown *in E. coli* that the cohesion responsible for the variation of segregation speed is modulated by Topoisomerase IV, a major decatenating enzyme (Wang et al., 2008). One of the identified partners of this decatenase is the SMC complex, MukBEF (Nicolas et al., 2014). Cells carrying a *mukB* deletion show a production of anucleate cells, and a mispositioned origin of replication. Chromosome segregation is impaired, and therefore sister chromatid cohesion is increased overall. The Topo IV-MukBEF interaction is regulated by MatP, which seems to displace MukBEF from the terminus of replication, facilitating the association of the MukBEF complex with the origin of replication (Nolivos et al., 2016). I therefore decided to investigate the role of MukB, MatP, and the partitioning system in the formation of the general patterns of cohesion in *V. cholerae*.

The first part of the results will focus on MatP and its action in the termini of replication. A series of various experiments were performed in collaboration with other members of the team to clarify MatP's role(s) in the *ter* domain, and whether he is the sole actor responsible for its cohesion. These investigations were done in a series of strains, some of them with rearranged chromosomes.

The roles of MukB and the partition system will be studied next as they are known actors of segregation. The extent of their collaboration will be explored as well, notably whether they are mutually exclusive and whether they operate together. These studies will make up the second part of the results section of this manuscript.

Each section of the results will be treated separately, and this work will be concluded by a general discussion followed by the perspectives for the projects that were presented.

Results

Chapter 1: Cohesion in the ter domain: the extent of MatP's involvement

Newly replicated sister copies of the *ter* domain of most bacterial chromosomes co-localize at mid-cell at the time of cell division. Fluorescence microscopy assays showed that sister copies of the *ter* domain of the chromosome 1 of *V. cholerae* (*ter1*) and chromosome 2 (*ter2*) migrate from the new pole of the cell to mid-cell before their replication **(Figure 19A and B)** (David et al., 2014; Demarre et al., 2014). Sister copies of *ter1* were further found to remain colocalized at mid-cell until after the initiation of septation **(Figure 19B)**. Sister copies of *ter2* were found to separate before the initiation of septation but they remained in close proximity to the septum **(Figure 19B and C)** (Demarre et al., 2014). The termination of Chr1 and Chr2 replication is synchronous. Therefore, a first suspect for the observed cohesion of newly replicated *ter1* and *ter2* copies was their actual timing of replication.

In addition, the *E. coli* Macrodomain terminus organizer protein, MatP, was shown to keep sister copies of the *ter* domain of the *E. coli* chromosome together until cell division (Espéli et al., 2012). It was also proposed to ensure the ordered segregation of loci within the *ter* domain (Stouf et al., 2013a). The genome of *V. cholerae* encodes a homologue of *E. coli* MatP. Fluorescence microscopy and site-specific recombination assays showed that *V. cholerae* MatP delayed the separation of *ter1* sister copies until cell division, and helped maintain *ter2* sister copies close to mid-cell during and after cell division (Demarre et al., 2014). Therefore, *V. cholerae* MatP was a second suspect for the observed cohesion of newly replicated *ter1* and *ter2* copies.

Along with Elisa Galli and Elena Espinosa, I set out to investigate the respective roles of MatP and the timing of replication in the cohesion of *ter1* and *ter2* behind replication forks and what mechanisms could be responsible for the different behaviors of sister copies of *ter1* and *ter2* during cell division.

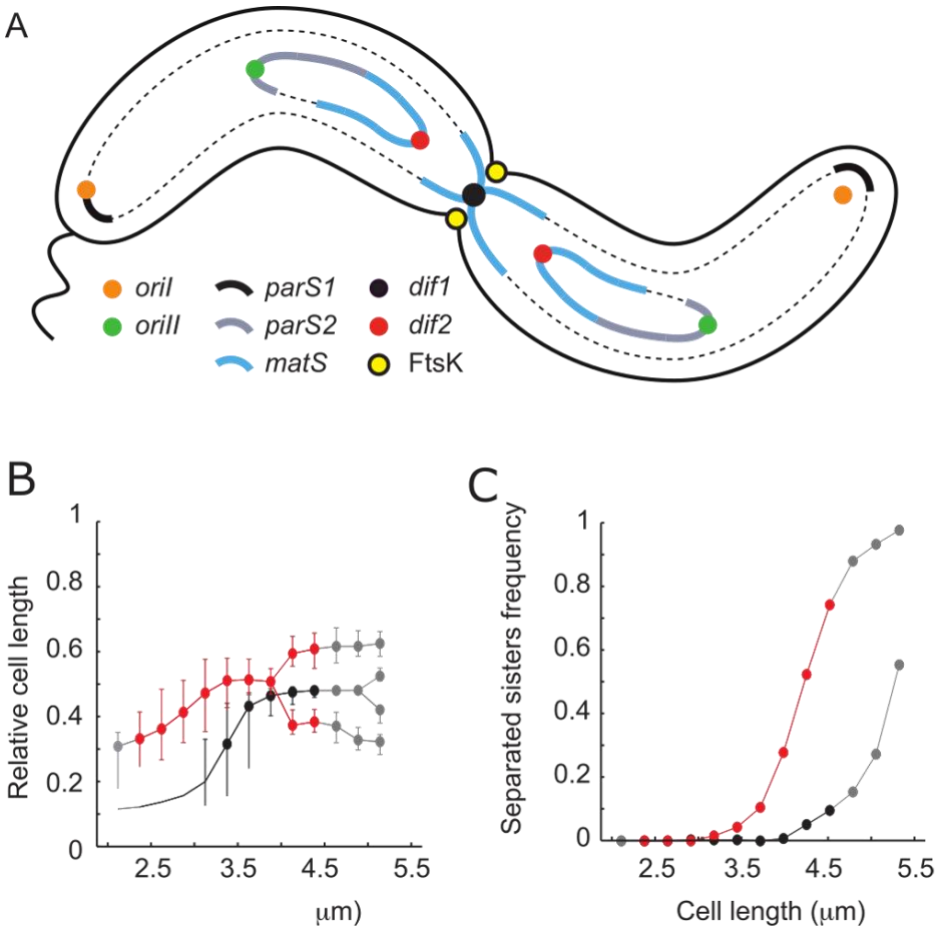

Figure 19: (A) Schematic representation of the two sister-chromatids of each *V. cholerae* chromosome (dotted lines) during septation. *Ori1* is represented by an orange circle and *ori2* by a green circle. *dif1* and *dif2* are represented by black and red circles respectively. The regions where *matS* sites are located are depicted by a blue line. The regions where *parS1* and *parS2* sites are located are shown in black and green lines respectively. Ftsk is represented by a yellow circle. **(B)** Relative position of *dif1* (in black) and *dif2* (in red) along the long axis of the cell as a function of cell length in WT cells. **(C)** Frequency of cells with separated *dif1* (in black) and *dif2* (in red) sisters as a function of cell length in WT cells. The plain red and black lines show the data for the bins containing at least 30 cells while the grey lines show the data for bins containing 3 to 29 cells. Taken from (Demarre et al., 2014).

1. Cohesion at the *ter* domain behind the replication fork

1.1. Replication termination is not responsible for cohesion at the *ter* domain

In order to investigate the potential role of replication termination in the cohesion of *ter* domains, we performed the Hi-SC2 assay in a synthetic *V. cholerae* mono-chromosomal strain, MCH1, which was engineered by the Mazel laboratory (Val et al., 2012). MCH1 was

built by integrating Chr2 into *ter1*. As a result, the *ter1* domain was split in two, with each half domain of *ter1* being located in a different replication arm, at ~1.5 Mbp from *ori1* and ~0.5 Mbp from *ter2* (Figure 20). In addition, *ori2*, the parAB2 partition genes and *dif1* were deleted in the process. Replication of the MCH1 chromosome was shown to initiate at *ori1* and terminate in *ter2* (Val et al., 2012).

As it had been observed on the two chromosomes of WT *V. cholerae* cells, we found that cohesion was elevated in the replication terminus region of the MCH1 chromosome, *ter2*, the replication origin region of the MCH1 chromosome, *ori1*, and around VPI-1 (**Figure 20**). However, we also found that cohesion was elevated at the positions corresponding to the two halves of *ter1,* 0.5 Mbp from the actual replication terminus of the MCH1 chromosome. This result suggested that the elevated cohesion in the *ter1* region was not due to its timing of replication but was linked to its genetic content.

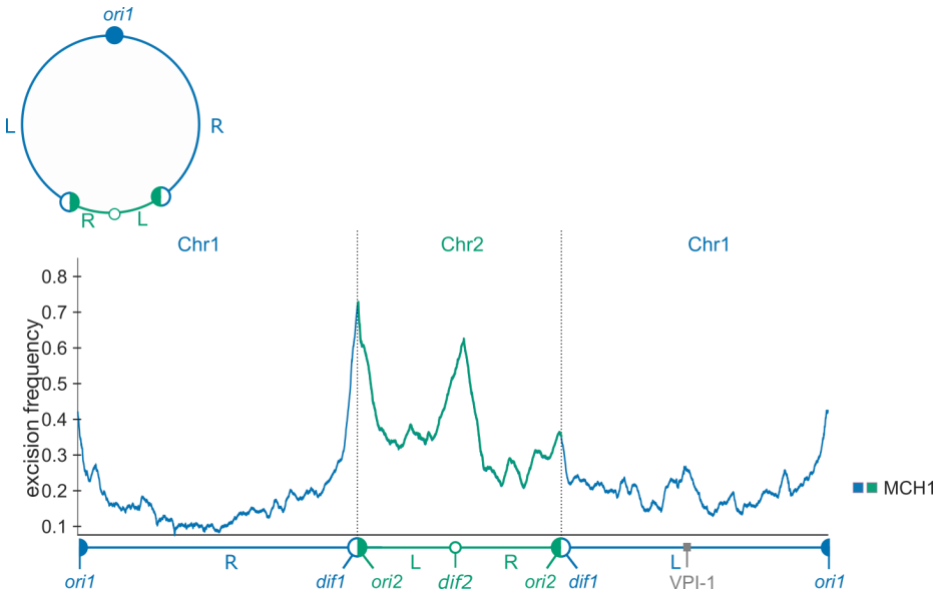

Figure 20: Hi-SC2 assay performed on a MCH1 strain. Chr1 and Chr2 DNA sequences are represented in blue and green respectively. The top panel contains a schematic representation of the rearranged chromosome plotted using a 40kb sliding window. *Ori1* and *ori2* are represented by blue and green full circles respectively, while *dif1* and *dif2* are represented by blue and green empty circles respectively.

1.2. Correlation between the local concentration of MatP and the Hi-SC2 profile at *ter1* and *ter2*

As stated in previous sections, *E.* coli MatP is known to specifically bind to *matS* sites enriched in the *ter* of the *E. coli* chromosome. Before I arrived in the lab, ChIP-seq experiments had shown that the *V. cholerae* homologue of *E. coli* MatP bound to specific sites with a DNA motif enriched in both *ter1* and *ter2* **(Figure 21A)**. The consensus DNA binding motif of *V. cholerae* MatP was found to be similar to the 13-mer GTGACRNYGTCAC *matS* binding motif found of *E. coli* MatP (Mercier et al., 2008). The sequence logo for *V. cholerae* MatP is in **(Figure 21A)**. Intriguingly, however, there was also a *matS* site close to *ori1* and another near *ori2* **(Figure 21B)**. Strikingly, plotting the ChIP-seq data at the same resolution as the Hi-SC2 profile (40kb sliding window) showed a correlation between the concentration of MatP and the cohesion of the *ter* regions of both chromosomes, in agreement with the idea that MatP is a major actor of the cohesion of the *ter* domains **(Figure 21C-21D)**.

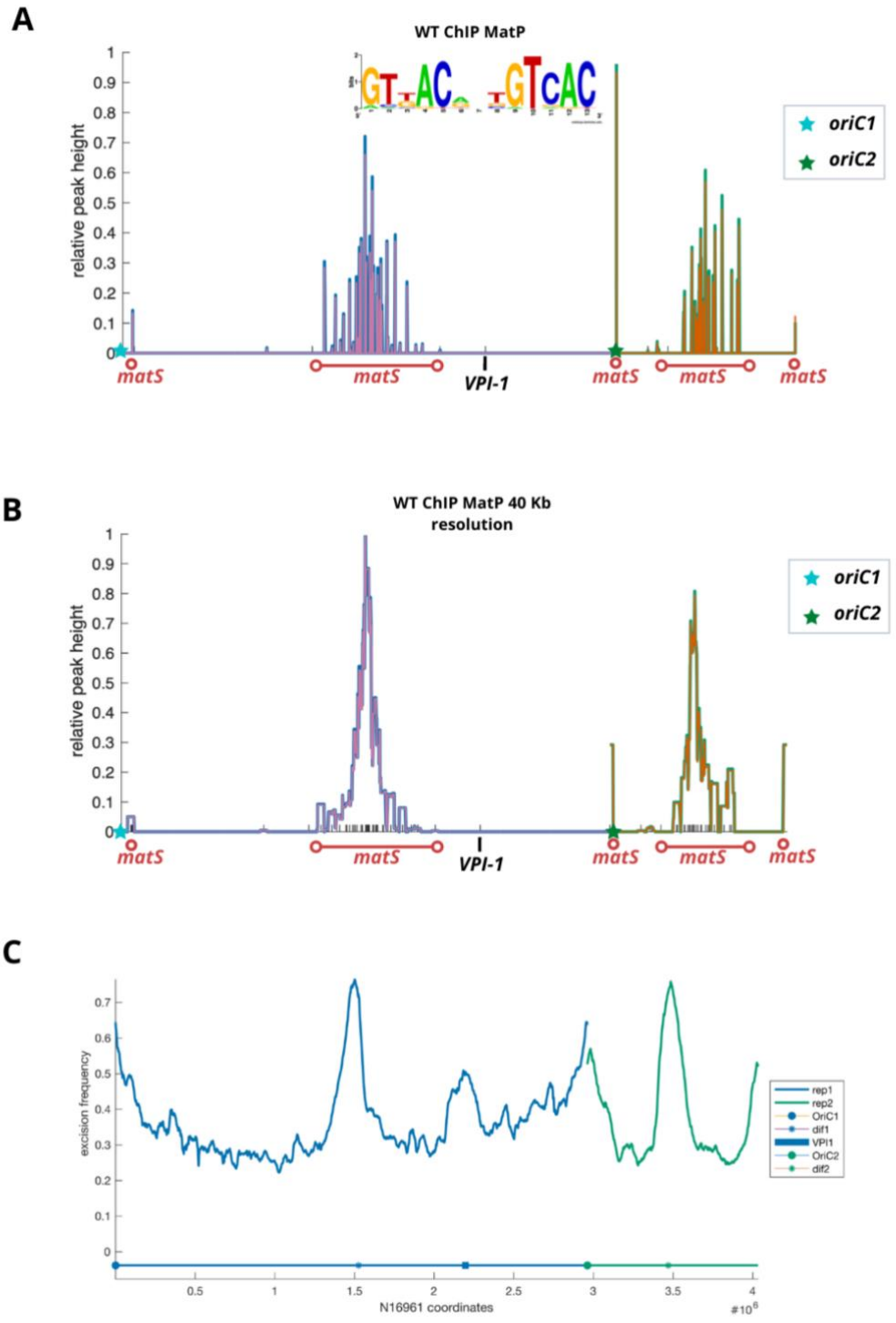

Figure 21: (A-B) ChIP-seq assay of MatP performed on WT cells. Chr1 is represented in purple and Chr2 is represented in orange. The unique copy of MatP is tagged with the 3X FLAG peptide. The relative peak height is plotted against the length of the genome. *OriC1* and *oriC2* are represented by a blue and green star respectively. The *matS* sites are represented by a clear red circle when alone, and a red line when grouped together. MatP binds on the *matS* sites around the *ter* region of each chromosome. The ChIP-seq assay is plotted at a 1kb resolution in **21A** and at 40kb resolution in **21B**. The top panel in **21A** contains a logo of *V. cholerae* MatP done using WebLogo (Crooks et al., 2004). **(C)** Hi-SC2 assay

performed on *V. cholerae* WT cells using the Cre recombinase, with the reporter excision frequency on the y axis and the reporter coordinates on the genome on the x axis. Chr1 and Chr2 are represented in blue and green respectively. *OriC1* and *oriC2* are represented by a blue and green circle respectively, while *dif1* and *dif2* are represented by a blue and green star respectively. VPI-1 is represented by a blue square.

To confirm this idea, I investigated the correspondence between the ChIP-seq profile of MatP and the sister-chromatid contacts profile in strains carrying two rearranged genomes: the MCH1 strain and a genetically engineered *V. cholerae* strain with Equal-Sized Chromosomes (ESC2), from the Mazel Lab (Val et al., 2012). One of the two chromosomes of ESC2 harbours *ori1, VPI-1,* and *ter2*; the second chromosome harbours *ori2* and *ter1* (Val et al., 2012). The results were striking as we observed a correlation between the regions of binding of MatP and the regions where sister-chromatid contacts were highest in both strains **(Figure 22)**.

In MCH1, MatP bound to the *matS* sites in both *ter2* and the two split in half *ter1* domains. The ChIP-seq peaks were reminiscent of those of the WT strain, with the *ter2* peak appearing between the two *ter1* halves but flipped. Interestingly, the ChIP-seq profile resembled the Hi-SC2 profile as the three eminent peaks stand from the tallest to the smallest from left to right in both assays **(Figure 20 and 22A)**. We further noted a correlation between the height of the MatP ChIP profile peaks and the height of the Hi-SC2 sister-chromatid cohesion peaks. Indeed, the highest peaks of sister-chromatid contacts were located at both *ter1* and *ter2*, where the highest ChIP profile peaks are situated **(Figure 20 and 22A)**.

In the ESC2 strain, we observed a much thinner peak at the *ter* of the first chromosome along with a larger, much higher peak on the *ter* of the second chromosome **(Figure 22B)**. This result fitted with the sister-chromatid contacts profile as the cohesion peak of the *ter* of the first chromosome was much thinner than that of the second chromosome **(Figure 22C)**. The difference in width was explained by the smaller number of *matS* sites in *ter2* than *ter1.*

Taken together, these results suggested a possible direct correlation between the presence and local concentration of MatP and the peaks of cohesion observed on the *ter* domains of each chromosome in *V. cholerae*.

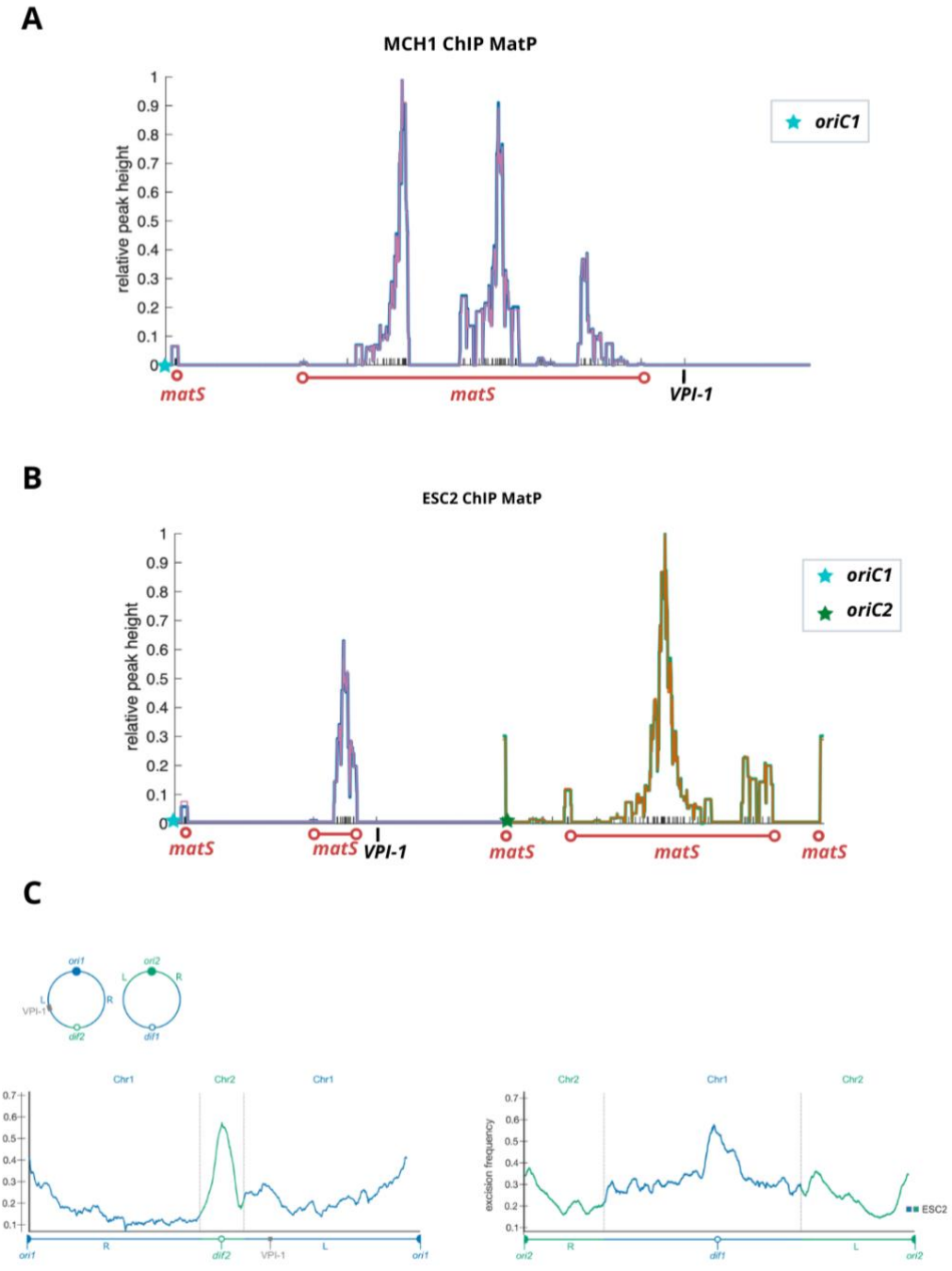

Figure 22: (A-B) ChIP-seq assay of MatP. Chr1 is represented in purple and Chr2 is represented in orange. The unique copy of MatP is tagged with the 3X FLAG peptide. The relative peak height is plotted against the length of the genome. *OriC1* and *oriC2* are represented by a blue and green star respectively. The *matS* sites are represented by a clear red circle when alone, and a red line when grouped together. MatP binds on the *matS* sites around the *ter* region of each chromosome. The ChIP-seq assay is performed on MCH1 cells in **22A** and on ESC2 cells in **22B**. **(C)** Hi-SC2 assay performed on

V. cholerae ESC2 cells using the Cre recombinase, with the reporter excision frequency on the y axis and the reporter coordinates on the genome on the x axis. Chr1 and Chr2 are represented in blue and green respectively. *Ori1* and *ori2* are represented by blue and green full circles respectively, while *dif1* and *dif2* are represented by blue and green empty circles respectively.

1.3. MatP is not the major factor in the cohesion at *ter* domains during replication

The correlation observed above between the presence of MatP and the peaks of sister-chromatid contacts at the *ter* domain fit with the hypothesis that MatP could be responsible for the cohesion at the *ter* domains behind the replication fork. To further investigate this possibility, we performed the Hi-SC2 assay in a strain lacking *matP* **(Figure 23)**. We observed a slight decrease in sister-chromatid contacts along both chromosomes. This decrease was more marked towards their terminus regions, as expected since almost all the *matS* sites are grouped together in the *ter* domains. However, the decrease in the frequency of sister-chromatid contacts of the two *ter* domains in the absence of MatP was very modest. Those results suggested that MatP was not the major factor in the cohesion at *ter* domains during replication.

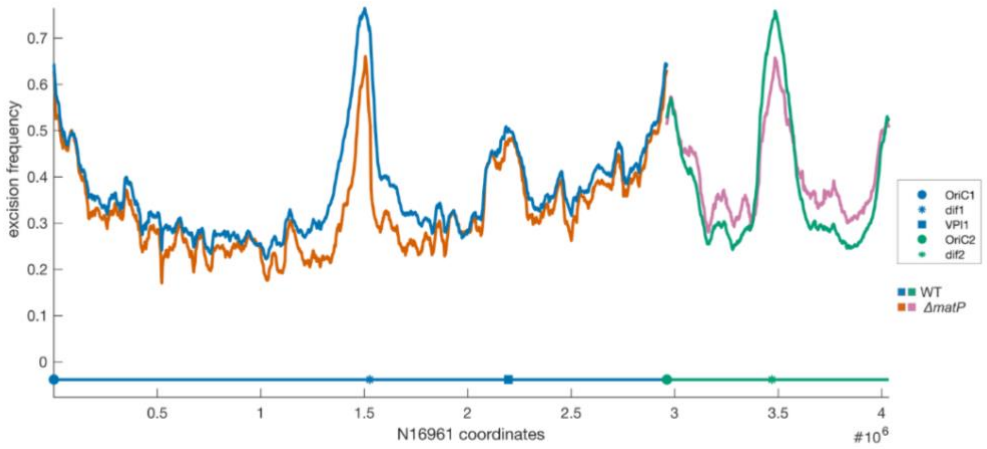

Figure 23: Hi-SC2 assay performed on *V. cholerae* WT (blue and green) and Δ*matP* (orange and pink) cells using the Cre recombinase, with the reporter excision frequency on the y axis and the reporter coordinates on the genome on the x axis. *OriC1* and *oriC2* are represented by a blue and green circle respectively, while *dif1* and *dif2* are represented by a blue and green star respectively. VPI-1 is represented by a blue square.

2. Cohesion at the *ter* domain at cell division

2.1. Cohesion between sister copies of the extreme *terminus* of replication of Chr1 and Chr2 during cell division

The above result was surprising since both fluorescent microscopy observations and the sister-chromatid contacts assays based on the XerC/D recombination system instead of the Cre recombinase had shown that MatP played an essential role in maintaining sister *ter1* and *ter2* sites together at mid-cell during cell division (Demarre et al., 2014). As mentioned earlier, XerD is dependent on the activity of FtsK, which is only active during septum constriction therefore limiting the action of XerC/D to the *dif* sites (Demarre et al., 2014; Val et al., 2008; Galli et al., 2017).

To confirm the role of MatP in the maintenance of sister *ter1* and *ter2* regions together at mid-cell during cell division, we decided to analyse sister-chromatid contacts using the XerC/D recombinase at a genomic scale. To do so, a short *dif1* cassette was inserted inside the transposon that had been used for the *loxP* cassette (Espinosa et al., 2020). Transposition was then used to insert a *dif1* cassette at different genomic random positions in strains in which XerC and XerD were expressed from an arabinose promoter.

We first performed the Hi-SC2 assay on a strain with a WT genome arrangement. The *dif1*-cassette excision frequency profile we obtained was very different from the *loxP*-cassette profile **(Figure 24A)**. We observed two peaks of sister-chromatid contacts: one per chromosome terminus, with *ter1* showing a much higher peak than *ter2*. The rest of the genome was flat as expected since the *ter1* domain is the only region in proximity of the cell division apparatus, and therefore of FtsK. However, these peaks were very sharp, and much thinner than the regions where FtsK was supposed to act. These observations suggested that only the extreme part of the *ter* domains were cohesive and remained at mid-cell during cell division. In addition, we observed that the peak of sister-chromatid contacts was significantly lower on *ter2*, indicating that this cohesion is much less frequent in the case of Chr2 than Chr1, which fit with the microscopic observations made by Demarre et al.

2.2. The genetic composition of *ter1* specifies the elevated frequency of *dif1* cassette excision

It was proposed in *E. coli* that the delayed segregation of the extreme terminus of the sister-chromatids was linked to the orderly removal of MatP from the *ter* when it translocated (Stouf et al., 2013a). To differentiate whether in *V. cholerae* the elevated frequency of *dif1* cassette excision in the middle of *ter1* was linked to the timing of replication, the orderly segregation of the terminus region by FtsK, or to the genetic composition of the *ter1* domain, we analyzed the *dif1*-cassette sister-chromatid contacts profile in MCH1. We observed elevated frequencies of cassette excision in the middle of *ter2*, which corresponds to the terminus of replication of the MCH1 chromosome **(Figure 24B)**. However, we also observed highly elevated excision frequencies in one of the two halves of the split *ter1* domain. This region is outside the replication terminus and is not the last region segregated by FtsK. This result suggested that sister-chromatid contacts during cell division were linked to the genetic content of *ter1*.

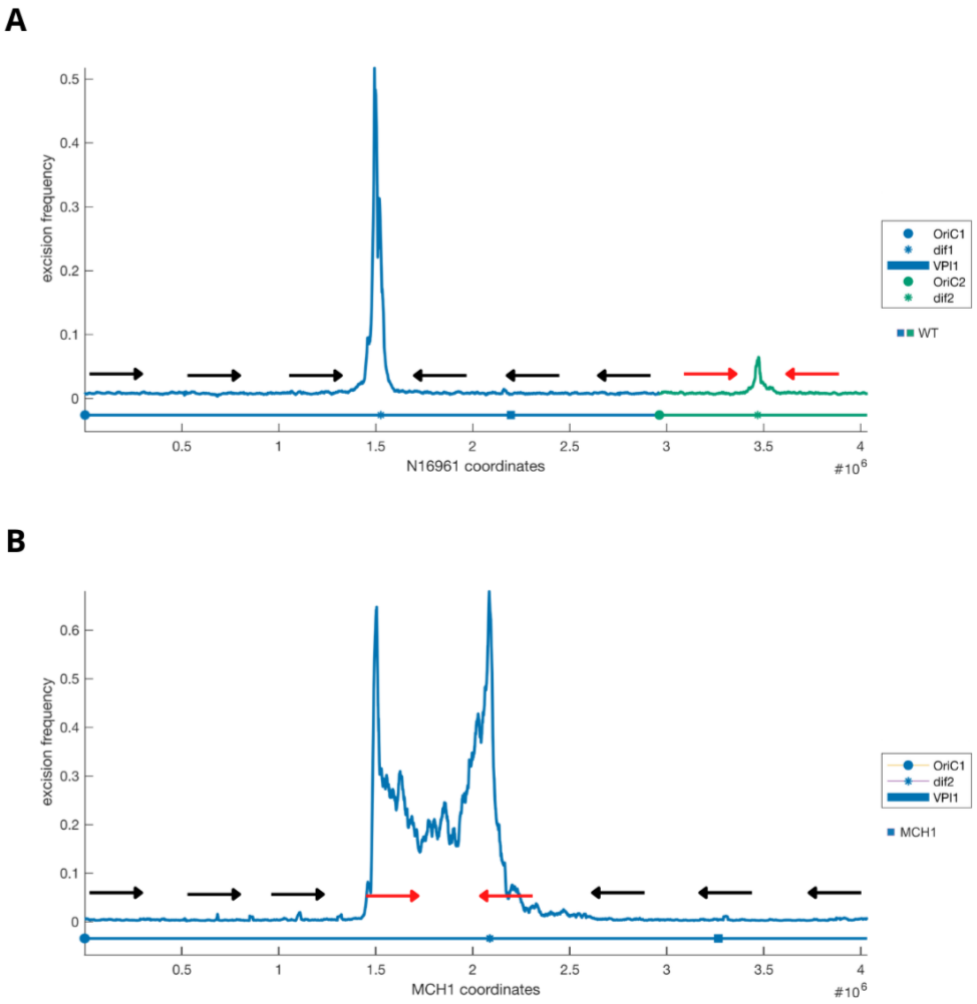

Figure 24: (A) Hi-SC2 assay performed on *V. cholerae* WT cells using the XerC/D recombinase, with the reporter excision frequency on the y axis and the reporter coordinates on the genome on the x axis. Chr1 and Chr2 are represented in blue and green respectively. *OriC1* and *oriC2* are represented by a blue and green circle respectively, while *dif1* and *dif2* are represented by a blue and green star respectively. VPI-1 is represented by a blue square. The arrows represent the direction of the FtsK-Oriented Polar Sequences (KOPS): black for Chr1 and red for Chr2. **(B)** Hi-SC2 assay performed on *V. cholerae* MCH1 cells using the XerC/D recombinase, with the reporter excision frequency on the y axis and the reporter coordinates on the genome on the x axis. *OriC1* is represented by a blue circle while *dif1* is represented by a blue star. VPI-1 is represented by a blue square. The arrows represent the direction of the FtsK-Oriented Polar Sequences (KOPS): black for Chr1 and red for Chr2.

2.3. MatP is responsible for sister-chromatid contacts of the *ter* domains at cell division

After establishing that sister-chromatid contacts of the *ter* domains at cell division was linked to its genetic context, we decided to further investigate the role of MatP in keeping the sister-copies of *ter1* together. The first step was to perform the Hi-SC2 assay on a strain

lacking *matP* **(Figure 25)**. The profile obtained *via* the XerC/D recombinase shows a drastic effect in sister chromatid contacts at *ter1*, therefore solidifying our hypothesis where MatP keeps the two sister copies of *ter1* together during septum constriction until cell division. The peak of cohesion of *ter2* disappeared in the Δ*matP* strain, hinting towards an involvement of MatP on the cohesion of the sister copies of *ter2* as well.

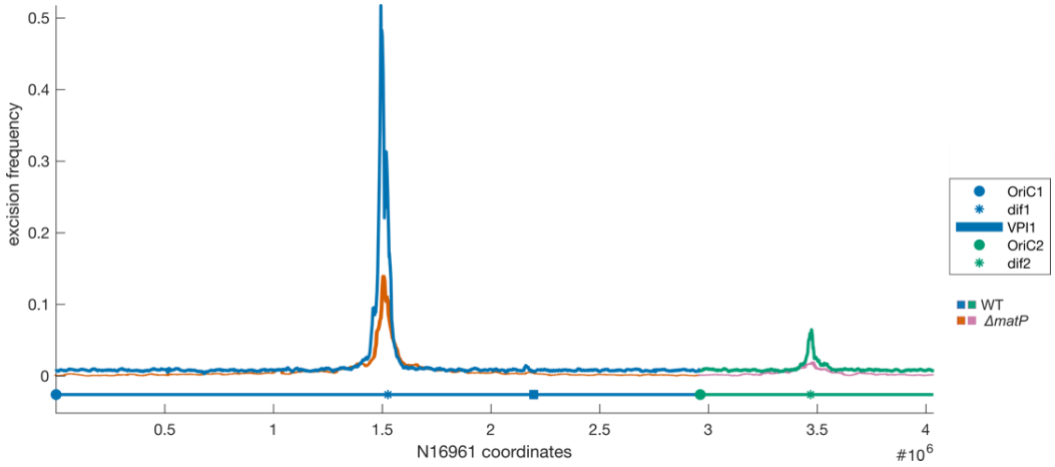

Figure 25: Comparison of the Hi-SC2 assay profiles performed on *V. cholerae* WT cells (blue and green) and Δ*matP* cells (orange and pink) using the XerC/D recombinase, with the reporter excision frequency on the y axis and the reporter coordinates on the genome on the x axis. *OriC1* and *oriC2* are represented by a blue and green circle respectively, while *dif1* and *dif2* are represented by a blue and green star respectively. VPI-1 is represented by a blue square. This assay was performed using the turbidostat.

2.4. The difference in the behavior of the *ter* domains is due to differences in the density of the *matS* sites

The difference between *ter1* and *ter2* in WT cells remained to be understood, and why only one of the halves of the split *ter1* region showed increased sister-chromatid contacts at cell division. We hypothesized that it was linked to relative density of MatP bound to those different regions. To test this hypothesis, we first performed the Hi-SC2 assays in two strains in which the *matS* arrangement had been modified.

First, we analyzed the *dif1* cassette excision frequency profile in a strain harboring an inversion of ~165 kilobases in the *ter1* region (between VC1616 at 1.3 Mb and *dif1* at 1.5 Mb). The *dif1*-cassette Hi-SC2 assay performed on this strain did not show a change in the height

of the peak at *ter1*. However, the peak profile was inverted **(Figure 26A)**. The small peak at *ter2* remained unchanged. The *dif1*-cassette Hi-SC2 profile correlated with the profile of the ChIP-seq of MatP as the shape of the peaks of binding of MatP at *ter*1 are inverted as well **(Figure 26B)**.

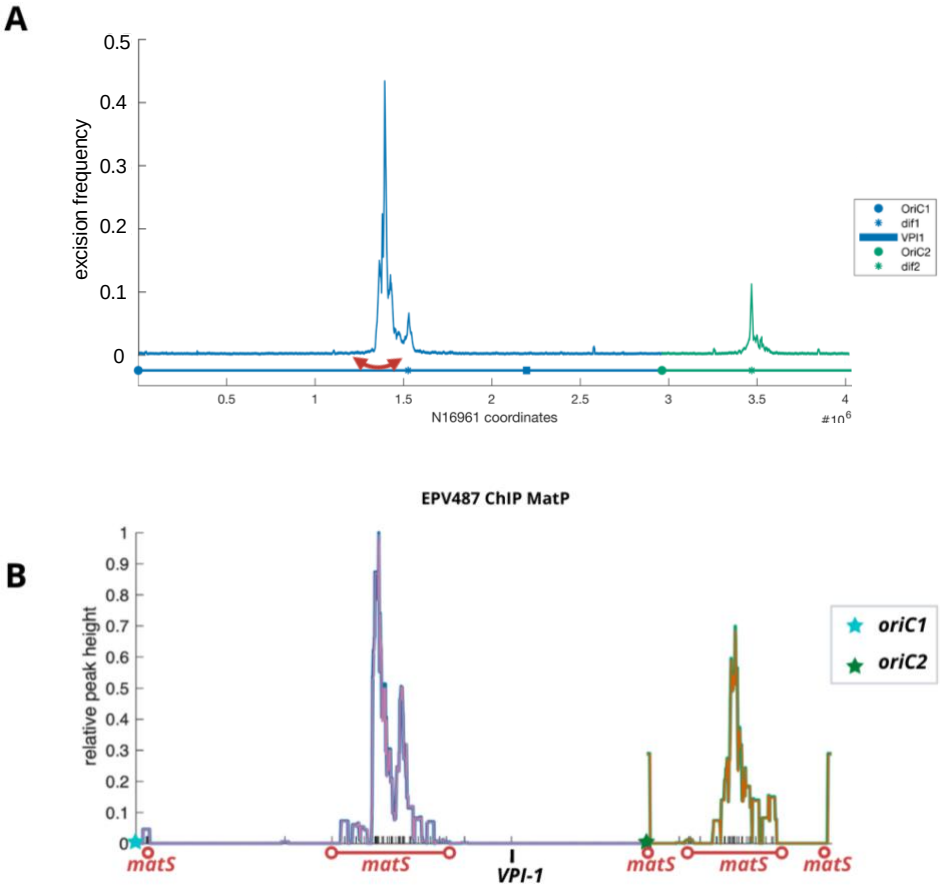

Figure 26: (A) Hi-SC2 assay performed on *V. cholerae* EPV487 cells with an inversion at the *ter* region using the XerC/D recombinase, with the reporter excision frequency on the y axis and the reporter coordinates on the genome on the x axis. The red arrow shows the region that has been inverted. This assay was performed using the turbidostat. **(B)** ChIP-seq assay of MatP performed on EPV487 cells that carry an inversion in *ter1*. Chr1 is represented in purple and Chr2 is represented in orange. The unique copy of MatP is tagged with the 3X FLAG peptide. The relative peak height is plotted against the length of the genome. *OriC1* and *oriC2* are represented by a blue and green star respectively. The *matS* sites are represented by a clear red circle when alone, and a red line when grouped together.

The results obtained with the strain harboring an inversion within the *ter1* domain prompted us to explore the effect of the number of *matS* sites. To this end, we displaced two of the *matS* sites from *ter1* to *ter2*, and performed the Hi-SC2 assay on this strain using the XerC/D recombinase **(Figure 27A)**. We found that the sister chromatid contact were significantly higher in the *ter2* domain with the displaced *matS* sites than in the WT strain. These data correlated with relative density of MatP bound at *ter2* as the ChIP-seq of MatP in this strain showed a higher peak at *ter2* while the rest of the profile remains unchanged **(Figure 27B)**. Taken together, the results obtained in the strain harboring an inversion in *ter1* and the strain in which two *matS* sites were displaced from *ter1* to *ter2* showed that the difference in the behavior of the *ter* domains is due to differences in the density of the *matS* sites.

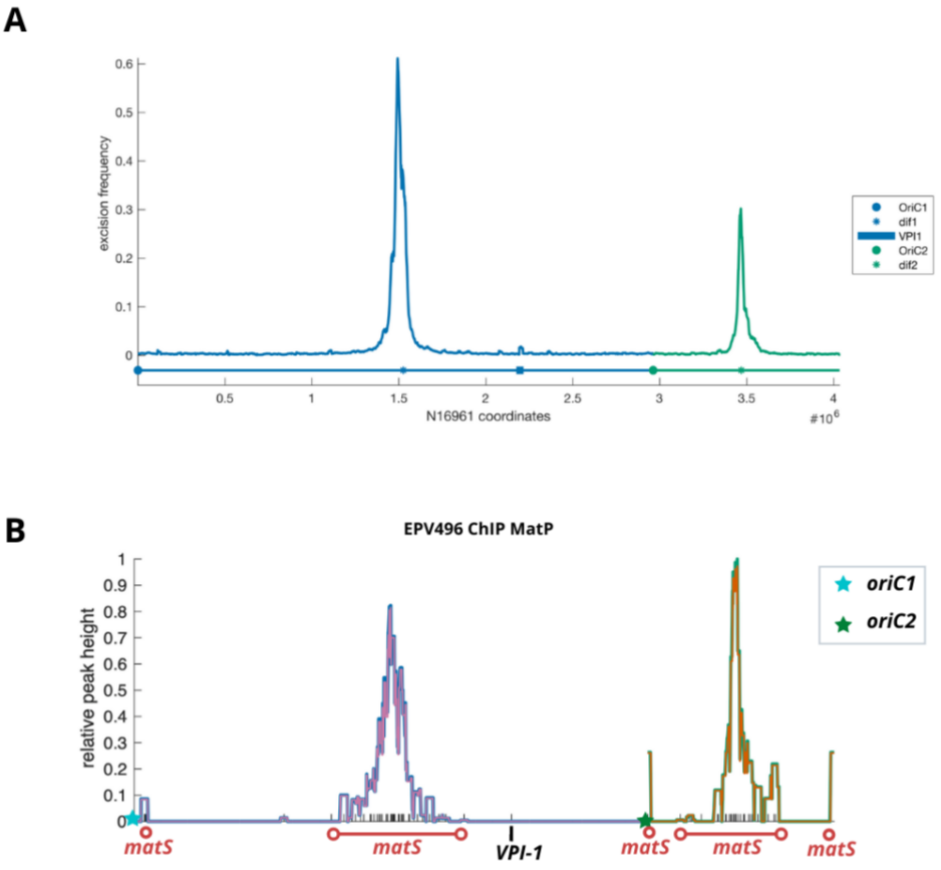

Figure 27: (A) Hi-SC2 assay profile performed on *V. cholerae* EPV496 cells with two displaced *matS* at *ter2* using the XerC/D recombinase, with the reporter excision frequency on the y axis and the reporter coordinates on the genome on the x axis. This assay was performed using the turbidostat. **(B)** ChIP-seq assay of MatP performed on EPV496 cells with two displaced *matS* at *ter2.* Chr1 is represented in purple and Chr2 is represented in orange. The unique copy of MatP is tagged with the 3X FLAG peptide.

The relative peak height is plotted against the length of the genome. *OriC1* and *oriC2* are represented by a blue and green star respectively. The *matS* sites are represented by a clear red circle when alone, and a red line when grouped together.

Chapter 2: The role of segregation factors in decohesion along the chromosome

It is no secret that replication and segregation are coordinated in bacteria. However, there is a lag between segregation and replication (Nielsen et al., 2006). This lag is supposed to be due to the time required for Topo IV to decatenate sister chromosomes (Wang et al., 2008). The MukB condensin was proposed to modulate the action of Topo IV (Hayama & Marians, 2010). Likewise, the partition machineries could influence the time of cohesion. Therefore, we decided to investigate the role of MukB and the parABS1 system in decohesion.

1. The binding pattern of MukB in *V. cholerae*

In *E. coli*, the deletion of MukB leads to severe phenotypes in cells, creating a high percentage of segregation defects and anucleate cells (Niki et al., 1991). This phenomenon raised the question of MukB's potential role in chromosome segregation as well as its involvement in sister chromatid cohesion. Interestingly, this severe phenotype was not observed in *V. cholerae* as the deletion of *mukB* does not impede the mutant's fitness in this organism, thus allowing us to explore the effect the absence of MukB had on the cohesion of its chromosomes.

The lack of severe phenotype however led us to question MukB's binding pattern in *V. cholerae*. In *E. coli*, Nolivos and colleagues suggested that MukBEF was displaced from the ter domain by MatP, which could explain the extended cohesion of this domain (Nolivos et al., 2016). My ChIP-seq experiments showed that MukB binds on the entire genome with a slight enrichment near the origin, which progressively lowers as it approaches the *ter* domain **(Figure 28A)**. In addition, I showed that the DNA surrounding *matS* sites was highly enriched in the ChIP-seq of MukB **(Figure 28B)**: it suggested that *V. cholerae* MukB interacted with *V. cholerae* MatP as observed in *E. coli* (Nolivos et al., 2016). This pattern suggests that MukB interacts with the *matS* sites in *V. cholerae* as it has been previously proposed for *E. coli* (Bürmann et al., 2021). We further notice that in contrary to the MatP ChIP-seq in which the enrichment along the genome was flat, we found that the *ori* regions are enriched while the

ter regions are depleted. In addition, Chr2 is relatively more depleted than Chr1. Plotting the ChIP-seq data at a smaller resolution (40kb) highlighted the enrichment near the origin **(Figure 28C)**. This 1.2-fold enrichment is low but nevertheless expected, as it agrees with the suggestion that MukB is displaced from the *ter* by MatP.

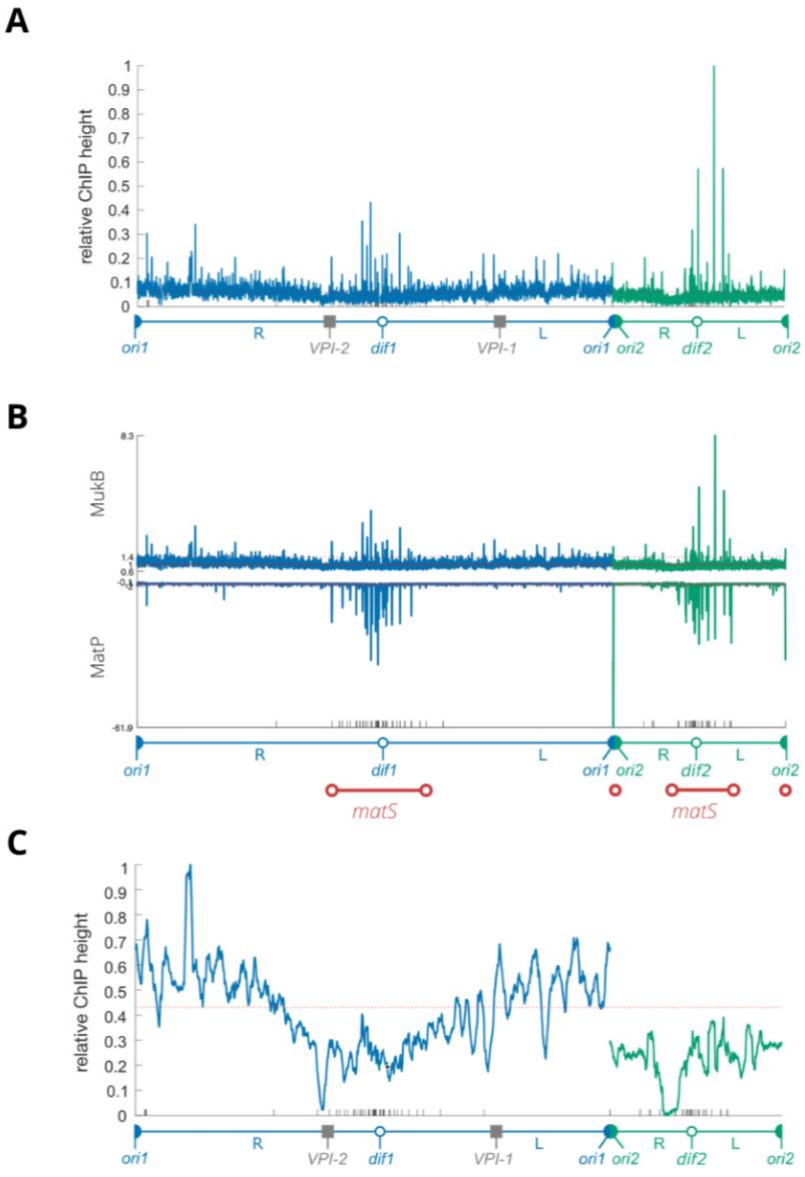

Figure 28: ChIP-seq assays of MukB and MatP performed on WT cells. Chr1 is represented in blue and Chr2 is represented in green. **(A)** ChIP-seq of MukB of both chromosomes at a high resolution. **(B)** The top panel shows the ChIP-seq of with a zoom on the peaks of MukB in the *ter* domain. The bottom panel shows the ChIP-seq of MatP of both chromosomes. The *matS* sites are represented by a clear red circle when alone, and a red line when grouped together. The red line is the mean of the DNA

enrichment. **(B)** ChIP-seq of MukB using a 40Kb sliding window. MukB is detected along both chromosomes with a slight enrichment far from the *ter* domain.

2. MukB in *V. cholerae* plays a role in chromosome decohesion

2.1. The role of MukB in a WT context

After having determined the binding pattern of MukB in *V. cholerae*, we investigated the potential role of MukB in removing cohesion along the genome. First, we compared the Hi-SC2 profile in WT and Δ*mukB* cells **(Figure 29A)**.

We observed an overall increase in cohesion levels following the deletion of MukB on Chr1, and little to no effect on Chr2. This increase was more pronounced as one moved away from *ori1*, with an emphasis on the left arm of Chr1, especially on the pathogenicity island VPI-1. Both *ori1* and *ter1* however, remained largely unchanged. The increase of cohesion due to the absence of MukB indicated that it played a role in the decohesion of Chr1, with its action being more obvious on the chromosome arms.

In order to confirm those results, I decided to follow the chromosome segregation of two loci on Chr1 by fluorescence microscopy. To be able to correlate the difference in segregation timing and the level of sister-chromatid contacts, I chose the R2 locus on the right arm of Chr1 and VC1042 on the left arm of Chr1 after the VPI-1, highly cohesive zone **(Figure 29B)**. In a WT strain, I observed more cells with a single VC1042 focus and two R2 foci than cells with two VC1042 foci and a single R2 focus with 5% and 17% respectively. This trend was more pronounced when MukB was deleted. The number of cells with a single VC1042 focus and two R2 foci significantly increases to reach 26%. These results indicated a delay in segregation of the VC1042 locus in the absence of MukB as opposed to the R2 locus, thus agreeing with the increase in cohesion in the area surrounding this locus observed in the Hi-SC2 assay.

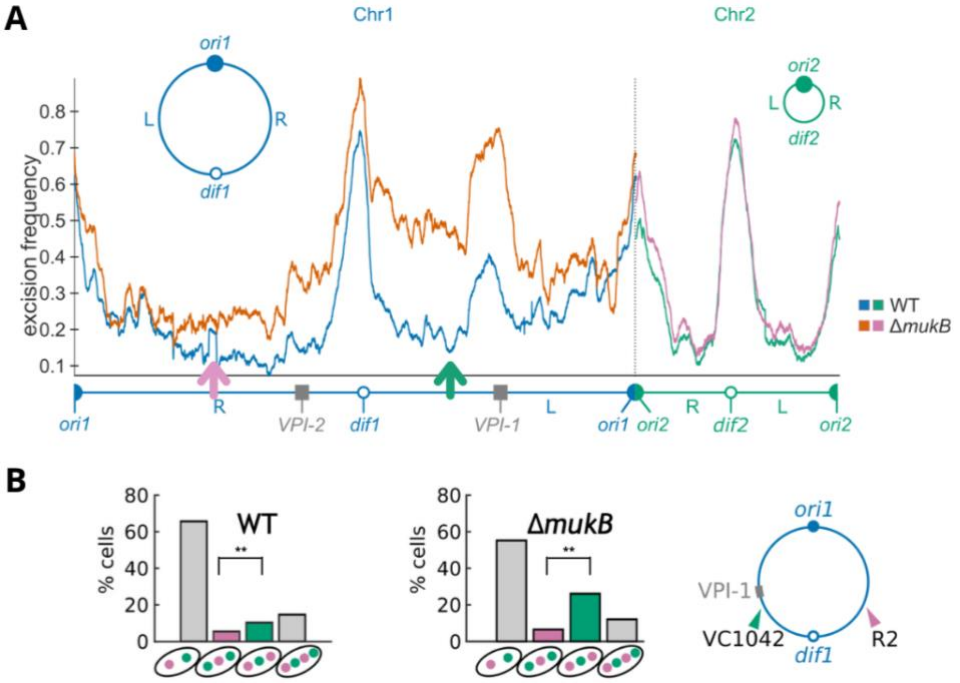

Figure 29: (A) Comparison of Cre-based Hi-SC2 assays performed on a WT, represented in blue and green, and a Δ*mukB* strain, represented in orange and pink. *Ori1* and *ori2* are represented by blue and green full circles respectively, while *dif1* and *dif2* are represented by blue and green empty circles respectively. The pink arrow shows the position of the R2 tag while the green arrow shows the position of the VC1042 tag. This assay was performed using the turbidostat. **(B)** Fluorescence microscopy analysis of the order of segregation of two loci on the opposite replication arms of Chr1. The graphs show the proportion of cells with the indicated number of foci observed. We analyzed >1,000 cells per strain per experiment. The two informative cell categories, i.e., the cells with 1 VC1042 and 2 R2 foci (1:2) and the cells with 2 VC1042 and 1 R2 foci (2:1), are highlighted in green and pink, respectively. On the right is a scheme of Chr1 with the position of each tag. *The difference is statistically different (Chi-Square test; $p<0.001$). Equivalent significance results were obtained using the data of each individual set of microscopy experiments.

2.2. Confirmation of the results in a Δ*VPI-1* context

The Hi-SC2 profile of Δ*mukB* cells suggested that MukB could have a more important role in highly cohesive regions. To demonstrate this possibility, we decided to check whether the apparent increased requirement for MukB to separate sister-copies of the VPI-1 region could be alleviated by the deletion of VPI-1. To this end, we studied the cohesion profile in a strain with a double Δ*VPI-1* Δ*mukB* mutation and compared it to the cohesion profile obtained in a Δ*VPI-1* strain. The deletion of VPI-1 leads to a decrease in sister chromatid contacts around the VPI-1 region **(Figure 30A)**, which caused the peak observed in a Δ*mukB* strain to largely decrease **(Figure 30B)**.

To confirm those results, I conducted the same fluorescence microscopy as for the Δ*mukB* strain to follow the chromosomal segregation of the two loci on Chr1, VC1042 for the left arm and R2 for the right arm **(Figure 30C)**. When compared to the foci count of the Δ*mukB* strain, we observe a dramatic decrease of the number of cells with a single VC1042 focus and two R2 foci compared to the number of cells with two VC1042 foci and a single R2 focus with 4% in the Δ*mukB* Δ*VPI* in contrast with 26% in the Δ*mukB* strain. This points to a significant decrease in segregation of the regions in the vicinity of VPI-1 in agreement with the sister chromatid contacts profile obtained *via* the Hi-SC2 assay.

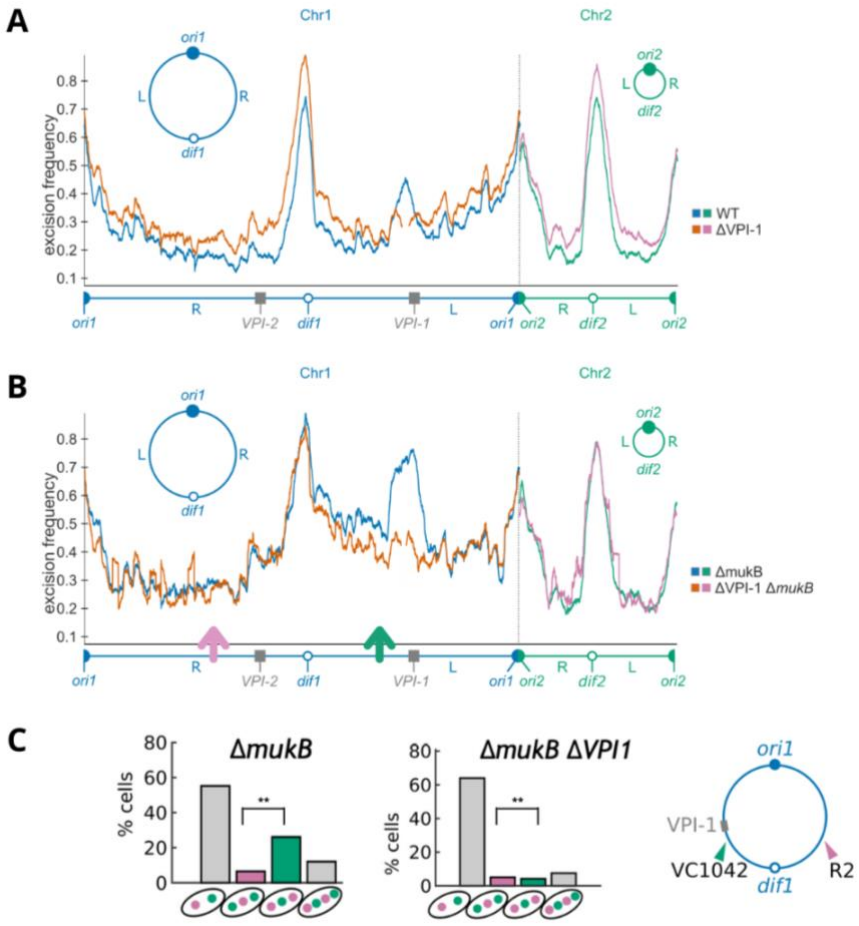

Figure 30: (A) Comparison of Cre-based Hi-SC2 assays performed on a WT, represented in blue and green, and a Δ*VPI-1* strain, represented in orange and pink. **(B)** Comparison of Cre-based Hi-SC2 assays performed on a Δ*mukB*, represented in blue and green, and a Δ*VPI-1* Δ*mukB* strain, represented in orange and pink. The pink arrow shows the position of the R2 tag while the green arrow shows the position of the VC1042 tag. *Ori1* and *ori2* are represented by blue and green full circles respectively, while *dif1* and *dif2* are represented by blue and green empty circles respectively. This assay was

performed using the turbidostat. **(C)** Fluorescence microscopy analysis of the order of segregation of two loci on the opposite replication arms of Chr1. The graphs show the proportion of cells with the indicated number of foci observed. We analyzed >1,000 cells per strain per experiment. The two informative cell categories, i.e., the cells with 1 VC1042 and 2 R2 foci (1:2) and the cells with 2 VC1042 and 1 R2 foci (2:1), are highlighted in green and pink, respectively. On the right is a scheme of Chr1 with the position of the tags. *The difference is statistically different (Chi-Square test; p<0.001). Equivalent significance results were obtained using the data of each individual set of microscopy experiments.

2. MukB and the partition system both play a role in chromosome decohesion

Taken together, the above results revealed the role of MukB in removing cohesion on the whole chromosome, with a more apparent action on HGT regions such as VPI-1. Another aspect of MukB is the more pronounced effect of its deletion the farther we move from *ori1*. As we reviewed these results, we speculated about the reason for this gradient and the partitioning system came to mind. Indeed, the three *parS* sites are located close to *ori1* and could explain the reduced effect of a *mukB* deletion in the *ori1* domain. The partitioning system could potentially mask the action of MukB with its own action on segregation.

2.1. The role of ParABS in chromosome decohesion

To investigate this hypothesis, I conducted a Hi-SC2 assay in the absence of the three *parS1* sites **(Figure 31)**. The profile obtained was similar to the one obtained for WT cells along the genome. However, there was a slight increase around *ori1* in the Δ*parS1* cells, demonstrating that ParAB1 participated to the separation of sister-chromatids through the *parS1* sites.

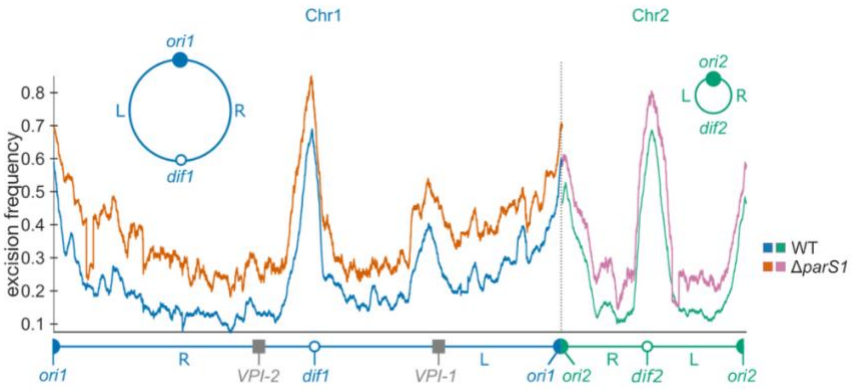

Figure 31: Comparison of Cre-based Hi-SC2 assays performed on a WT, represented in blue and green, and a Δ*parS1* strain, represented in orange and pink. *Ori1* and *ori2* are represented by blue and green full circles respectively, while *dif1* and *dif2* are represented by blue and green empty circles respectively.

2.2. The effect of a double mutation on chromosome cohesion

The double deletion of Δ*mukB* Δ*parS1* led to a very interesting result **(Figure 32)**. This double mutation was done in a Δ*VPI-1* strain in order to have a clearer view of the sister chromatid contacts level on the left arm of Chr1. We compared the Hi-SC2 profile of the Δ*VPI-1* Δ*mukB* Δ*parS1* strain to that of the Δ*VPI-1* Δ*mukB* strain in order to focus on the effect of the deletion of the three *parS1* sites on *ori1* and we observed a large increase of sister chromatid cohesion on the right arm of Chr1, from *ori1* to *ter1*. These results imply that while MukB is acting on the arms of Chr1, its action is masked by that of the ParABS system that segregates *ori1*, thus reducing cohesion near the origin. Based on these results, we are able to present a model of decohesion on Chr1 where ParABS and MukB have similar but non-redundant actions, where they act mainly on the origin and the chromosomal arms respectively. We also noticed a slight increase in cohesion near *ori2*, which is not yet understood.

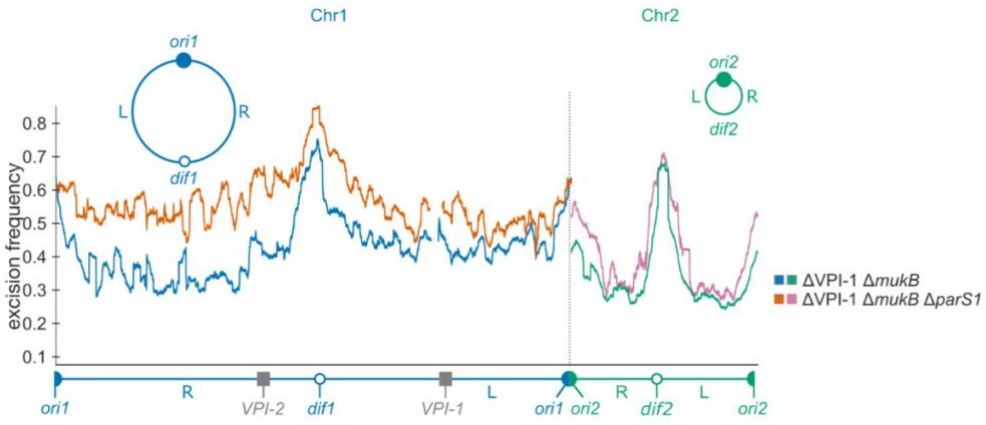

Figure 32: Comparison of Cre-based Hi-SC2 assays performed on a Δ*VPI-1* Δ*mukB*, represented in blue and green, and a Δ*VPI-1* Δ*mukB* Δ*parS1* strain, represented in orange and pink. *Ori1* and *ori2* are represented by blue and green full circles respectively, while *dif1* and *dif2* are represented by blue and green empty circles respectively. This assay was performed using the turbidostat.

2.3. Confirmation of the results with different microscopy tags

I have tagged different loci on Chr1 and Chr2 in order to confirm the observations described above. Among those tested were the two combinations *ori1* and L3 on Chr1, with L3 being located in the vicinity of VPI-1; and R1 I and R1 II with tagged loci close to *ori1* and *ori2* respectively **(Figure 33)**. The first combination was chosen upon viewing of the first results of the Hi-SC2 assay on the Δ*mukB* strain. The L3 tag was chosen to monitor segregation on a locus within close vicinity of the VPI-1 region with the *ori1* tag serving as a reference as the sister chromatid contacts level did not appear to change with and without *mukB*. In the WT strain, we observe a higher percentage of cells with one L3 spot and two *ori1* spots (15%) than cells with two L3 spots and one *ori1* spots (4%). The gap between the two percentages is diminished in a Δ*mukB* strain however, with the increase in the number of cells with one *ori1* spots and two L3 spots to reach 10%, indicating an increase in cohesion in *ori1*. These results were not expected as we believed that the deletion of MukB should not affect the level of cohesion at *ori1*. These results will be confirmed with further investigation of sister-chromatid levels at *ori1*.

In the second combination, we wanted to follow the segregation of a loci near *ori1*: R1 I. We decided to tag R1 II as a reference as *ori2* and its neighboring regions did not appear to change in the Hi-SC2 assays previously performed investigating MukB. In the WT strain, we observe a smaller percentage of cells (7%) with one R1 I spot and two R1 II spots than cells with one R1 II spot and two R1 I spots (15%). In a Δ*mukB* context however, the percentage of cells with one R1 I spot and two R1 II spots increases and is now equal to the percentage of cells with one R1 II spot and two R1 I spots, suggesting an increase in the cohesion of the regions next to *ori1* compared to *ori2*. The results for this combination are still preliminary but the Hi-SC2 assays conducted in the absence of the three *parS1* sites seem to hint towards a slight change in Chr2 that is yet to be understood.

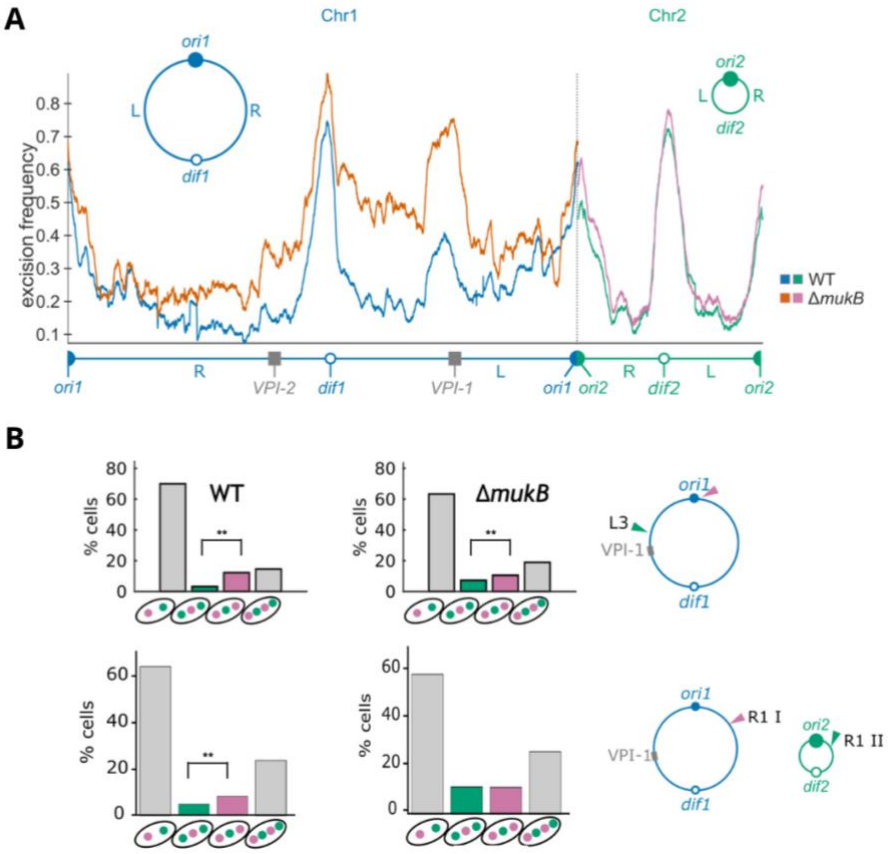

Figure 33: (A) Comparison of Cre-based Hi-SC2 assays performed on a WT, represented in blue and green, and a Δ*mukB* strain, represented in orange and pink. *Ori1* and *ori2* are represented by blue and green full circles respectively, while *dif1* and *dif2* are represented by blue and green empty circles respectively. This assay was performed using the turbidostat. **(B)** The top panel shows a fluorescence microscopy analysis of the order of segregation of two loci on Chr1, *ori1* and L3 on the left arm of Chr1. The graphs show the proportion of cells with the indicated number of foci observed. The two informative cell categories, i.e., the cells with 1 L3 and 2 *ori1* foci (1:2) and the cells with 2 L3 and 1 *ori1* foci (2:1), are highlighted in green and pink, respectively. The bottom panel shows a fluorescence microscopy analysis of the order of segregation of two loci R1 I and R1 II near *ori1* and *ori2* respectively. The graphs show the proportion of cells with the indicated number of foci observed. The two informative cell categories, i.e., the cells with 1 R1 II and 2 R1 I foci (1:2) and the cells with 2 R1 II and 1 R1 I foci (2:1), are highlighted in green and pink, respectively. We analyzed >1,000 cells per strain per experiment. Schematic representations of the positions of each tag are on the right. *The difference is statistically different (Chi-Square test; $p<0.001$). Equivalent significance results were obtained using the data of each individual set of microscopy experiments.

3. The effect of MukB on Chr2 is masked

Several questions came to mind while studying these results, especially the different effects the deletion of MukB has on the cohesion of each chromosome. We wondered whether it was due to the origins of replication, the partition systems, or the DNA context as all three are unique to each chromosome. To investigate, I performed the Hi-SC2 assay on the

MCH1 strain. It is important to note that with the integration of Chr2 in *ter1*, *ori2* and parAB2 are now absent. The deletion of MukB in the MCH1 strain leads to an increase in cohesion along the fused chromosome, including the DNA context of Chr2 **(Figure 34)**. The level of sister chromatid contacts in most of the chromosome is reminiscent of Chr1 in a Δ*mukB* strain, including the peak around the VPI-1 region. Furthermore, the sudden increase in sister chromatid contacts on the regions belonging to Chr2 when placed in a MCH1 context implied that DNA context itself does not prevent the action of MukB, but that another factor was masking its action.

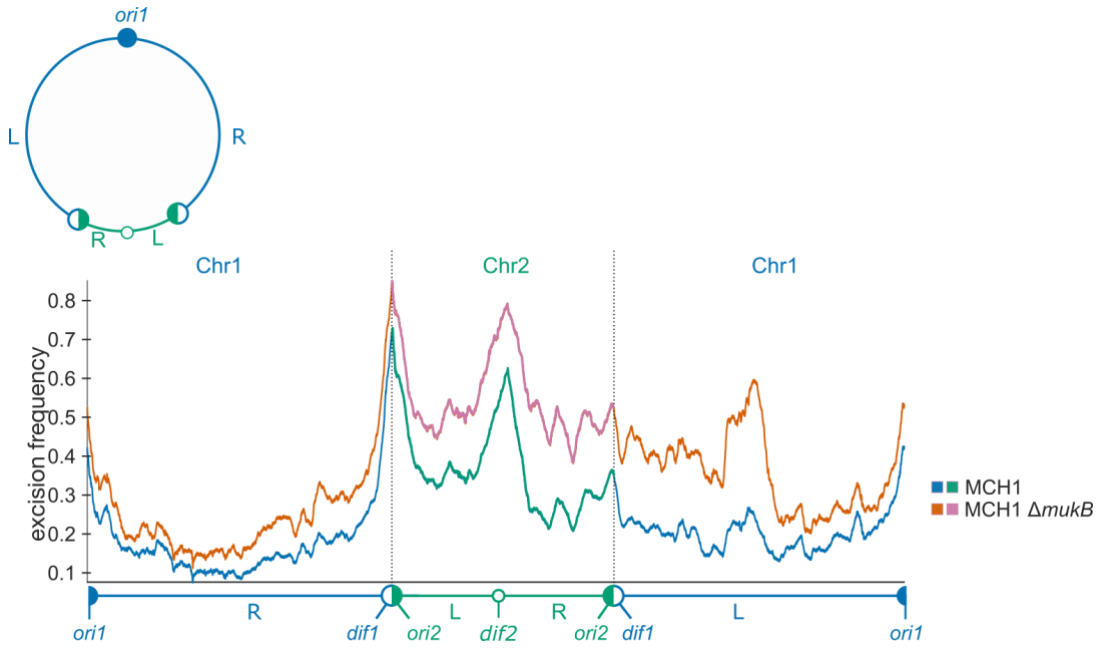

Figure 34: Comparison of Cre-based Hi-SC2 assays performed on a MCH1 strain, represented in blue and green, and a MCH1 Δ*mukB* strain, represented in orange and pink. *Ori1* and *ori2* are represented by blue and green full circles respectively, while *dif1* and *dif2* are represented by blue and green empty circles respectively. The top panel contains a schematic representation of the rearranged chromosome.

4. The length of the arms of Chr1 and Chr2 do not play a role in masking the effect of MukB

One of the hypotheses that came to mind after studying the results of the MCH1 strain was that the reason for the absence of a role of MukB on the decohesion of Chr2 was that the arms of Chr2 are much shorter than those of Chr1. Indeed, with MatP chasing MukB away from *ter1*, MukB would be free to act on the arms away from *ter1*. In Chr2, however, the arms

are much shorter than in Chr1, leaving MukB with relatively no freedom to act after being chased from *ter2* as suggested by the ChIP-seq profile of MukB **(Figure 28)**. To test this hypothesis, I performed the Hi-SC2 assay in ESC2, with and without *mukB* **(Figure 35)**. The profile obtained showed an increase in sister chromatid contacts on the first chromosome, while the second chromosome remains unchanged. Interestingly, regions that showed an increase in a Δ*mukB* strain (Chr1) did not change when placed under *ori2*, while regions that did not show an increase in a Δ*mukB* strain (Chr2) showed an increased level of sister chromatid contacts when placed under *ori1*. These results invalidated the hypothesis that the length of the arms is responsible for the lack of effect the MukB deletion has on Chr2.

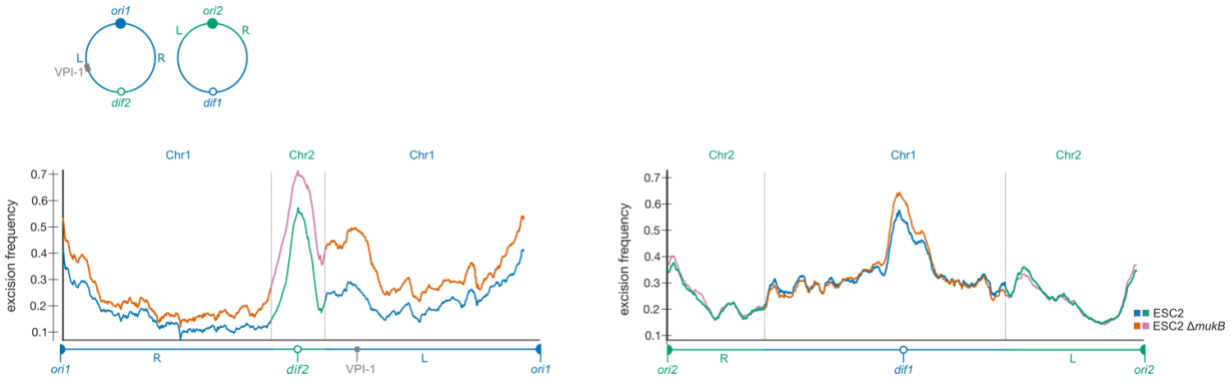

Figure 35: Comparison of Cre-based Hi-SC2 assays performed on a ESC2 strain, represented in blue and green, and a ESC2 Δ*mukB* strain, represented in orange and pink. The top panel contains a schematic representation of the rearranged chromosome. The left panel shows the Hi-SC2 profile of the first chromosome (containing *ori1* and *ter2*) while the right panel shows the Hi-SC2 profile of the second chromosome (containing *ori2* and *ter1*). *Ori1* and *ori2* are represented by blue and green full circles respectively, while *dif1* and *dif2* are represented by blue and green empty circles respectively.

Chapter 3: Supplementary data

Transposon insertion plots for Hi-SC2 experiments

While performing the Hi-SC2 assays, a big concern was the distribution of transposon insertion along the genome. We plotted the transposon insertion of each sequenced experiment to check that the insertions are evenly distributed **(Figure 36)**. The flatter the graph, the more evenly the transposon was inserted along the genome. We can see for example that the Hi-SC2 assay performed on Δ*parS1,* Δ*matP* using the Cre/*loxP* assay, and WT using the XerC/D assay do not have a transposon insertion distribution as even as the rest of the strains, and we will be performing a replicate of this assay. As for the drops, they represent a locus that was not/could not be mapped. This typically happens when the transposon is inserted in an essential gene in which case the cell dies, and the data is not recovered.

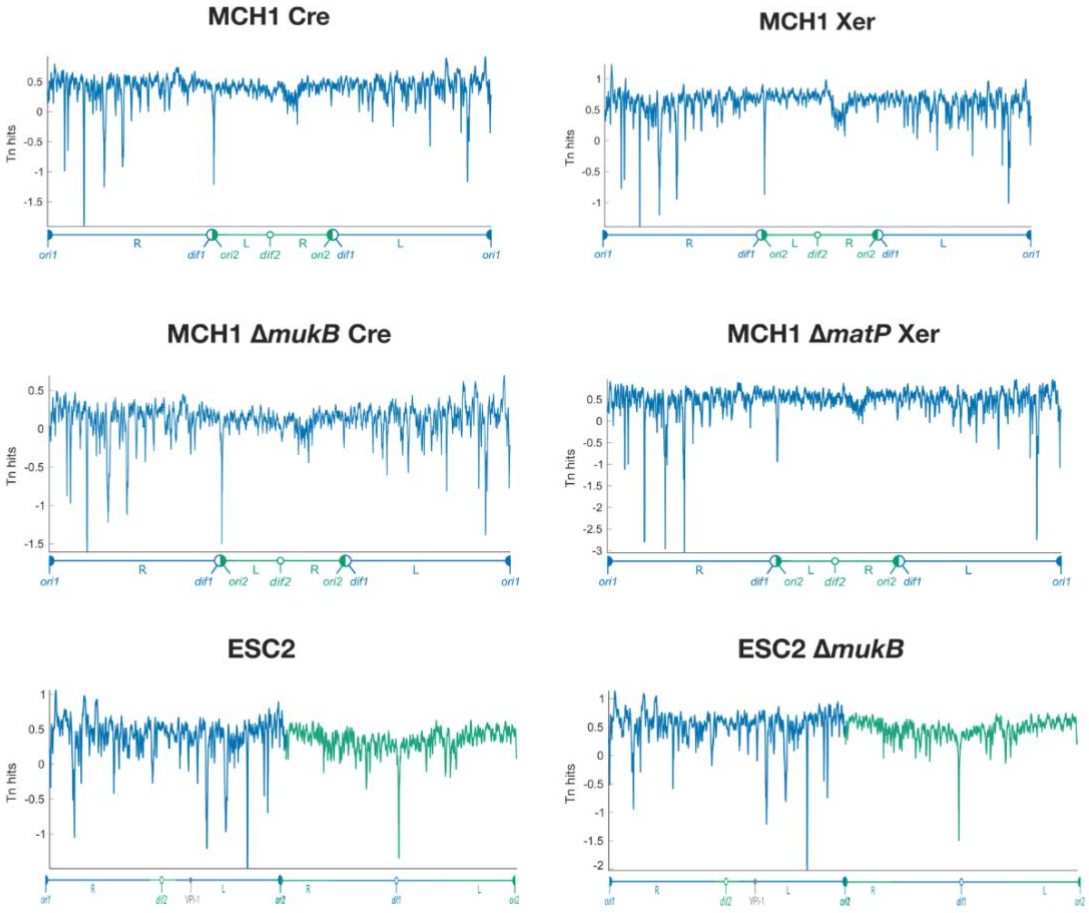

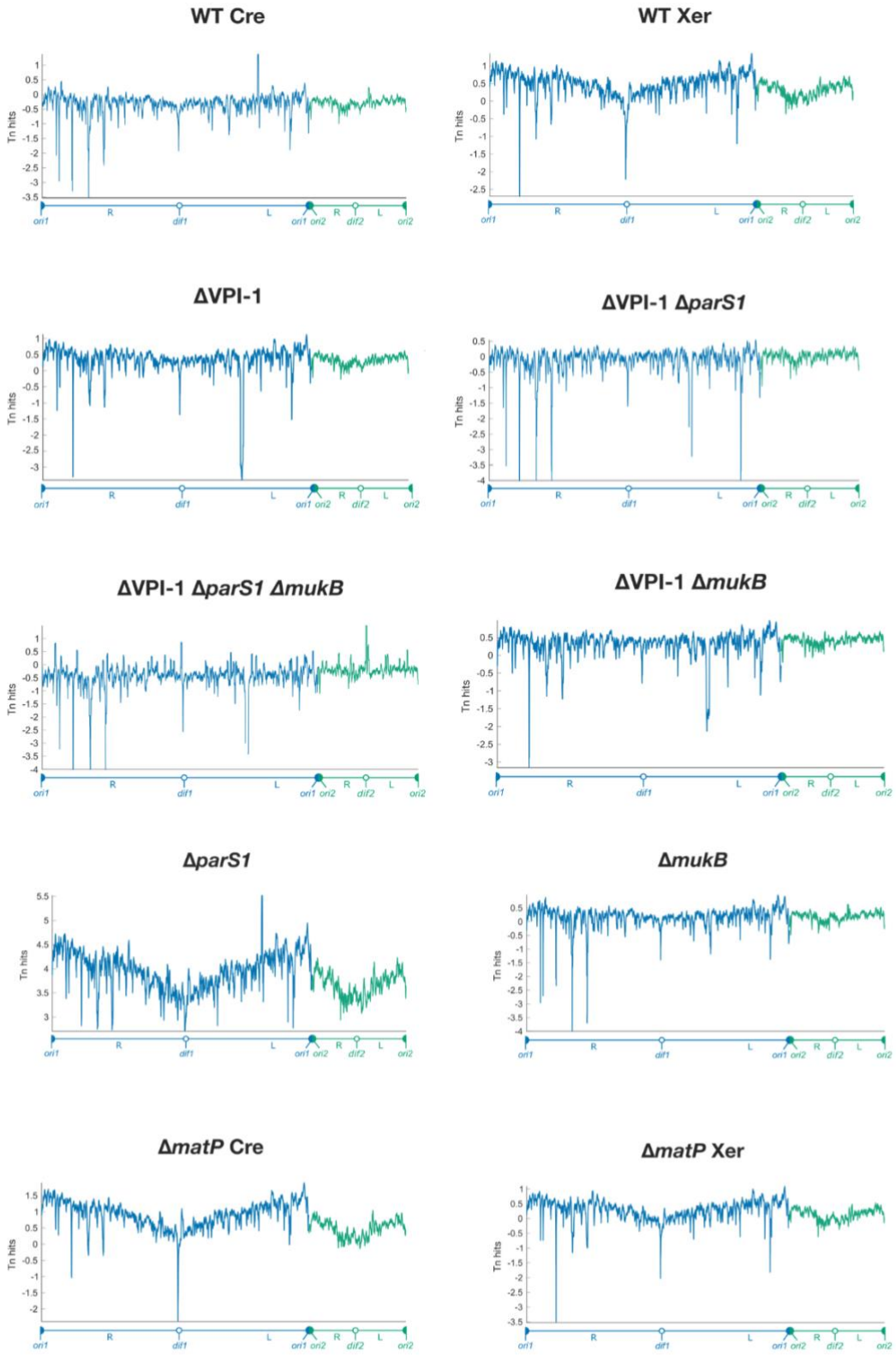

Figure 36: Plots of the insertions of the transposons for each Hi-SC2 assay performed for this thesis. Chr1 is represented in blue and Chr2 is represented in green. The transposon insertions are plotted using a logarithmic scale (log10) as a function of its position on the genome.

Discussion and Perspectives

DNA has been studied for several decades and will likely remain the center of attention for decades to come. Every aspect of the double helix is being scrutinized, and each interaction with either internal or external factors are being studied. As knowledge about chromosomes and cell cycles grew, so did the interest in that field. Labs rushed to uncover the mechanisms behind DNA replication and subsequent segregation, and details about what became known as "bacterial cohesion" started to emerge. The development of new techniques helped us progressively learn about the concomitance of replication and segregation in bacteria as well as the delay in certain regions of the chromosome that was later called sister-chromatid contacts (Lesterlin et al., 2012; Nielsen et al., 2006; Wang et al., 2006). It is now clear that the loci of a bacterial chromosome do not segregate at the same speed after replication as some sister copies remain together for a longer time post-replication, suggesting differences of cohesion along the genome. These sister-chromatid contacts can be monitored in different ways including microscopy and high-throughput whole genome sequencing (Hi-SC2) (Joshi et al., 2011; Espinosa et al., 2020). These techniques brought to light a list of potential candidates responsible for either adding or removing cohesion along the chromosome and thanks to continuous work on the subject, the list keeps on growing.

The sister-chromatid contacts profile of the WT strain in *V. cholerae* showed three domains of extensive cohesion: *ori*, *ter*, and the pathogenicity island VPI-1. The aim of my PhD was to explore potential actors involved such as MatP for cohesion in the *ter* domain, as well as actors that might participate to its removal: MukB and ParABS1.

1. Potential actors of cohesion in the ter domain: the role of MatP

The idea that MatP played a possible role in the cohesion of the *ter* domain started with the observation that MatP contributes to the condensation of the *ter* of the *E. coli* chromosome by forming tetramers before linking the *matS* sites together through a bridging mechanism (Dupaigne et al., 2012). This study came hand-in-hand with the one

demonstrating that MatP is responsible for sequestering the sister-copies of the *ter* together at mid-cell *via* its interaction with the divisome, particularly with ZapB (Espéli et al., 2012). Fluorescence microscopy assays later proposed that FtsK progressively unloads MatP from the *matS* sites in order to promote the segregation of the sister-copies of the *ter*, therefore making MatP a potential actor of cohesion in the *ter* domain behind the replication fork. (Stouf et al., 2013b). This hypothesis was solidified when microscopy observations coupled with genetic assays using XerC/D / *dif* demonstrated that MatP played a role in keeping the sister-copies of *ter1* together until cell division in *V. cholerae* (Demarre et al., 2014). However, a study using the Cre/*loxP* genetic assay targeting two loci in the *ter* region of the *E. coli* chromosome did not show any significant cohesion decrease in these loci with the deletion of *matP*. Therefore, there was a controversy around whether MatP was responsible for the cohesion behind the replication fork in the *ter* domain.

During my PhD, we observed a correlation between the peaks of binding of the protein and the peaks of cohesion of the *ter* domains using ChIP-seq and Hi-SC2 assays. We later found however that MatP is not the only factor responsible for the high cohesiveness of these regions behind the replication forks as its deletion only led to a minor decrease of said cohesion, in agreement with the observations of Lesterlin et al.. When investigating cohesion of the *ter* domains at cell division however, we found that MatP plays a major role in keeping the sister-copies of *ter1* together. Next, we investigated the drastic difference in cohesion levels between *ter1* and *ter2* and found that it was not the position nor the orientation of the *matS* sites that are behind it, but the density of *matS* sites present in each *ter* domain. These results lead to the following question: how does MatP keep the sister-copies of *ter1* together? Does it achieve so through certain interactions with the divisome, or does it alter the conformation of the DNA *via* its binding as a tetramer, thus “forcing it” into condensation? Future work is needed to test these hypotheses, such conformation studies using 3C assays and protein-protein interaction analysis using co-IP or pull-down assays.

As MatP is not a major actor of cohesion on the *ter* domain behind the replication fork, this leaves room for other actors that could participate *via* the organization of the chromosome such as the HU nucleoid-associated protein (NAP). It has been shown that HU promotes DNA contacts in the megabase range outside of the *ter* region in *E. coli* (Lioy et.al,

2018). Thus, the absence of HU in the *ter* could be the reason for the high cohesiveness of this region. The binding pattern of HU is reflective of relatively non-specific binding to the chromosome although with a preference for A/T-rich DNA sequences (Prieto et al., 2012). The exclusion of the action of HU on the *ter* region remains to be studied and makes for a very interesting potential candidate for the cohesion of the *ter* domain.

2. Potential actors of cohesion in the *ori* domain

The sister-chromatid contacts profile behind the replication fork of the WT strain clearly shows two highly cohesive regions in both Chr1 and Chr2: the origin and the terminus of replication. The cohesiveness of these two regions come as no surprise as they constitute key parts of the cell cycle. The origin of replication for instance, is home to many factors regulating the initiation of replication notably the SeqA protein. SeqA is known to bind hemimethylated DNA at the origin and preventing its rapid methylation in a phenomenon called origin sequestration (Egan & Waldor, 2003). The overexpression of SeqA leads to an increase in DNA condensation as well as a severe filamentous phenotype in *V. cholerae*, making it an interesting candidate for the cohesiveness of the origins (Saint-Dic et al., 2008). Unfortunately, a SeqA deletion could not be obtained in *V. cholerae* although, interestingly enough, it is possible in *E. coli* (Lu et al., 1994; Egan & Waldor, 2003).

3. The contribution of MukB and the partition system to cohesion behind the replication fork

In *E. coli*, MukB has been shown to interact with Topo-IV multiple studies throughout the years. It was shown to interact with the ParC subunit of Topo-IV, thus stimulating catalysis by the topoisomerase (Nicolas et al., 2014). It was later demonstrated that this interaction is modulated by MatP, which is proposed to unload MukB from the *ter* domain (Nolivos et al., 2016). However, such studies had not yet been performed in *V. cholerae*, as not much is known about MukB's role and action on cohesion behind the replication fork in our model organism.

Unlike *E. coli* that showcases a severe phenotype when MukB is deleted, *V. cholerae* does not exhibit strong segregation defects in the same context. The lack of obvious impact

on viability prompted us to start with ChIP-seq experiments to identify its binding pattern in our model organism. What we found however, remains elusive as it is still unclear whether MukB loads near the *ori* and is moved away due to cell elongation, or if it is MatP that unloads it from the *ter*, thus creating a gradient. This gradient itself is still under investigation as well since the enrichment observed in our ChIP-seq assays is too low (1.2x fold) to settle the question. With studies demonstrating the active unloading of MukB from the *ter* domain at the hands of MatP in *E. coli*, further research needs to be conducted in order to either confirm or deny this rather attractive model in *V. cholerae* (Nolivos et al., 2016).

The lack of defect in segregation in a Δ*mukB* strain was attributed to the presence of a partition system which is not the case in *E. coli*. This theory was upheld by the sister-chromatid contacts profile of the Δ*mukB* strain showing a bigger increase in cohesion as one moves away from the *ori*. This observation led us to scavenge for reasons as to why MukB's action was less obvious near *ori1,* and the partition system came to mind. Indeed, the three *parS1* sites being located next to *ori1* made the partition system of Chr1 the main candidate for this matter. We subsequently found that the deletion of those three sites have a minor effect on the cohesion of Chr1. Interestingly, we found an increase in cohesion on this region in a double Δ*parS1* Δ*mukB* context, implying that the cell has established a rescue system where MukB is able to compensate for the absence of ParABS and vice-versa, thus keeping the cell alive with little to no phenotypic defects. Future work is needed to validate that model through phenotypical characterization as well viability tests of the doubly mutated strain.

This model can be extrapolated to Chr2 where we observe little to no effect of the deletion of MukB on cohesion. Unlike the three *parS1* that are located near *ori1*, the ten *parS2* sites are scattered along the length of Chr2. This distribution could explain the lack of obvious effect of MukB as it allows ParAB2 to reduce cohesion along the length of Chr2 all by itself, therefore shielding it from the repercussions of the absence of MukB. The sister-chromatid contacts profile of the MCH1 Δ*mukB* strain heavily leans into this hypothesis as we suddenly observe an increase in cohesion on regions belonging to Chr2 that were not affected in a Δ*mukB* strain, especially with the knowledge that MCH1 lacks ParAB2. This model has to be verified by performing the Hi-SC2 assay on a strain lacking ParAB2. Unfortunately, this

deletion leads to a severe phenotype that highly complicates manipulating the mutated cells. We have started to build a system that would help us bypass this hurdle by having ParAB2 inside a *loxP-loxP* cassette that would be excised at the start of the experiment, thus allowing us to grow the cells without any viability defect and observe the effects of the deletion of ParAB2 in real time.

4. Small local variations of cohesion

Plotting the Hi-SC2 assay using a 10kb sliding window allows for a more detailed view of sister-chromatid contacts on a smaller, local scale. We observe small variations along the genome that are as reproducible as they are detailed (Espinosa et al., 2020). The reason behind these variations is still unknown although we suspect gene expression plays a role in this process. In fact, one hypothesis states that the more a locus is transcribed, the less it is cohesive. We plan on performing RNA-seq assays on WT *V. cholerae* cells in different conditions that alter gene expression and correlating them to Hi-SC2 assays to either validate or invalidate this hypothesis.

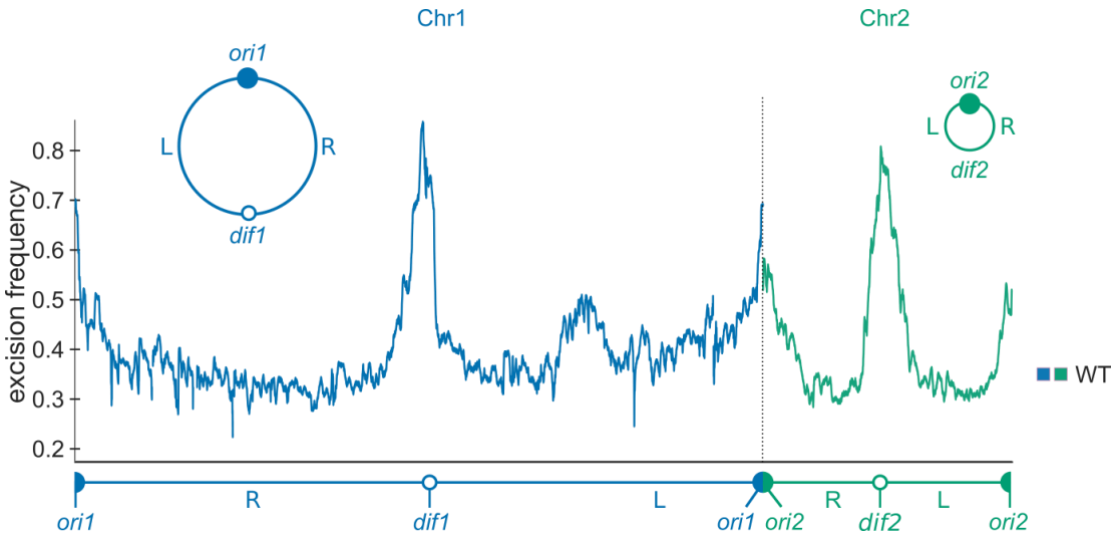

Figure 35: Hi-SC2 profile of a *V. cholerae* WT strain. Chromosome one is represented in blue, while chromosome two is represented in green. The excision frequency of the *loxP* sites is plotted according to their position on the genome. Below the X axis is a linear map of each chromosome with the *oriC* and *dif* domains (1 and 2 for each chromosome). R and L indicate the right and left arm of the chromosomes. The two chromosomes are separated by a dotted line, and a schematic representation of each chromosome is displayed as well. The excision frequency of the loxP cassettes is plotted at a

10-kbp window, which permits to see both types of cohesion patterns. Adapted from (Espinosa et al., 2020).

5. Segregation versus decohesion – the role of cohesion in bacteria

In my thesis, I brought support to the respective roles of MukBEF and ParABS1 in the process of decohesion. However, a role of MukBEF in stimulating the decatenation activity of Topo-IV was also reported (Nolivos et al., 2016). Hence, these factors thus far referred to as segregation factors could also have a role in the process of decohesion. In contrast, the factor which is supposed to be a cohesion factor, MatP, did not lead to a significant phenotype once inactivated. Therefore, the only factors whose action mechanism was characterized are stimulating or inhibiting the activity of Topo-IV. Hence, no cohesion factor might be at play. Their only mission is to ensure decatenation, which is not equally efficient on all loci. Unlike plasmids, chromosomes are fully catenated after replication due to their structure in the absence of Topo-IV. The role of the chromosomal partition system could be merely to promote decatenation instead of the precise positioning of the sister replication origins of chromosomes, *oriC*.

Globally, the segregation step might only be a decohesion step supported by a precise chromosome organization. In fact, the choreography of chromosome organization reconstitution was interpreted as segregation when it could only be an improved method of decohesion. The extensive displacement during the segregation step in eukaryotes (anaphase) is crucial for genome equipartition while no large displacement is required in bacteria. The individualization of the two chromosomes *via* decohesion and self-organization could be sufficient to ensure partitioning.

Different constrains could provoke different levels of contacts along the chromosome and the biological role of the modulation is not clear. As mentioned earlier, cohesion could be reduced with higher expression/activity of Topo-IV or lower levels of SeqA. This could suggest that the cohesion step is under selective pressure to perform a biological role: ensuring that the replication forks would not be dismantled because of fast sister chromatids separation and protecting the chromosome's self-organization.

Materials and Methods

1. Bacterial strains and growth conditions

The experimental model for this study was the El Tor N16961 *Vibrio cholerae* isolate. The strains and plasmids used in this study are listed in the Supplementary Tables 1 and 2 respectively. The El Tor derivatives were constructed using natural transformation (Meibom et al., 2005) as well as standard methods of bacterial transformation such as integration/excision. Cells were grown in different media throughout the study: M9 minimal medium (M9 minimal salts: KH_2PO_4 15 g/L, NaCl 2,5g/L, Na_2HPO_4 33,9 g/L, NH_4Cl 5 g/L) was supplemented with fructose, $MgSO_4$, $CaCl_2$, and thiamine. As for the rich media: LB broth (Sigma-Aldrich) (Yeast Extract 5 g/L, Tryptone 10 g/L, NaCl 5 g/L), and AKI medium mimicking infectious conditions such as the epithelial lining of the gut (0.5% NaCl, 0.15% KCl, 0.4% $NaHCO_3$, 0.4% Yeast Extract, 1% peptide) (Iwanaga M, 1985). For the AKI medium to mimic infectious conditions as closely as possible, the cells were grown in static conditions: the cell culture vessels were placed in an incubator and grown without shaking to achieve anaerobic conditions.

As for growth in solid media, all strains were grown in LB Agar (Sigma-Aldrich) (1.25% Bacto-Tryptone, 0.625% Yeast Extract, 1.25% NaCl).

Antibiotics and other chemicals were added to the growth medium to the final concentrations shown in the Supplementary Table 3.

For some Hi-SC2 assays, cells were grown in the turbidostat (**Figure M1**) to maintain a steady-state of growth throughout the experiment (Hoffmann et al., 2017). The turbidostat is composed of 4 distinct units: a central unit that holds the culture vessel as well sensory and control electronics, a medium and air peristaltic pump, a fresh medium reservoir, and a waste reservoir. The culture vessel is flat-bottom test tube that holds a magnetic stir bar for agitation. The culture volume is regulated by the position of the liquid in the tube and is aerated by pressurized sterile air from the air pump. The turbidostat measures the optical density (OD) *via* a beam of 650 nm laser diode that goes through the culture vessel, is detected by a light-to-frequency converter on the other side. The OD is measured every

second and compared to the target OD set by the user. As soon as the current OD of the culture volume surpasses the target OD, a pump event is triggered, and the culture is diluted.

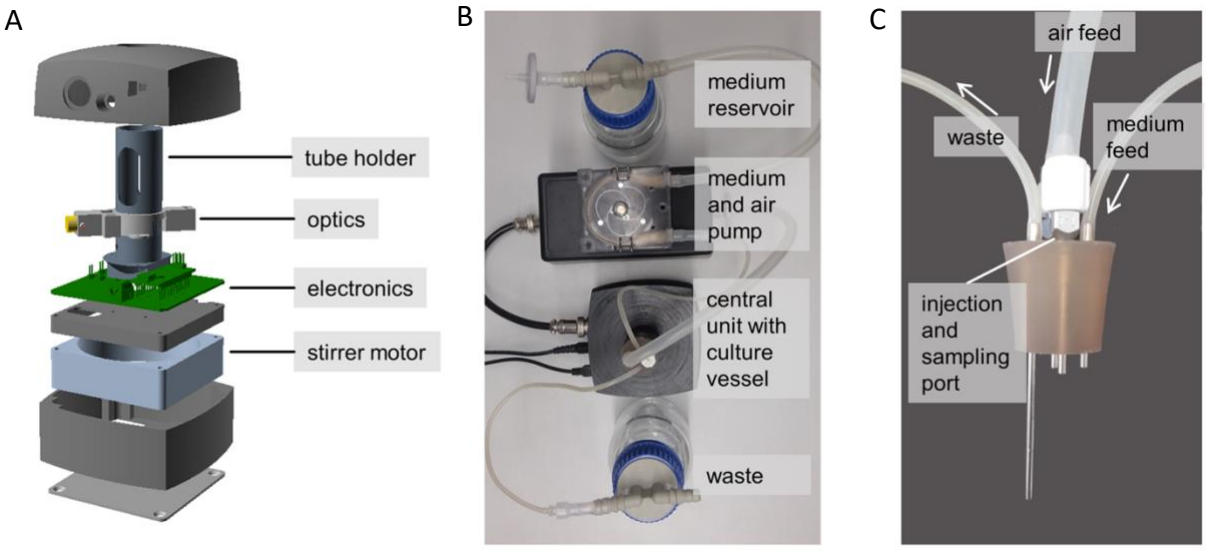

Figure M1: (A) Scheme of the central unit of the turbidostat. (B) Photograph of the assembled turbidostat with the waste and medium reservoirs, the central unit, and the medium and air pump (top view). (C) Photograph of the silicone plug of the central unit with four ports: an air feed, a medium feed, an injection and sampling port, and a waste ejecting vent. This figure was adapted from (Hoffmann et al., 2017).

2. High-resolution whole-genome assay of Sister-Chromatid Contacts (Hi-SC2)

Principle of the assay

This experiment was carried based on the Hi-SC2 assay developed in the laboratory (Espinosa et al., 2020). A Cre recombination site (*loxP-loxP* cassette) was inserted in the different strains using a Mariner transposon (Lampe et al., 1999) prior to the experiment, with a rate of approximately 400 000 unique insertions per strain, thus covering the entire genome. A scheme of the assay is shown in **Figure M2**.

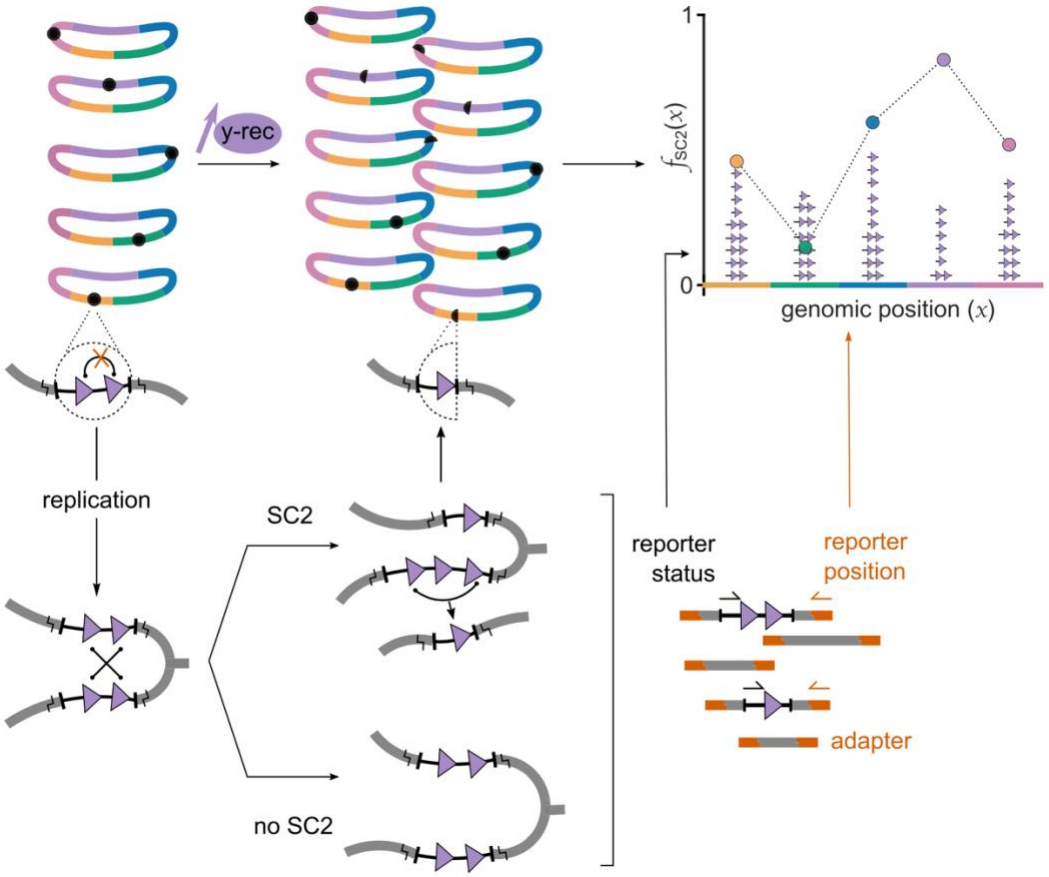

Figure M2: Scheme of the Hi-SC2 assay. The SC2 reporters made of two *loxP-loxP* sites are inserted at random positions in a library of cells. Following the expression of the recombinase, intermolecular recombination can occur if two sister chromatids are close together, resulting in a copy with a single *loxP* site while the others harbors three. The three recombination sites are subsequently converted into a single *loxP* site *via* intramolecular recombination. The DNA is extracted and sequenced using paired-end sequencing to determine both the reporter status and its position on the genome. This figure is adapted from (Espinosa et al., 2020).

Cell growth

The turbidostat was used to maintain a steady-state growth during the Hi-SC2 assays. The cells were grown overnight at target OD_{600}=0.1 at 30°C in M9 minimal medium supplemented with IPTG at 0.1 mM. Arabinose was added to the culture at a concentration of 0.02% and 10 mL were taken from the culture at each timepoint. The samples were centrifuged for 10 mins at 5000 rpm at room temperature and the pellets were frozen in dry ice.

Library construction

The genomic DNA was extracted using GenElute™ Bacterial Genomics DNA kit (Sigma Aldrich) and the recombination status of the samples was checked by PCR using the oligonucleotides

3459 and 1514; the list of oligonucleotides used in this study can be found in Supplementary Table 4. The DNA was later digested with *MmeI* (NEB) for 4 hours at 37°C and the enzyme was inactivated by incubating the samples at 65°C for 20 mins. The DNA samples were purified using the Qiagen MinElute Reaction Cleanup kit and run through the Pippin Prep (Sage Science) a first time inside a 1.5% agarose-dye free gel cassette to recover DNA fragments between 800 bp – 2000 bp that contain the transposon. The samples were next ligated to double-stranded adapters (list of the adapters can be found in Supplementary Table 4) overnight at 16°C, then purified again with the MinElute kit. The libraries were amplified by a 17 cycles PCR run and verified by a 2% agarose gel. Scale-up PCR runs can be done to increase the quantity of DNA of each sample. The PCR reactions were then pooled and purified again in the Pippin Prep, this time using a 2% agarose-dye free agarose gel cassette to recover fragments between 160 bp – 400 bp. The fragments obtained contain the recombined and non-recombined DNA (Espinosa et al., 2020). A quality check of the libraries was performed, and the samples were sequenced by the next generation sequencing facility using NextSeq 500/550 Illumina sequencing.

Data analysis

The samples were sequenced by a sequencing platform using Next Generation Sequencing with 75 cycles (Paired End). The sequencing kit used was the NextSeq 500/550 High Output kit v2 (150 cycles). For the analysis, the pipeline used by by the platform was demultiplex, trim the adapters using Cutadapt 1.15, and perform a quality control of the sequences using FastQC v0.11.5.

After receiving the sequences in the format of fastQ files, cutadapt was used to trim the adapters and the transposon in both the recombined reads and the total reads. Reads with more than 5 consecutive Ns were discarded, as well as those that don't exceed 14 base pairs. The bwa program was next used to map the samples against the genome, thus creating a sam file. Once the reads are mapped, MATLAB was used to combine both the recombined and the total reads files, and the final files were plotted using MATLAB as well. The scripts used for the data analysis are available upon demand at: francois-xavier.barre@i2bc.paris-saclay.fr

Figure M3 showcases the importance of growing the cells using the turbidostat. Two replicates of the same WT strain grown without the turbidostat have the same profile with a

different overall excision frequency level **(Figure M3A)**. The recombination profile of replicate 1 is higher than replicate 2 for both chromosomes, showcasing the fluctuation in level of excisions depending on the differences in growth rates of the same strain during different experiments. When comparing mutant strains, it is imperative to know whether the changes in recombination profiles are due to the mutations themselves or to the growth rate of the strains themselves. When grown using the turbidostat, the three WT replicates tested align almost perfectly, leading us to conduct all further Hi-SC2 assays *via* the turbidostat **(Figure M3B)**.

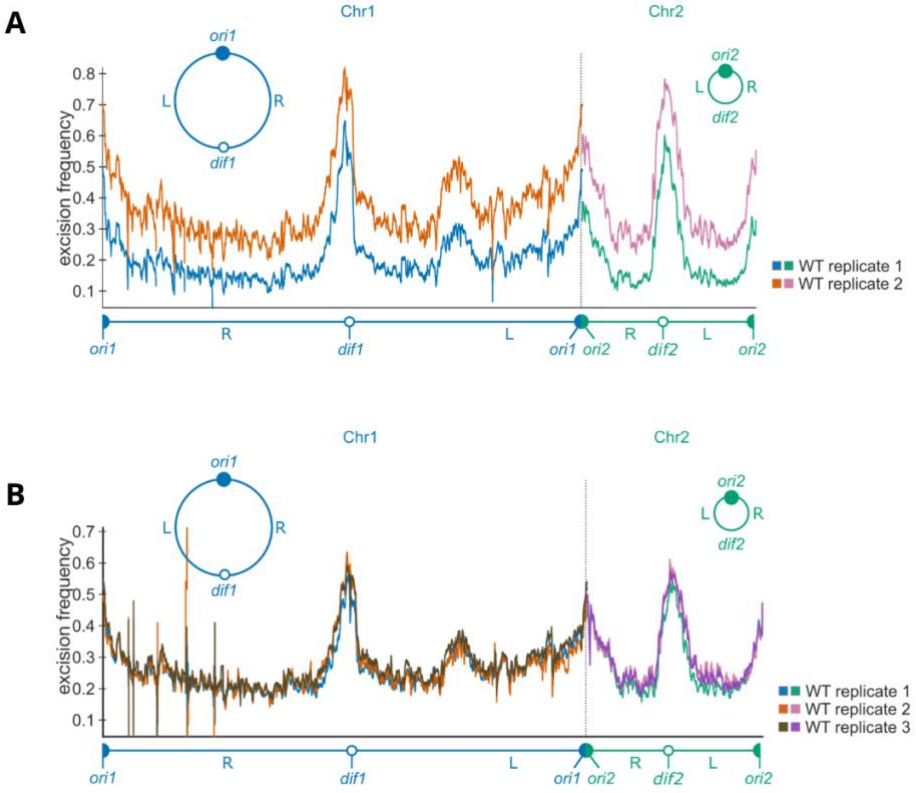

Figure M3: Plots of Hi-SC2 assays in 10kb sliding window resolution. **(A)** Comparison of the recombination profile of two replicates of the WT strain done without the turbidostat, with the excision frequency of the reporter on the y axis and its location on the genome on the x axis. Replicate 1 is represented in blue and green while replicate 2 is represented in orange and pink. **(B)** Comparison of the recombination profile of three replicates of the WT strain done using the turbidostat, with the excision frequency of the reporter on the y axis and its location on the genome on the x axis. Replicate 1 is represented in blue and green, replicate 2 is represented in orange and pink, and replicate 3 is represented in brown and purple.

3. ChIP-seq assays

ChIP-seq assays were performed on *V. cholerae* strains to investigate the binding pattern of condensin MukBEF. A frozen stock of *E. coli* SPA-tagged MatP was added to the samples as a control.

Cell growth

The *E.* coli strain was grown in M9 supplemented with glucose and casamino acids at 30°C and frozen at OD_{600}=0.3. The *E. coli* stock was stored at -80°C and an aliquot was used for each ChIP-seq assay.

As for *V. cholerae*, cells were grown overnight in M9 supplemented with fructose at 30°C and diluted the next day in 100 mL of M9 fructose at a concentration of 10^9 cells. At OD_{600}=0.3, the cultures were diluted again to the same concentration in 50 mL of M9 fructose. 5% of the *E. coli* frozen stock was added to the sample after 1h30 of growth at 30°C.

Cross-linking

Formaldehyde was carefully added to each sample at a final concentration of 1% and they were incubated at room temperature (RT) for 30 minutes with gentle agitation. Glycine was added next at a final concentration of 250mM, and the samples were incubated for 15 mins at RT with gentle agitation. Two consecutive cold TBS (Tris-HCl pH=4,7 50mM, NaCl 150mM) washes were performed by centrifuging the samples for 10 mins at 5000 rpm ay 4°C, keeping the pellets at each step. 500µL of lysis buffer I (Sucrose 20%, Tris-HCl pH=8 10mM, NaCl 50mM, EDTA 10mM, lysozyme 1 mg/mL) were added to the cells, followed by an incubation of 30 mins at 37°C. 500 µL of lysis buffer II (Tris-HCl pH=7,4 50mM, NaCl 150mM, EDTA 1mM, Triton X100 1%, Complete Mini Protease Inhibitor Cocktail (Roche) (1 tablet/10mL) were added next and the samples were directly taken to the Covaris S220 for sonication.

Sonication using the Covaris S220 to obtain 800 bp fragments

The parameters used for this sonication are:

- Duration: 10 mins
- Intensity: 4
- Peak incident power: 140 Watts

- Duty cycle: 5%
- Cycles per burst: 200

The cells were then centrifuged for 30 mins at 13 000 rpm at 4°C to eliminate all cell debris and the supernatant was recovered. 50µL of the samples were stored and later used as the input.

Immuno Precipitation of flag fusions proteins

The cell extracts were incubated with the correct amount of ANTI-FLAG M2 (A2220) (Sigma Aldrich) affinity gel overnight at 4°C with gentle mixing. The samples were centrifuged the next day for 30 seconds at 8000 g at4°C and the supernatant was discarded. Five consecutive washes were performed using volumes that were 20 times the total gel volume of the sample, each lasting 10 mins at 4°C with gentle mixing. The first two washes were done with TBS + 0.05% of Tween, and the last three washes were done with TBS only. For the elution, 2.5 times of the sample volume of 3xFLAG peptide solution (F4799) (Sigma Aldrich) (150 ng/µL) was added to each sample, followed by a 30-minute incubation at 4°C with gentle agitation. The resin was centrifuged, and the elution step repeated with the supernatant, thereafter referred to as the IP sample.

Decrosslinking of both the input and the IP samples was performed using 30 µg/mL of RNase (10109134001) (Sigma Aldrich) followed by an incubation of 1h at 37°C. 20 mg/mL of Proteinase K (1.24568) (Sigma Aldrich) was added to each sample, and they were left to incubate overnight at 65°C.

Library construction

The genomic DNA was extracted using the Qiagen kit for the input samples, and the MinElute Qiagen kit for the IP samples and the libraries were constructed as per the Illumina protocol. The DNA was sheared a second time with the Covaris to obtain 200bp fragments. The End-repair/dA-tailing of the fragments was performed following the instructions provided by NEB in NEBNext® Ultra™ II End Repair/dA-Tailing Module kit and the reactions were purified using AMPure beads (1.6x) (A63880) (Beckman-Coulter) following the manufacturer's protocol. The samples were ligated to Illumina adapters for 15 mins at 20°C, using a different indexed adapter for each sample. The reactions were then purified twice using the AMPure beads for

a double-sided purification, using 1.1x-0.75x. The ligation was amplified by a 12 cycles PCR run using the Kapa Hifi Hotstart Polymerase with oligonucleotides C and D, whose sequences can be found in Supplementary Table 4. The PCR products were purified with 1.1x AMPure XP beads (A63880) (Beckman-Coulter) and stored at -20°C. The samples were sent to a sequencing facility where a quality check was also performed.

Data Analysis

The samples were sequenced by a sequencing platform using Next Generation Sequencing with 75 sequencing cycles (Single read). The sequencing kit used was the NextSeq 500/550 High Output Kit v2 (75 cycles). About the analysis, the pipeline used by the platform was demultiplex, trim the adapters using Cutadapt 1.15, and perform a quality control of the sequences using FastQC v0.11.5.

After receiving the sequences in the format of fastQ files, cutadapt was used to trim the adapters, the first 9 bases of each read, repeated T bases (7 repeats), and any reads that are under 14 bases. A sam file was then generated from the fastQ files to map the reads against the reference genome. MATLAB was later used to combine the IP and the input files, and the results are then plotted in the same program. The scripts used for the data analysis are available upon demand at: francois-xavier.barre@i2bc.paris-saclay.fr

4. RNA-seq assays

Cells were grown in the appropriate flasks until OD_{600}=0.2 in shaking conditions for the LB samples, and static conditions for the AKI samples. This assay was done in two biological replicates, with two technical replicates of each. The biological and technical replicates were pelleted and resuspended in 250 µl of LB and AKI respectively. 500 µl of RNA protect (RNeasy Qiagen kit) were added to each sample, and they were incubated at room temperature for 5 mins. The cells were pelleted, and the supernatant was discarded. The pellets were frozen in dry ice and stored at -80°C for the night, and the RNA extraction was performed the next day using the Qiagen RNeasy kit (74004). The samples were sent to a sequencing facility where a quality check was also performed.

Data analysis

The analysis was done using Miniconda3 and the R package SARTools (Varet et al., 2016), along with MATLAB using scripts developed in the lab. The scripts used for the data analysis are available upon demand at: francois-xavier.barre@i2bc.paris-saclay.fr

5. Microscopy assays

Cells were grown overnight in M9 fructose at 30°C and were diluted the next day in 5mL of M9 fructose at OD_{600}=0.02 and grown at 30°C until they reached OD_{600}=0.2. Snapshots of the cells were taken, and the number of green and red spots was counted for each strain. The analysis was done using MATLAB, mainly the software packages Microbe Tracker version 0.937.

6. Cell count monitoring

Cell cultures were grown in M9 minimal medium until OD_{600}=0.1. Once this target OD was reached, 20 μl of cells were added to 180 μl of LB broth and serially diluted (1:10) 8 times in LB. 20 μl of the dilutions were spotted on LB Agar plates and grown overnight at 30°C.

Annexes

Supplementary Table 1: *V. cholerae* strains used in this study

Name	Genotype	Reference
EPV50	*N16961 ChapR ΔlacZ*	*David et.al, 2014*
EEV29	*N16961 ChapR ΔlacZ P_{ara}-Cre-invP_{lac}::Zeo^R::FRT*	*Espinosa et.al, 2020*
EPV530	*N16961 ChapR ΔlacZ P_{ara}-Cre-invP_{lac}::Zeo^R::FRT ΔmukB::aadA1*	This study
EEV104[1]	MCH1 *ChapR ΔlacZ P_{ara}-Cre-invP_{lac}::Zeo^R::FRT*	*Espinosa et.al, 2020*
EEV111	*N16961 ChapR ΔlacZ P_{ara}-Cre-invP_{lac}::Zeo^R::FRT ΔVPI FRT::Amp ::FRT*	*Espinosa et.al, 2020*
JCV001[1]	MCH1 *ChapR ΔlacZ P_{ara}-Cre-invP_{lac}::Zeo^R::FRT ΔmukB::aadA1*	This study
JCV005[2]	ESC2 *ChapR ΔlacZ P_{ara}-Cre-invP_{lac}::Zeo^R::FRT*	This study
JCV007[2]	ESC2 *ChapR ΔlacZ P_{ara}-Cre-invP_{lac}::Zeo^R::FRT ΔmukBEF*	This study
JCV009[2]	ESC2 *ChapR ΔlacZ P_{ara}-Cre-invP_{lac}::Zeo^R::FRT mukB::spa tag*	This study
JCV011[1]	MCH1 *ChapR ΔlacZ P_{ara}-Cre-invP_{lac}::Zeo^R::FRT mukB::spa tag*	This study
JCV012	*N16961 ChapR ΔlacZ P_{ara}-Cre-invP_{lac}::Zeo^R::FRT ΔmukB::aadA1 ΔVPI-1*	This study
JCV014	*N16961 ChapR ΔlacZ P_{ara}-Cre-invP_{lac}::Zeo^R::FRT ΔmukB::aadA1 ΔmatP*	This study
JCV022	*N16961 ChapR lacO::Km::FRT inserted at 852955 tetR-parST1::Cm^R::FRT-tetR inserted at 1980369*	This study
JCV023	*N16961 ChapR ΔlacZ P_{lac}::lacI-RFPT-YGFP-$parB_{pMT1}$::Zeo::FRT lacO::Km::FRT inserted at 852955 tetR-parST1::Cm^R::FRT-tetR inserted at 1980369*	This study
JCV025	*N16961 ChapR ΔlacZ P_{lac}::lacI-RFPT-YGFP-$parB_{pMT1}$::Zeo::FRT lacO::Km::FRT inserted at 852955 tetR-parST1::Cm^R::FRT-tetR inserted at 1980369 ΔmukB::aadA1*	This study
JCV029	*N16961 ChapR ΔlacZ P_{lac}::lacI-RFPT-YGFP-$parB_{pMT1}$::Zeo::FRT lacO::Km::FRT inserted at 852955*	This study

	tetR-parST1::Cm^R::FRT-tetR inserted at 1980369 ΔmukB::aadA1 ΔVPI-1	
EGV23	*N16961 ChapR ΔlacZ Δ3parS1::aadA1*	This study
EGV23+212	*N16961 ChapR ΔlacZ Δ3parS1::aadA1 ΔmukB*	This study
ADV25	*N16961 ChapR ΔlacZ P$_{lac}$::lacI-RFPT-YGFP-parB$_{pMT1}$::Zeo::FRT lacO::Km::FRT inserted at 852955 tetR-parST1::Cm^R::FRT-tetR inserted at 2315403*	This study
ADV41	*N16961 ChapR ΔlacZ P$_{lac}$::lacI-RFPT-YGFP-parB$_{pMT1}$::Zeo::FRT lacO::Km::FRT inserted at 852955 tetR-parST1::Cm^R::FRT-tetR inserted at 2315403 ΔparS1*	This study
CP629	*N16961 ChapR ΔlacZ P$_{lac}$::lacI-RFPT-YGFP-parB$_{pMT1}$::Zeo::FRT lacO::Km::FRT inserted at 852955 tetR-parST1::Cm^R::FRT-tetR inserted at 2315403 ΔparS1 ΔmukB*	This study
JCV037	*N16961 ChapR ΔlacZ P$_{lac}$::lacI-RFPT-YGFP-parB$_{pMT1}$::Zeo::FRT lacO::Km::FRT inserted at 588074 tetR-parST1::Cm^R::FRT-tetR inserted at 64080 chr2*	This study
JCV038	*N16961 ChapR ΔlacZ P$_{lac}$::lacI-RFPT-YGFP-parB$_{pMT1}$::Zeo::FRT lacO::Km::FRT inserted at 588074 tetR-parST1::Cm^R::FRT-tetR inserted at 64080 chr2 ΔmukB*	This study
JCV040	*N16961 ChapR ΔlacZ P$_{lac}$::lacI-RFPT-YGFP-parB$_{pMT1}$::Zeo::FRT lacO::Km::FRT inserted at 588074 tetR-parST1::Cm^R::FRT-tetR inserted at 64080 chr2 ΔVPI-1 ΔparS1*	This study
JCV041	*N16961 ChapR ΔlacZ P$_{lac}$::lacI-RFPT-YGFP-parB$_{pMT1}$::Zeo::FRT lacO::Km::FRT inserted at 588074 tetR-parST1::Cm^R::FRT-tetR inserted at 64080 chr2 parS1 inserted at 5437ΔVPI-1 ΔparS1*	This study
JCV042	*N16961 ChapR ΔlacZ P$_{lac}$::lacI-RFPT-YGFP-parB$_{pMT1}$::Zeo::FRT lacO::Km::FRT inserted at 588074 tetR-parST1::Cm^R::FRT-tetR inserted at 64080 chr2 parS1 inserted at 5437ΔVPI-1 ΔparS1 ΔmukB*	This study
JCV043	*N16961 ChapR ΔlacZ P$_{lac}$::lacI-RFPT-YGFP-parB$_{pMT1}$::Zeo::FRT lacO::Km::FRT inserted at 588074 tetR-parST1::Cm^R::FRT-tetR inserted at 64080 chr2 ΔVPI-1 ΔparS1 ΔmukB*	This study
CP1023	*N16961 ChapR ΔlacZ P$_{ara}$-Cre-invP$_{lac}$::Zeo^R::FRT Δ3parS1::aadA1*	This study
CP902	*N16961 ChapR ΔlacZ ΔhubP:: Zeo^R*	This study

CP2131	*N16961 ChapR ⊿lacZ P_{ara}-Cre-invP_{lac}::Zeo^R::FRT ⊿VPI-1 ⊿parS1 ::aadA1*	This study
CP2136	*N16961 ChapR ⊿lacZ P_{ara}-Cre-invP_{lac}::Zeo^R::FRT ⊿VPI-1 ⊿parS1 ::aadA1 ⊿mukB*	This study
GDV28	*N16961 ChapR ⊿lacZ inducible xerC-aad1*	This study
EGV638[1]	*MCH1 ChapR ⊿matP inducible xerC-aad1*	This study
EGV641	*N16961 ChapR ⊿lacZ pBAD-Vib XerC-plac repression matS15 (all VC1488 between VCA0560 and VCA0561) matS15 (in VC1488) deletion with FRT-spec-FRT*	This study
JVV013	*N16961 ChapR ΔlacZ | lacZ::attP::lacZ inserted at 1360156 ViXerC-D -VC1465 arabinose inducible in Ts vector with inversion seq between attP site and dif1 (VC1616 to VC1452: 1360160 to dif) pBAD-Vib XerC-plac repression*	This study
JVV018	*N16961 ChapR ΔlacZ | lacZ::attP::lacZ inserted at 1360156 ViXerC-D -VC1465 arabinose inducible in Ts vector with inversion seq between attP site and dif1 (VC1616 to VC1452: 1360160 to dif) pBAD-Vib XerC-plac repression ⊿matP*	This study
JMDV53	*N16961 ChapR ⊿lacZ mukB-3xFlag*	This study

[1]: Derived from MonoChromosomal strain (MCH1)
[2]: Derived from Equal Sized Chromosomes strain (ESC2)
Both strains are described in (Val et al., 2014)

E. coli strains used in this study

Strain	Genotype	Reference
MG1655-matP	*MG1655 matP::spatag*	Boccard Laboratory

Supplementary Table 2: plasmids used in this study

Name	Description	Reference
pPOS175	Up region-*mukB*-DW region, Cml^R, Spec^R	This study
pJMD19	FRT-*mukB::spatag*-FRT, Amp^R, Zeo^R	This study
pEE54	tetR FRT-parST1-FRT at VC1042, Cml^R	This study
pEE44	VPI-1, Amp^R, Cml^R	*Espinosa et.al, 2020*

pPOS188	*parS1*, Zeo^R	This study
pPOS185	*parS1* at R1I	This study

Supplementary Table 3: final concentration of antibiotics and other chemicals used in this study

Chemical	Final concentration
Antibiotics	
Ampicillin	100 µg/mL
Chloramphenicol	5 µg/mL (*V. cholerae*) / 25 µg/mL (*E. coli*)
Gentamycin	10 µg/mL
Kanamycin	50 µg/mL
Rifampicin	1 µg/mL (*V. cholerae*) / 150 µg/mL (*E. coli*)
Spectinomycin	50 µg/mL
Streptomycin	200 µg/mL
Zeocin	25 µg/mL
Other chemicals	
IPTG	0.1-1 mM
DAP	0.3 mM

Supplementary Table 4: List of oligonucleotides and adapters used for the construction of the Hi-SC2 libraries in this study

Oligonucleotides	Source
3459: 5'- TTGGATGATAAGTCCCCGGTC-3'	(Espinosa et al., 2020)
1514: 5'- TGACGAGTTCTTCTGAGCGGGACTCTGG-3'	(Espinosa et al., 2020)
Adapter 3455: 5'- TTCCCTACACGACGCTCTTCCGATCTCAGTNN-3'	(Espinosa et al., 2020)
Adapter 3456: 5'- ACTGAGATCGGAAGAGCGTCGTGTAGGG-3'	(Espinosa et al., 2020)
Adapter 3811: 5'- TTCCCTACACGACGCTCTTCCGATCTCGTANN-3'	(Espinosa et al., 2020)
Adapter 3812: 5'- TACGAGATCGGAAGAGCGTCGTGTAGGG-3'	(Espinosa et al., 2020)
Adapter 3813: 5'- TTCCCTACACGACGCTCTTCCGATCTACAGTNN-3'	(Espinosa et al., 2020)
Adapter 3814: 5'- ACTGTAGATCGGAAGAGCGTCGTGTAGGG-3'	(Espinosa et al., 2020)
Adapter 3815: 5'- TTCCCTACACGACGCTCTTCCGATCTTACTCNN-3'	(Espinosa et al., 2020)

Adapter 3816: 5’- GAGTAAGATCGGAAGAGCGTCGTGTAGGG-3’	(Espinosa et al., 2020)
Adapter 3817: 5’- TTCCCTACACGACGCTCTTCCGATCTCTAGTNN-3’	(Espinosa et al., 2020)
Adapter 3818: 5‘- ACTAGAGATCGGAAGAG CGTCGTGTAGGG-3’	(Espinosa et al., 2020)
Adapter 3819: 5’- TTCCCTACACGACGCTCTTCCGATCTTGACTCNN-3’	(Espinosa et al., 2020)
Adapter 3820: 5’- GAGTCAAGATCGGAAGAGCGTCGTGTAGGG-3’	(Espinosa et al., 2020)
Adapter 3821: 5’- TTCCCTACACGACGCTCTTCCGATCTATGCTANN-3’	(Espinosa et al., 2020)
Adapter 3822: 5’- TAGCATAGATCGGAAGAGCGTCGTGTAGGG-3’	(Espinosa et al., 2020)
Adapter 3823: 5’- TTCCCTACACGACGCTCTTCCGATCTAGCATANN-3’	(Espinosa et al., 2020)
Adapter 3824: 5’- TATGCTAGATCGGAAGAGCGTCGTGTAGGG-3’	(Espinosa et al., 2020)
P5 NGS 3457: 5’- AATGATACGGCGACCACCGAGATCTACACTCTTTCCCTACACGACGCTCTTCCGATCTCAGT-3’	(Espinosa et al., 2020)
P5 NGS 3825: 5’- AATGATACGGCGACCACCGAGATCTACACTCTTTCCCTACACGACGCTCTTCCGATCTCGTA-3’	(Espinosa et al., 2020)
P5 NGS 3826: 5’- AATGATACGGCGACCACCGAGATCTACACTCTTTCCCTACACGACGCTCTTCCGATCTACAGT-3’	(Espinosa et al., 2020)
P5 NGS 3827: 5’- AATGATACGGCGACCACC GAGATCTACACTCTTTCCCT ACACGACGCTCTTCCGATCTTACTC-3’	(Espinosa et al., 2020)
P5 NGS 3828: 5’- AATGATACGGCGACCACCGAGATCTACACTCTTTCCCTACACGACGCTCTTCCGATCTCTAGT-3’	(Espinosa et al., 2020)
P5 NGS 3829: 5’- AATGATACGGCGACCACCGAGATCTACACTCTTTCCCTACACGACGCTCTTCCGATCTTGACTC-3’	(Espinosa et al., 2020)
P5 NGS 3830: 5’- AATGATACGGCGACCACCGAGATCTACACTCTTTCCCTACACGACGCTCTTCCGATCTATGCTA-3’	(Espinosa et al., 2020)
P5 NGS 3831: 5’- AATGATACGGCGACCACCGAGATCTACACTCTTTCCCTACACGACGCTCTTCCGATCTAGCATA-3’	(Espinosa et al., 2020)
P7 NGS*: 5’- CAAGCAGAAGACG GCATACGAGATxxxxxxGTGACTGGAGTTCAGACGTGTGCTCTTCCGATCTTCTA-3’	(Espinosa et al., 2020)
C : 5’- ATGATACGGCGACCACCGAGATCTACAC-3’	I2BC sequencing platform
D: 5’- CAAGCAGAAGACGGCATACGAGAT-3’	I2BC sequencing platform

* xxxxxx corresponds to a six-based sequence index for Illumina. Multiple primers with different barcodes were prepared for this study as each sample needed its own barcode.

Supplementary Table 5: List of the Hi-SC2 experiments with total number of reads

Strain	Sequencing run	SSR system	Time point (mins)	Total number of reads
EEV105	FX404	Cre	90	14 358 163
EEV29	FX779	Cre	90	18 417 701
JCV005	FX385	Cre	90	17 896 572

EEV95	FX408	Cre	90	50 280 228
EEV29	FX205	XerC/D	300	17 064 073
EGV637	FX777	XerC/D	300	21 427 829
EGV638	FX807	XerC/D	300	7 793 010
EEV92	FX379	XerC/D	300	10 867 436
JVV013	FX700	XerC/D	300	24 027 138
EGV641	FX801	XerC/D	300	7 385 917
EPV530	FX785	Cre	90	20 756 844
EEV112	FX243	Cre	90	20 007 446
JCV012	FX813_3	Cre	90	13 934 430
CP1023	FX813_5	Cre	90	13 884 945
CP2131	FX809	Cre	90	15 900 680
CP2136	FX811	Cre	90	16 606 168
JCV001	FX406	Cre	90	10 334 811
JCV007	FX383	Cre	90	16 866 695

Bibliography

Abeles, A. L., Friedman, S. A., & Austin, S. J. (1985). Partition of unit-copy miniplasmids to daughter cells. *Journal of Molecular Biology*, *185*(2), 261–272. https://doi.org/10.1016/0022-2836(85)90402-4

Adachi, S., Fukushima, T., & Hiraga, S. (2008). Dynamic events of sister chromosomes in the cell cycle of Escherichia coli: Chromosomal events in E. coli. *Genes to Cells*, *13*(2), 181–197. https://doi.org/10.1111/j.1365-2443.2007.01157.x

Ah-Seng, Y., Rech, J., Lane, D., & Bouet, J.-Y. (2013). Defining the Role of ATP Hydrolysis in Mitotic Segregation of Bacterial Plasmids. *PLoS Genetics*, *9*(12), e1003956. https://doi.org/10.1371/journal.pgen.1003956

Albert, M. J. (1996). Epidemiology & molecular biology of *Vibrio cholerae* O139 Bengal. *The Indian Journal of Medical Research*, *104*, 14–27.

Allman, R., Schjerven, T., & Boye, E. (1991). Cell cycle parameters of Escherichia coli K-12. *Journal of Bacteriology*, *173*(24), 7970–7974. https://doi.org/10.1128/jb.173.24.7970-7974.1991

Ashley, R. E., Dittmore, A., McPherson, S. A., Turnbough, C. L., Neuman, K. C., & Osheroff, N. (2017). Activities of gyrase and topoisomerase IV on positively supercoiled DNA. *Nucleic Acids Research*, *45*(16), 9611–9624. https://doi.org/10.1093/nar/gkx649

Ayala, J. C., Silva, A. J., & Benitez, J. A. (2017). H-NS: An overarching regulator of the *Vibrio cholerae* life cycle. *Research in Microbiology*, *168*(1), 16–25. https://doi.org/10.1016/j.resmic.2016.07.007

Azam, T. A., & Ishihama, A. (1999). Twelve Species of the Nucleoid-associated Protein from Escherichia coli. *Journal of Biological Chemistry*, *274*(46), 33105–33113. https://doi.org/10.1074/jbc.274.46.33105

Baek, J. H., & Chattoraj, D. K. (2014). Chromosome I Controls Chromosome II Replication in *Vibrio cholerae*. *PLoS Genetics*, *10*(2), e1004184. https://doi.org/10.1371/journal.pgen.1004184

Baker, T. A., Sekimizu, K., Funnell, B. E., & Kornberg, A. (1986). Extensive unwinding of the plasmid template during staged enzymatic initiation of DNA replication from the origin of the Escherichia coli chromosome. *Cell*, *45*(1), 53–64. https://doi.org/10.1016/0092-8674(86)90537-4

Basu, A., Parente, A. C., & Bryant, Z. (2016). Structural Dynamics and Mechanochemical Coupling in DNA Gyrase. *Journal of Molecular Biology*, *428*(9), 1833–1845. https://doi.org/10.1016/j.jmb.2016.03.016

Bates, D., & Kleckner, N. (2005). Chromosome and Replisome Dynamics in E. coli: Loss of Sister Cohesion Triggers Global Chromosome Movement and Mediates Chromosome Segregation. *Cell*, *121*(6), 899–911. https://doi.org/10.1016/j.cell.2005.04.013

Beattie, T. R., & Reyes-Lamothe, R. (2015). A Replisome's journey through the bacterial chromosome. *Frontiers in Microbiology*, *6*. https://doi.org/10.3389/fmicb.2015.00562

Bi, E., & Lutkenhaus, J. (1991). FtsZ ring structure associated with division in Escherichia coli. *Nature*, *354*(6349), 161–164. https://doi.org/10.1038/354161a0

Bigot, S., Saleh, O. A., Cornet, F., Allemand, J.-F., & Barre, F. (2006). Oriented loading of FtsK on KOPS. *Nature Structural & Molecular Biology*, *13*(11), 1026–1028. https://doi.org/10.1038/nsmb1159

Bigot, S., Saleh, O. A., Lesterlin, C., Pages, C., El Karoui, M., Dennis, C., Grigoriev, M., Allemand, J.-F., Barre, F.-X., & Cornet, F. (2005). KOPS: DNA motifs that control E. coli chromosome segregation by orienting the FtsK translocase. *The EMBO Journal*, *24*(21), 3770–3780. https://doi.org/10.1038/sj.emboj.7600835

Boucher, Y., Labbate, M., Koenig, J. E., & Stokes, H. W. (2007). Integrons: Mobilizable platforms that promote genetic diversity in bacteria. *Trends in Microbiology*, *15*(7), 301–309. https://doi.org/10.1016/j.tim.2007.05.004

Bouet, J.-Y., & Funnell, B. E. (2019). Plasmid Localization and Partition in *Enterobacteriaceae*. *EcoSal Plus*, *8*(2), ecosalplus.ESP-0003-2019. https://doi.org/10.1128/ecosalplus.ESP-0003-2019

Bouet, J.-Y., Stouf, M., Lebailly, E., & Cornet, F. (2014). Mechanisms for chromosome segregation. *Current Opinion in Microbiology*, *22*, 60–65. https://doi.org/10.1016/j.mib.2014.09.013

Brezellec, P., Hoebeke, M., Hiet, M.-S., Pasek, S., & Ferat, J.-L. (2006). DomainSieve: A protein domain-based screen that led to the identification of dam-associated genes with potential link to DNA maintenance. *Bioinformatics*, *22*(16), 1935–1941. https://doi.org/10.1093/bioinformatics/btl336

Brézellec, P., Vallet-Gely, I., Possoz, C., Quevillon-Cheruel, S., & Ferat, J.-L. (2016). DciA is an ancestral replicative helicase operator essential for bacterial replication initiation. *Nature Communications*, *7*(1), 13271. https://doi.org/10.1038/ncomms13271

Brown, P. O., & Cozzarelli, N. R. (1979). A Sign Inversion Mechanism for Enzymatic Supercoiling of DNA. *Science*, *206*(4422), 1081–1083. https://doi.org/10.1126/science.227059

Broyles, S. S., & Pettijohn, D. E. (1986). Interaction of the Escherichia coli HU protein with DNA. *Journal of Molecular Biology*, *187*(1), 47–60. https://doi.org/10.1016/0022-2836(86)90405-5

Bürmann, F., Funke, L. F. H., Chin, J. W., & Löwe, J. (2021). Cryo-EM structure of MukBEF reveals DNA loop entrapment at chromosomal unloading sites. *Molecular Cell*, *81*(23), 4891-4906.e8. https://doi.org/10.1016/j.molcel.2021.10.011

Cairns, J. (1963). The bacterial chromosome and its manner of replication as seen by autoradiography. *Journal of Molecular Biology*, *6*(3), 208-IN5. https://doi.org/10.1016/S0022-2836(63)80070-4

Cho, H., McManus, H. R., Dove, S. L., & Bernhardt, T. G. (2011). Nucleoid occlusion factor SlmA is a DNA-activated FtsZ polymerization antagonist. *Proceedings of the National Academy of Sciences*, *108*(9), 3773–3778. https://doi.org/10.1073/pnas.1018674108

Cobbe, N., & Heck, M. M. S. (2004). The Evolution of SMC Proteins: Phylogenetic Analysis and Structural Implications. *Molecular Biology and Evolution*, *21*(2), 332–347. https://doi.org/10.1093/molbev/msh023

Collis, C. M., Grammaticopoulos, G., Briton, J., Stokes, H. W., & Hall, R. M. (1993). Site-specific insertion of gene cassettes into integrons. *Molecular Microbiology*, *9*(1), 41–52. https://doi.org/10.1111/j.1365-2958.1993.tb01667.x

Conin, B., Billault-Chaumartin, I., El Sayyed, H., Quenech'Du, N., Cockram, C., Koszul, R., & Espéli, O. (2022). Extended sister-chromosome catenation leads to massive reorganization of the *E. coli* genome. *Nucleic Acids Research*, gkac105. https://doi.org/10.1093/nar/gkac105

Crisona, N. J., Strick, T. R., Bensimon, D., Croquette, V., & Cozzarelli, N. R. (2000). Preferential relaxation of positively supercoiled DNA by E. coli topoisomerase IV in single-molecule and ensemble measurements. *Genes & Development*, *14*(22), 2881–2892. https://doi.org/10.1101/gad.838900

Crooks, G. E., Hon, G., Chandonia, J.-M., & Brenner, S. E. (2004). WebLogo: A sequence logo generator. *Genome Research*, *14*(6), 1188–1190. https://doi.org/10.1101/gr.849004

Crozat, E., Tardin, C., Salhi, M., Rousseau, P., Lablaine, A., Bertoni, T., Holcman, D., Sclavi, B., Cicuta, P., & Cornet, F. (2019). *Post-replicative pairing of sister* ter *regions in* Escherichia coli *involves multiple activities of MatP* [Preprint]. Microbiology. https://doi.org/10.1101/755397

Cui, Y., Petrushenko, Z. M., & Rybenkov, V. V. (2008). MukB acts as a macromolecular clamp in DNA condensation. *Nature Structural & Molecular Biology*, *15*(4), 411–418. https://doi.org/10.1038/nsmb.1410

David, A., Demarre, G., Muresan, L., Paly, E., Barre, F.-X., & Possoz, C. (2014). The Two Cis-Acting Sites, parS1 and oriC1, Contribute to the Longitudinal Organisation of *Vibrio cholerae* Chromosome I. *PLoS Genetics*, *10*(7), e1004448. https://doi.org/10.1371/journal.pgen.1004448

Demarre, G., Galli, E., & Barre, F.-X. (2013). The FtsK Family of DNA Pumps. In M. Spies (Ed.), *DNA Helicases and DNA Motor Proteins* (Vol. 767, pp. 245–262). Springer New York. https://doi.org/10.1007/978-1-4614-5037-5_12

Demarre, G., Galli, E., Muresan, L., Paly, E., David, A., Possoz, C., & Barre, F.-X. (2014). Differential Management of the Replication Terminus Regions of the Two *Vibrio cholerae* Chromosomes during Cell Division. *PLoS Genetics*, *10*(9), e1004557. https://doi.org/10.1371/journal.pgen.1004557

den Blaauwen, T. (2013). Prokaryotic cell division: Flexible and diverse. *Current Opinion in Microbiology*, *16*(6), 738–744. https://doi.org/10.1016/j.mib.2013.09.002

diCenzo, G. C., & Finan, T. M. (2017). The Divided Bacterial Genome: Structure, Function, and Evolution. *Microbiology and Molecular Biology Reviews*, *81*(3). https://doi.org/10.1128/MMBR.00019-17

Ding, Q., & Tan, K. S. (2017). Himar1 Transposon for Efficient Random Mutagenesis in Aggregatibacter actinomycetemcomitans. *Frontiers in Microbiology*, *8*, 1842. https://doi.org/10.3389/fmicb.2017.01842

Dorman, C. J. (2004). H-NS: A universal regulator for a dynamic genome. *Nature Reviews Microbiology*, *2*(5), 391–400. https://doi.org/10.1038/nrmicro883

Du, S., & Lutkenhaus, J. (2017). Assembly and activation of the *Escherichia coli* divisome: The *E. coli* divisome. *Molecular Microbiology*, *105*(2), 177–187. https://doi.org/10.1111/mmi.13696

Duderstadt, K. E., & Berger, J. M. (2008). AAA+ ATPases in the Initiation of DNA Replication. *Critical Reviews in Biochemistry and Molecular Biology*, *43*(3), 163–187. https://doi.org/10.1080/10409230802058296

Duggin, I. G., Wake, R. G., Bell, S. D., & Hill, T. M. (2008). The replication fork trap and termination of chromosome replication. *Molecular Microbiology*, *70*(6), 1323–1333. https://doi.org/10.1111/j.1365-2958.2008.06500.x

Dumont, S., & Mitchison, T. J. (2009). Force and Length in the Mitotic Spindle. *Current Biology*, *19*(17), R749–R761. https://doi.org/10.1016/j.cub.2009.07.028

Durand, D., Li de la Sierra-Gallay, I., Brooks, M. A., Thompson, A. W., Lazar, N., Lisboa, J., van Tilbeurgh, H., & Quevillon-Cheruel, S. (2012). Expression, purification and preliminary structural analysis of *Escherichia coli* MatP in complex with the *matS* DNA site. *Acta Crystallographica Section F Structural Biology and Crystallization Communications*, *68*(6), 638–643. https://doi.org/10.1107/S1744309112011062

Ebersbach, G., Galli, E., Møller-Jensen, J., Löwe, J., & Gerdes, K. (2008). Novel coiled-coil cell division factor ZapB stimulates Z ring assembly and cell division. *Molecular Microbiology*, *68*(3), 720–735. https://doi.org/10.1111/j.1365-2958.2008.06190.x

Ebersbach, G., & Gerdes, K. (2001). The double par locus of virulence factor pB171: DNA segregation is correlated with oscillation of ParA. *Proceedings of the National Academy of Sciences*, *98*(26), 15078–15083. https://doi.org/10.1073/pnas.261569598

El Sayyed, H., Le Chat, L., Lebailly, E., Vickridge, E., Pages, C., Cornet, F., Cosentino Lagomarsino, M., & Espéli, O. (2016). Mapping Topoisomerase IV Binding and Activity Sites on the E. coli Genome. *PLOS Genetics*, *12*(5), e1006025. https://doi.org/10.1371/journal.pgen.1006025

Espéli, O., Borne, R., Dupaigne, P., Thiel, A., Gigant, E., Mercier, R., & Boccard, F. (2012). A MatP-divisome interaction coordinates chromosome segregation with cell division in *E. coli*: Chromosome-divisome interplay. *The EMBO Journal*, *31*(14), 3198–3211. https://doi.org/10.1038/emboj.2012.128

Espeli, O., & Marians, K. J. (2004). Untangling intracellular DNA topology: Untwisting the chromosome. *Molecular Microbiology*, *52*(4), 925–931. https://doi.org/10.1111/j.1365-2958.2004.04047.x

Espinosa, E., Barre, F.-X., & Galli, E. (2017). Coordination between replication, segregation and cell division in multi-chromosomal bacteria: Lessons from *Vibrio cholerae*. *International Microbiology. Official Journal of the Spanish Society for Microbiology*, *20*, 121–129. https://doi.org/10.2436/20.1501.01.293

Espinosa, E., Paly, E., & Barre, F.-X. (2020). High-Resolution Whole-Genome Analysis of Sister-Chromatid Contacts. *Molecular Cell*, *79*(5), 857-869.e3. https://doi.org/10.1016/j.molcel.2020.06.033

Espinosa, E., Yamaichi, Y., & Barre, F.-X. (2020). Protocol for High-Throughput Analysis of Sister-Chromatids Contacts. *STAR Protocols*, *1*(3), 100202. https://doi.org/10.1016/j.xpro.2020.100202

Ferrandiz, M.-J., Martin-Galiano, A. J., Schvartzman, J. B., & de la Campa, A. G. (2010). The genome of Streptococcus pneumoniae is organized in topology-reacting gene clusters. *Nucleic Acids Research*, *38*(11), 3570–3581. https://doi.org/10.1093/nar/gkq106

Fiebig, A., Keren, K., & Theriot, J. A. (2006). Fine-scale time-lapse analysis of the biphasic, dynamic behaviour of the two *Vibrio cholerae* chromosomes. *Molecular Microbiology*, *60*(5), 1164–1178. https://doi.org/10.1111/j.1365-2958.2006.05175.x

Fitzgerald, S., Kary, S. C., Alshabib, E. Y., MacKenzie, K. D., Stoebel, D. M., Chao, T.-C., & Cameron, A. D. S. (2020). Redefining the H-NS protein family: A diversity of specialized core and accessory forms exhibit hierarchical transcriptional network integration. *Nucleic Acids Research*, *48*(18), 10184–10198. https://doi.org/10.1093/nar/gkaa709

Forterre, P., & Gadelle, D. (2009). Phylogenomics of DNA topoisomerases: Their origin and putative roles in the emergence of modern organisms. *Nucleic Acids Research*, *37*(3), 679–692. https://doi.org/10.1093/nar/gkp032

Fung, E. (2001). Probing the ATP-binding site of P1 ParA: Partition and repression have different requirements for ATP binding and hydrolysis. *The EMBO Journal*, *20*(17), 4901–4911. https://doi.org/10.1093/emboj/20.17.4901

Funnell, B. E. (2016). ParB Partition Proteins: Complex Formation and Spreading at Bacterial and Plasmid Centromeres. *Frontiers in Molecular Biosciences*, *3*. https://doi.org/10.3389/fmolb.2016.00044

Gadde, S., & Heald, R. (2004). Mechanisms and Molecules of the Mitotic Spindle. *Current Biology*, *14*(18), R797–R805. https://doi.org/10.1016/j.cub.2004.09.021

Galli, E., Ferat, J.-L., Desfontaines, J.-M., Val, M.-E., Skovgaard, O., Barre, F.-X., & Possoz, C. (2019). Replication termination without a replication fork trap. *Scientific Reports*, *9*(1), 8315. https://doi.org/10.1038/s41598-019-43795-2

Galli, E., Poidevin, M., Le Bars, R., Desfontaines, J.-M., Muresan, L., Paly, E., Yamaichi, Y., & Barre, F.-X. (2016). Cell division licensing in the multi-chromosomal *Vibrio cholerae* bacterium. *Nature Microbiology*, *1*(9), 16094. https://doi.org/10.1038/nmicrobiol.2016.94

Galli, E., Midonet, C., Paly, E., & Barre, F.-X. (2017). Fast growth conditions uncouple the final stages of chromosome segregation and cell division in Escherichia coli. *PLOS Genetics*, *13*(3), e1006702. https://doi.org/10.1371/journal.pgen.1006702

Gerdes, K., Møller-Jensen, J., & Jensen, R. B. (2002). Plasmid and chromosome partitioning: Surprises from phylogeny: Phylogeny of partitioning ATPases. *Molecular Microbiology*, *37*(3), 455–466. https://doi.org/10.1046/j.1365-2958.2000.01975.x

Gilson, P. R., & Beech, P. L. (2001). Cell division protein FtsZ: Running rings around bacteria, chloroplasts and mitochondria. *Research in Microbiology*, *152*(1), 3–10. https://doi.org/10.1016/S0923-2508(00)01162-1

Graham, T. G. W., Wang, X., Song, D., Etson, C. M., van Oijen, A. M., Rudner, D. Z., & Loparo, J. J. (2014). ParB spreading requires DNA bridging. *Genes & Development*, *28*(11), 1228–1238. https://doi.org/10.1101/gad.242206.114

Grill, S. W., & Hyman, A. A. (2005). Spindle Positioning by Cortical Pulling Forces. *Developmental Cell*, *8*(4), 461–465. https://doi.org/10.1016/j.devcel.2005.03.014

Gueiros-Filho, F. J., & Losick, R. (2002). A widely conserved bacterial cell division protein that promotes assembly of the tubulin-like protein FtsZ. *Genes & Development*, *16*(19), 2544–2556. https://doi.org/10.1101/gad.1014102

Haering, C. H., Löwe, J., Hochwagen, A., & Nasmyth, K. (2002). Molecular Architecture of SMC Proteins and the Yeast Cohesin Complex. *Molecular Cell*, *9*(4), 773–788. https://doi.org/10.1016/S1097-2765(02)00515-4

Harrison, P. W., Lower, R. P. J., Kim, N. K. D., & Young, J. P. W. (2010). Introducing the bacterial 'chromid': Not a chromosome, not a plasmid. *Trends in Microbiology*, *18*(4), 141–148. https://doi.org/10.1016/j.tim.2009.12.010

Hayakawa, T., Tanaka, T., Sakaguchi, K., Otake, N., & Yonehara, H. (1979). A linear plasmid-like DNA in Streptomyces SP producting lankacidin group antibiotics. *The Journal of General and Applied Microbiology*, *25*(4), 255–260. https://doi.org/10.2323/jgam.25.255

Hayama, R., & Marians, K. J. (2010). Physical and functional interaction between the condensin MukB and the decatenase topoisomerase IV in *Escherichia coli*. *Proceedings of the National Academy of Sciences*, *107*(44), 18826–18831. https://doi.org/10.1073/pnas.1008140107

Hayes, F., & Barillà, D. (2006). The bacterial segrosome: A dynamic nucleoprotein machine for DNA trafficking and segregation. *Nature Reviews Microbiology*, *4*(2), 133–143. https://doi.org/10.1038/nrmicro1342

Heidelberg, J. F., Eisen, J. A., Nelson, W. C., Clayton, R. A., Gwinn, M. L., Dodson, R. J., Haft, D. H., Hickey, E. K., Peterson, J. D., Umayam, L., Gill, S. R., Nelson, K. E., Read, T. D., Tettelin, H., Richardson, D., Ermolaeva, M. D., Vamathevan, J., Bass, S., Qin, H., … Fraser, C. M. (2000). DNA sequence of both chromosomes of the cholera pathogen *Vibrio cholerae*. *Nature*, *406*(6795), 477–483. https://doi.org/10.1038/35020000

Hill, T. M., & Marians, K. J. (1990). Escherichia coli Tus protein acts to arrest the progression of DNA replication forks in vitro. *Proceedings of the National Academy of Sciences*, *87*(7), 2481–2485. https://doi.org/10.1073/pnas.87.7.2481

Hoess, R. H., & Abremski, K. (1985). Mechanism of strand cleavage and exchange in the Cre-lox site-specific recombination system. *Journal of Molecular Biology*, *181*(3), 351–362. https://doi.org/10.1016/0022-2836(85)90224-4

Hofmann, A., Mäkelä, J., Sherratt, D. J., Heermann, D., & Murray, S. M. (2019). Self-organised segregation of bacterial chromosomal origins. *ELife*, *8*, e46564. https://doi.org/10.7554/eLife.46564

Hoffmann, S. A., Wohltat, C., Müller, K. M., & Arndt, K. M. (2017). A user-friendly, low-cost turbidostat with versatile growth rate estimation based on an extended Kalman filter. *PLOS ONE*, *12*(7), e0181923. https://doi.org/10.1371/journal.pone.0181923

Hołówka, J., & Zakrzewska-Czerwińska, J. (2020). Nucleoid Associated Proteins: The Small Organizers That Help to Cope With Stress. *Frontiers in Microbiology*, *11*, 590. https://doi.org/10.3389/fmicb.2020.00590

Hyperactive transposase mutants of the Himar1 mariner transposon. *Proceedings of the National Academy of Sciences*, *96*(20), 11428–11433. https://doi.org/10.1073/pnas.96.20.11428

Iwanaga M, Y. K. (1985). New Medium for the Production of Cholera Toxin by *Vibrio cholerae* O1 Biotype El Tor. *Journal of Clinical Biology*, *22*(3), 405–408.

Jacob, F., Brenner, S., & Cuzin, F. (1963). On the Regulation of DNA Replication in Bacteria. *Cold Spring Harbor Symposia on Quantitative Biology*, *28*(0), 329–348. https://doi.org/10.1101/SQB.1963.028.01.048

Jalal, A. S., Tran, N. T., & Le, T. B. (2020). ParB spreading on DNA requires cytidine triphosphate in vitro. *ELife*, *9*, e53515. https://doi.org/10.7554/eLife.53515

Jensen, R. B. (2001). A moving DNA replication factory in Caulobacter crescentus. *The EMBO Journal*, *20*(17), 4952–4963. https://doi.org/10.1093/emboj/20.17.4952

Johnson, R. C., Johnson, L. M., Schmidt, J. W., & Gardner, J. F. (2014). Major Nucleoid Proteins in the Structure and Function of the *Escherichia coli* Chromosome. In N. P. Higgins (Ed.), *The Bacterial Chromosome* (pp. 65–132). ASM Press. https://doi.org/10.1128/9781555817640.ch5

Joshi, M. C., Bourniquel, A., Fisher, J., Ho, B. T., Magnan, D., Kleckner, N., & Bates, D. (2011). *Escherichia coli* sister chromosome separation includes an abrupt global transition with concomitant release of late-splitting intersister snaps. *Proceedings of the National Academy of Sciences*, *108*(7), 2765–2770. https://doi.org/10.1073/pnas.1019593108

Joshi, M. C., Magnan, D., Montminy, T. P., Lies, M., Stepankiw, N., & Bates, D. (2013). Regulation of Sister Chromosome Cohesion by the Replication Fork Tracking Protein SeqA. *PLoS Genetics*, *9*(8), e1003673. https://doi.org/10.1371/journal.pgen.1003673

Junier, I., Boccard, F., & Espéli, O. (2014). Polymer modeling of the E. coli genome reveals the involvement of locus positioning and macrodomain structuring for the control of chromosome conformation and segregation. *Nucleic Acids Research*, *42*(3), 1461–1473. https://doi.org/10.1093/nar/gkt1005

Kaguni, J. M. (2011). Replication initiation at the Escherichia coli chromosomal origin. *Current Opinion in Chemical Biology*, *15*(5), 606–613. https://doi.org/10.1016/j.cbpa.2011.07.016

Kaguni, J. M. (2014). DnaA, DnaB, and DnaC. In E. Bell (Ed.), *Molecular Life Sciences* (pp. 1–14). Springer New York. https://doi.org/10.1007/978-1-4614-6436-5_142-1

Kahramanoglou, C., Seshasayee, A. S. N., Prieto, A. I., Ibberson, D., Schmidt, S., Zimmermann, J., Benes, V., Fraser, G. M., & Luscombe, N. M. (2011). Direct and indirect effects of H-NS and Fis on global gene expression control in Escherichia coli. *Nucleic Acids Research*, *39*(6), 2073–2091. https://doi.org/10.1093/nar/gkq934

Kamashev, D. (2000). The histone-like protein HU binds specifically to DNA recombination and repair intermediates. *The EMBO Journal*, *19*(23), 6527–6535. https://doi.org/10.1093/emboj/19.23.6527

Kang, S., Han, J. S., Park, J. H., Skarstad, K., & Hwang, D. S. (2003). SeqA Protein Stimulates the Relaxing and Decatenating Activities of Topoisomerase IV. *Journal of Biological Chemistry*, *278*(49), 48779–48785. https://doi.org/10.1074/jbc.M308843200

Karaboja, X., Ren, Z., Brandão, H. B., Paul, P., Rudner, D. Z., & Wang, X. (2021). XerD unloads bacterial SMC complexes at the replication terminus. *Molecular Cell*, *81*(4), 756-766.e8. https://doi.org/10.1016/j.molcel.2020.12.027

Katayama, T., Ozaki, S., Keyamura, K., & Fujimitsu, K. (2010). Regulation of the replication cycle: Conserved and diverse regulatory systems for DnaA and oriC. *Nature Reviews Microbiology*, *8*(3), 163–170. https://doi.org/10.1038/nrmicro2314

Kawakami, H., Keyamura, K., & Katayama, T. (2005). Formation of an ATP-DnaA-specific Initiation Complex Requires DnaA Arginine 285, a Conserved Motif in the AAA+ Protein Family. *Journal of Biological Chemistry*, *280*(29), 27420–27430. https://doi.org/10.1074/jbc.M502764200

Kawalek, A., Wawrzyniak, P., Bartosik, A. A., & Jagura-Burdzy, G. (2020). Rules and Exceptions: The Role of Chromosomal ParB in DNA Segregation and Other Cellular Processes. *Microorganisms*, *8*(1), 105. https://doi.org/10.3390/microorganisms8010105

Kemter, F. S., Messerschmidt, S. J., Schallopp, N., Sobetzko, P., Lang, E., Bunk, B., Spröer, C., Teschler, J. K., Yildiz, F. H., Overmann, J., & Waldminghaus, T. (2018). Synchronous termination of replication of the two chromosomes is an evolutionary selected feature in Vibrionaceae. *PLOS Genetics*, *14*(3), e1007251. https://doi.org/10.1371/journal.pgen.1007251

Kirkup, B. C., Chang, L., Chang, S., Gevers, D., & Polz, M. F. (2010). Vibrio chromosomes share common history. *BMC Microbiology*, *10*(1), 137. https://doi.org/10.1186/1471-2180-10-137

Kleine Borgmann, L. A. K., Hummel, H., Ulbrich, M. H., & Graumann, P. L. (2013). SMC Condensation Centers in Bacillus subtilis Are Dynamic Structures. *Journal of Bacteriology*, *195*(10), 2136–2145. https://doi.org/10.1128/JB.02097-12

Koch, B., Ma, X., & Løbner-Olesen, A. (2010). Replication of *Vibrio cholerae* Chromosome I in Escherichia coli: Dependence on Dam Methylation. *Journal of Bacteriology*, *192*(15), 3903–3914. https://doi.org/10.1128/JB.00311-10

Kornberg, A., & Baker, T. A. (2005). *DNA replication* (2. ed., paperback ed). University Science Books.

Kreuzer, K. N., & Cozzarelli, N. R. (1980). Formation and resolution of DNA catenanes by DNA gyrase. *Cell*, *20*(1), 245–254. https://doi.org/10.1016/0092-8674(80)90252-4

Lang, B., Blot, N., Bouffartigues, E., Buckle, M., Geertz, M., Gualerzi, C. O., Mavathur, R., Muskhelishvili, G., Pon, C. L., Rimsky, S., Stella, S., Babu, M. M., & Travers, A. (2007). High-affinity DNA binding sites for H-NS provide a molecular basis for selective silencing within proteobacterial genomes. *Nucleic Acids Research*, *35*(18), 6330–6337. https://doi.org/10.1093/nar/gkm712

Le, T. B. K., Imakaev, M. V., Mirny, L. A., & Laub, M. T. (2013). High-Resolution Mapping of the Spatial Organization of a Bacterial Chromosome. *Science*, *342*(6159), 731–734. https://doi.org/10.1126/science.1242059

Lemon, K. P., & Grossman, A. D. (1998). Localization of Bacterial DNA Polymerase: Evidence for a Factory Model of Replication. *Science*, *282*(5393), 1516–1519. https://doi.org/10.1126/science.282.5393.1516

Leng, F., Chen, B., & Dunlap, D. D. (2011). Dividing a supercoiled DNA molecule into two independent topological domains. *Proceedings of the National Academy of Sciences*, *108*(50), 19973–19978. https://doi.org/10.1073/pnas.1109854108

Leonard, A. C., & Grimwade, J. E. (2011). Regulation of DnaA Assembly and Activity: Taking Directions from the Genome. *Annual Review of Microbiology*, *65*(1), 19–35. https://doi.org/10.1146/annurev-micro-090110-102934

Lesterlin, C., Barre, F.-X., & Cornet, F. (2004). Genetic recombination and the cell cycle: What we have learned from chromosome dimers: Genetic recombination and the cell cycle. *Molecular Microbiology*, *54*(5), 1151–1160. https://doi.org/10.1111/j.1365-2958.2004.04356.x

Lesterlin, C., Gigant, E., Boccard, F., & Espéli, O. (2012). Sister chromatid interactions in bacteria revealed by a site-specific recombination assay: Sister chromatid cohesion in E. coli. *The EMBO Journal*, *31*(16), 3468–3479. https://doi.org/10.1038/emboj.2012.194

Li, Y., Stewart, N. K., Berger, A. J., Vos, S., Schoeffler, A. J., Berger, J. M., Chait, B. T., & Oakley, M. G. (2010). Escherichia coli condensin MukB stimulates topoisomerase IV activity by a direct physical interaction. *Proceedings of the National Academy of Sciences*, *107*(44), 18832–18837. https://doi.org/10.1073/pnas.1008678107

Lin, D. C.-H., & Grossman, A. D. (1998). Identification and Characterization of a Bacterial Chromosome Partitioning Site. *Cell*, *92*(5), 675–685. https://doi.org/10.1016/S0092-8674(00)81135-6

Lioy, V. S., Cournac, A., Marbouty, M., Duigou, S., Mozziconacci, J., Espéli, O., Boccard, F., & Koszul, R. (2018). Multiscale Structuring of the E. coli Chromosome by Nucleoid-Associated and Condensin Proteins. *Cell*, *172*(4), 771-783.e18. https://doi.org/10.1016/j.cell.2017.12.027

Livny, J., Yamaichi, Y., & Waldor, M. K. (2007). Distribution of Centromere-Like parS Sites in Bacteria: Insights from Comparative Genomics. *Journal of Bacteriology*, *189*(23), 8693–8703. https://doi.org/10.1128/JB.01239-07

Lu, M., CampBell, JL., Boye, E., Kleckner, N. (1994). SeqA: A negative modulator of replication initiation in E. coli. *Cell*, *77*(3), 413–426. https://doi.org/10.1016/0092-8674(94)90156-2

Luijsterburg, M. S., Noom, M. C., Wuite, G. J. L., & Dame, R. Th. (2006). The architectural role of nucleoid-associated proteins in the organization of bacterial chromatin: A molecular perspective. *Journal of Structural Biology*, *156*(2), 262–272. https://doi.org/10.1016/j.jsb.2006.05.006

Lutkenhaus, J. (2007). Assembly Dynamics of the Bacterial MinCDE System and Spatial Regulation of the Z Ring. *Annual Review of Biochemistry*, *76*(1), 539–562. https://doi.org/10.1146/annurev.biochem.75.103004.142652

Lutkenhaus, J. F., Wolf-Watz, H., & Donachie, W. D. (1980). Organization of genes in the ftsA-envA region of the Escherichia coli genetic map and identification of a new fts locus (ftsZ). *Journal of Bacteriology*, *142*(2), 615–620. https://doi.org/10.1128/jb.142.2.615-620.1980

Madrid, C., Balsalobre, C., García, J., & Juárez, A. (2007). The novel Hha/YmoA family of nucleoid-associated proteins: Use of structural mimicry to modulate the activity of the H-NS family of proteins. *Molecular Microbiology*, *63*(1), 7–14. https://doi.org/10.1111/j.1365-2958.2006.05497.x

Mahone, C. R., & Goley, E. D. (2020). Bacterial cell division at a glance. *Journal of Cell Science*, *133*(7), jcs237057. https://doi.org/10.1242/jcs.237057

Mäkelä, J., & Sherratt, D. J. (2020). Organization of the Escherichia coli Chromosome by a MukBEF Axial Core. *Molecular Cell*, *78*(2), 250-260.e5. https://doi.org/10.1016/j.molcel.2020.02.003

Männik, J., Castillo, D. E., Yang, D., Siopsis, G., & Männik, J. (2016). The role of MatP, ZapA and ZapB in chromosomal organization and dynamics in *Escherichia coli*. *Nucleic Acids Research*, *44*(3), 1216–1226. https://doi.org/10.1093/nar/gkv1484

Marsin, S., Adam, Y., Cargemel, C., Andreani, J., Baconnais, S., Legrand, P., Li de la Sierra-Gallay, I., Humbert, A., Aumont-Nicaise, M., Velours, C., Ochsenbein, F., Durand, D., Le Cam, E., Walbott, H., Possoz, C., Quevillon-Cheruel, S., & Ferat, J.-L. (2021). Study of the DnaB:DciA interplay reveals insights into the primary mode of loading of the bacterial replicative helicase. *Nucleic Acids Research*, *49*(11), 6569–6586. https://doi.org/10.1093/nar/gkab463

Mazel, D. (2006). Integrons: Agents of bacterial evolution. *Nature Reviews Microbiology*, *4*(8), 608–620. https://doi.org/10.1038/nrmicro1462

Mazel, D., Dychinco, B., Webb, V. A., & Davies, J. (1998). A Distinctive Class of Integron in the *Vibrio cholerae* Genome. *Science*, *280*(5363), 605–608. https://doi.org/10.1126/science.280.5363.605

McClintock, B. (1932). A Correlation of Ring-Shaped Chromosomes with Variegation in Zea Mays. *Proceedings of the National Academy of Sciences*, *18*(12), 677–681. https://doi.org/10.1073/pnas.18.12.677

McNally, F. J. (2013). Mechanisms of spindle positioning. *Journal of Cell Biology*, *200*(2), 131–140. https://doi.org/10.1083/jcb.201210007

Meibom, K. L., Blokesch, M., Dolganov, N. A., Wu, C.-Y., & Schoolnik, G. K. (2005). Chitin Induces Natural Competence in *Vibrio cholerae*. *Science*, *310*(5755), 1824–1827. https://doi.org/10.1126/science.1120096

Melby, T. E., Ciampaglio, C. N., Briscoe, G., & Erickson, H. P. (1998). The Symmetrical Structure of Structural Maintenance of Chromosomes (SMC) and MukB Proteins: Long, Antiparallel Coiled Coils, Folded at a Flexible Hinge. *Journal of Cell Biology*, *142*(6), 1595–1604. https://doi.org/10.1083/jcb.142.6.1595

Mercier, R., Petit, M.-A., Schbath, S., Robin, S., El Karoui, M., Boccard, F., & Espéli, O. (2008). The MatP/matS Site-Specific System Organizes the Terminus Region of the E. coli Chromosome into a Macrodomain. *Cell*, *135*(3), 475–485. https://doi.org/10.1016/j.cell.2008.08.031

Midonet, C., & Barre, F.-X. (2014). Xer Site-Specific Recombination: Promoting Vertical and Horizontal Transmission of Genetic Information. *Microbiology Spectrum*, *2*(6). https://doi.org/10.1128/microbiolspec.MDNA3-0056-2014

Mizuuchi, K., O'Dea, M. H., & Gellert, M. (1978). DNA gyrase: Subunit structure and ATPase activity of the purified enzyme. *Proceedings of the National Academy of Sciences*, *75*(12), 5960–5963. https://doi.org/10.1073/pnas.75.12.5960

Nasmyth, K., & Haering, C. H. (2009). Cohesin: Its Roles and Mechanisms. *Annual Review of Genetics*, *43*(1), 525–558. https://doi.org/10.1146/annurev-genet-102108-134233

Nicolas, E., Upton, A. L., Uphoff, S., Henry, O., Badrinarayanan, A., & Sherratt, D. (2014). The SMC Complex MukBEF Recruits Topoisomerase IV to the Origin of Replication Region in Live Escherichia coli. *MBio*, *5*(1), e01001-13. https://doi.org/10.1128/mBio.01001-13

Nievera, C., Torgue, J. J.-C., Grimwade, J. E., & Leonard, A. C. (2006). SeqA Blocking of DnaA-oriC Interactions Ensures Staged Assembly of the E. coli Pre-RC. *Molecular Cell*, *24*(4), 581–592. https://doi.org/10.1016/j.molcel.2006.09.016

Nielsen, H. J., Li, Y., Youngren, B., Hansen, F. G., & Austin, S. (2006). Progressive segregation of the Escherichia coli chromosome. *Molecular Microbiology*, *61*(2), 383–393. https://doi.org/10.1111/j.1365-2958.2006.05245.x

Niki, H., Jaffé, A., Imamura, R., Ogura, T., & Hiraga, S. (1991). The new gene mukB codes for a 177 kd protein with coiled-coil domains involved in chromosome partitioning of E. coli. *The EMBO Journal*, *10*(1), 183–193. https://doi.org/10.1002/j.1460-2075.1991.tb07935.x

Nolivos, S., & Sherratt, D. (2014). The bacterial chromosome: Architecture and action of bacterial SMC and SMC-like complexes. *FEMS Microbiology Reviews*, *38*(3), 380–392. https://doi.org/10.1111/1574-6976.12045

Nolivos, S., Upton, A. L., Badrinarayanan, A., Müller, J., Zawadzka, K., Wiktor, J., Gill, A., Arciszewska, L., Nicolas, E., & Sherratt, D. (2016). MatP regulates the coordinated action of topoisomerase IV and MukBEF in chromosome segregation. *Nature Communications*, *7*(1), 10466. https://doi.org/10.1038/ncomms10466

Oberto, J., Nabti, S., Jooste, V., Mignot, H., & Rouviere-Yaniv, J. (2009). The HU Regulon Is Composed of Genes Responding to Anaerobiosis, Acid Stress, High Osmolarity and SOS Induction. *PLoS ONE*, *4*(2), e4367. https://doi.org/10.1371/journal.pone.0004367

O'Donnell, M., Langston, L., & Stillman, B. (2013). Principles and Concepts of DNA Replication in Bacteria, Archaea, and Eukarya. *Cold Spring Harbor Perspectives in Biology*, *5*(7), a010108–a010108. https://doi.org/10.1101/cshperspect.a010108

O'gara, J. P., & Dorman, C. J. (2000). Effects of local transcription and H-NS on inversion of the fim switch of Escherichia coli. *Molecular Microbiology*, *36*(2), 457–466. https://doi.org/10.1046/j.1365-2958.2000.01864.x

Ogasawara, N., & Yoshikawa, H. (1992). Genes and their organization in the replication origin region of the bacterial chromosome. *Molecular Microbiology*, *6*(5), 629–634. https://doi.org/10.1111/j.1365-2958.1992.tb01510.x

Ogura, T., & Hiraga, S. (1983). Partition mechanism of F plasmid: Two plasmid gene-encoded products and a cis-acting region are involved in partition. *Cell*, *32*(2), 351–360. https://doi.org/10.1016/0092-8674(83)90454-3

Ojeda Rodriguez, J. A., & Kahwaji, C. I. (2022). *Vibrio cholerae*. In *StatPearls*. StatPearls Publishing. http://www.ncbi.nlm.nih.gov/books/NBK526099/

Onogi, T., Miki, T., & Hiraga, S. (2002). Behavior of Sister Copies of Mini-F Plasmid after Synchronized Plasmid Replication in Escherichia coli Cells. *Journal of Bacteriology*, *184*(11), 3142–3145. https://doi.org/10.1128/JB.184.11.3142-3145.2002

Pant, A., Bag, S., Saha, B., Verma, J., Kumar, P., Banerjee, S., Kumar, B., Kumar, Y., Desigamani, A., Maiti, S., Maiti, T. K., Banerjee, S. K., Bhadra, R. K., Koley, H., Dutta, S., Nair, G. B., Ramamurthy, T., & Das, B. (2020). Molecular insights into the genome dynamics and interactions between core and acquired genomes of *Vibrio cholerae*. *Proceedings of the National Academy of Sciences*, *117*(38), 23762–23773. https://doi.org/10.1073/pnas.2006283117

Peter, B. J., Arsuaga, J., Breier, A. M., Khodursky, A. B., Brown, P. O., & Cozzarelli, N. R. (2004). Genomic transcriptional response to loss of chromosomal supercoiling in Escherichia coli. *Genome Biology*, *5*(11), R87. https://doi.org/10.1186/gb-2004-5-11-r87

Pillet, F., Sanchez, A., Lane, D., Anton Leberre, V., & Bouet, J.-Y. (2011). Centromere binding specificity in assembly of the F plasmid partition complex. *Nucleic Acids Research*, *39*(17), 7477–7486. https://doi.org/10.1093/nar/gkr457

Prieto, A. I., Kahramanoglou, C., Ali, R. M., Fraser, G. M., Seshasayee, A. S. N., & Luscombe, N. M. (2012). Genomic analysis of DNA binding and gene regulation by homologous nucleoid-associated proteins IHF and HU in Escherichia coli K12. *Nucleic Acids Research*, *40*(8), 3524–3537. https://doi.org/10.1093/nar/gkr1236

Prosser, S. L., & Pelletier, L. (2017). Mitotic spindle assembly in animal cells: A fine balancing act. *Nature Reviews Molecular Cell Biology*, *18*(3), 187–201. https://doi.org/10.1038/nrm.2016.162

Ramachandran, R., Jha, J., & Chattoraj, D. K. (2014). Chromosome Segregation in *Vibrio cholerae. Journal of Molecular Microbiology and Biotechnology*, *24*(5–6), 360–370. https://doi.org/10.1159/000368853

Rapa, R. A., & Labbate, M. (2013). The function of integron-associated gene cassettes in Vibrio species: The tip of the iceberg. *Frontiers in Microbiology*, *4*. https://doi.org/10.3389/fmicb.2013.00385

Reyes-Lamothe, R., Possoz, C., Danilova, O., & Sherratt, D. J. (2008). Independent Positioning and Action of Escherichia coli Replisomes in Live Cells. *Cell*, *133*(1), 90–102. https://doi.org/10.1016/j.cell.2008.01.044

Robinson, A., J. Causer, R., & E. Dixon, N. (2012). Architecture and Conservation of the Bacterial DNA Replication Machinery, an Underexploited Drug Target. *Current Drug Targets*, *13*(3), 352–372. https://doi.org/10.2174/138945012799424598

Roca, J., & Wang, J. C. (1992). The capture of a DNA double helix by an ATP-dependent protein clamp: A key step in DNA transport by type II DNA topoisomerases. *Cell*, *71*(5), 833–840. https://doi.org/10.1016/0092-8674(92)90558-T

Roecklein, B., Pelletier, A., & Kuempel, P. (1991). The tus gene of Escherichia coli: Autoregulation, analysis of flanking sequences and identification of a complementary system in Salmonella typhimurium. *Research in Microbiology*, *142*(2–3), 169–175. https://doi.org/10.1016/0923-2508(91)90026-7

Rosenberg, C., Boistard, P., Dénarié, J., & Casse-Delbart, F. (1981). Genes controlling early and late functions in symbiosis are located on a megaplasmid in Rhizobium meliloti. *Molecular and General Genetics MGG*, *184*(2), 326–333. https://doi.org/10.1007/BF00272926

Rouvière-Yaniv, J., Yaniv, M., & Germond, J.-E. (1979). E. coli DNA binding protein HU forms nucleosome-like structure with circular double-stranded DNA. *Cell*, *17*(2), 265–274. https://doi.org/10.1016/0092-8674(79)90152-1

Roy, S., Dimitriadis, E. K., Kar, S., Geanacopoulos, M., Lewis, M. S., & Adhya, S. (2005). Gal Repressor−Operator−HU Ternary Complex: Pathway of Repressosome Formation. *Biochemistry*, *44*(14), 5373–5380. https://doi.org/10.1021/bi047720t

Rozgaja, T. A., Grimwade, J. E., Iqbal, M., Czerwonka, C., Vora, M., & Leonard, A. C. (2011). Two oppositely oriented arrays of low-affinity recognition sites in oriC guide progressive binding of DnaA during Escherichia coli pre-RC assembly: DnaA-oriC interaction at arrayed sites. *Molecular Microbiology*, *82*(2), 475–488. https://doi.org/10.1111/j.1365-2958.2011.07827.x

Ryan, V. T., Grimwade, J. E., Nievera, C. J., & Leonard, A. C. (2002). IHF and HU stimulate assembly of pre-replication complexes at Escherichia coli oriC by two different mechanisms: Unwinding E. coli replication origins. *Molecular Microbiology*, *46*(1), 113–124. https://doi.org/10.1046/j.1365-2958.2002.03129.x

Rybenkov, V. V., Herrera, V., Petrushenko, Z. M., & Zhao, H. (2014). MukBEF, a Chromosomal Organizer. *Journal of Molecular Microbiology and Biotechnology*, *24*(5–6), 371–383. https://doi.org/10.1159/000369099

Saitoh, S., Takahashi, K., & Yanagida, M. (1997). Mis6, a Fission Yeast Inner Centromere Protein, Acts during G1/S and Forms Specialized Chromatin Required for Equal Segregation. *Cell*, *90*(1), 131–143. https://doi.org/10.1016/S0092-8674(00)80320-7

Sakiyama, Y., Kasho, K., Noguchi, Y., Kawakami, H., & Katayama, T. (2017). Regulatory dynamics in the ternary DnaA complex for initiation of chromosomal replication in Escherichia coli. *Nucleic Acids Research*, *45*(21), 12354–12373. https://doi.org/10.1093/nar/gkx914

Samadpour, A. N., & Merrikh, H. (2018). DNA gyrase activity regulates DnaA-dependent replication initiation in *Bacillus subtilis*: DNA gyrase regulates DnaA-dependent initiation. *Molecular Microbiology*, *108*(2), 115–127. https://doi.org/10.1111/mmi.13920

Sanchez, A., Rech, J., Gasc, C., & Bouet, J.-Y. (2013). Insight into centromere-binding properties of ParB proteins: A secondary binding motif is essential for bacterial genome maintenance. *Nucleic Acids Research*, *41*(5), 3094–3103. https://doi.org/10.1093/nar/gkt018

Sato, Y. T., Watanabe, S., Kenmotsu, T., Ichikawa, M., Yoshikawa, Y., Teramoto, J., Imanaka, T., Ishihama, A., & Yoshikawa, K. (2013). Structural Change of DNA Induced by Nucleoid Proteins: Growth Phase-Specific Fis and Stationary Phase-Specific Dps. *Biophysical Journal*, *105*(4), 1037–1044. https://doi.org/10.1016/j.bpj.2013.07.025

Schumacher, M. A., Piro, K. M., & Xu, W. (2010). Insight into F plasmid DNA segregation revealed by structures of SopB and SopB–DNA complexes. *Nucleic Acids Research*, *38*(13), 4514–4526. https://doi.org/10.1093/nar/gkq161

Shahul Hameed, U. F., Liao, C., Radhakrishnan, A. K., Huser, F., Aljedani, S. S., Zhao, X., Momin, A. A., Melo, F. A., Guo, X., Brooks, C., Li, Y., Cui, X., Gao, X., Ladbury, J. E., Jaremko, Ł., Jaremko, M., Li, J., & Arold, S. T. (2019). H-NS uses an autoinhibitory conformational switch for environment-controlled gene silencing. *Nucleic Acids Research*, *47*(5), 2666–2680. https://doi.org/10.1093/nar/gky1299

She, W., Mordukhova, E., Zhao, H., Petrushenko, Z. M., & Rybenkov, V. V. (2013). Mutational analysis of MukE reveals its role in focal subcellular localization of MukBEF: Mutational analysis of MukE. *Molecular Microbiology*, *87*(3), 539–552. https://doi.org/10.1111/mmi.12112

Sheng, D., Chen, X., Li, Y., Wang, J., Zhuo, L., & Li, Y. (2021). ParC, a New Partitioning Protein, Is Necessary for the Active Form of ParA From Myxococcus pMF1 Plasmid. *Frontiers in Microbiology*, *11*, 623699. https://doi.org/10.3389/fmicb.2020.623699

Sissi, C., & Palumbo, M. (2010). In front of and behind the replication fork: Bacterial type IIA topoisomerases. *Cellular and Molecular Life Sciences*, *67*(12), 2001–2024. https://doi.org/10.1007/s00018-010-0299-5

Stepankiw, N., Kaidow, A., Boye, E., & Bates, D. (2009). The right half of the Escherichia coli replication origin is not essential for viability, but facilitates multi-forked replication. *Molecular Microbiology*, *74*(2), 467–479. https://doi.org/10.1111/j.1365-2958.2009.06877.x

Stouf, M., Meile, J.-C., & Cornet, F. (2013). FtsK actively segregates sister chromosomes in *Escherichia coli*. *Proceedings of the National Academy of Sciences*, *110*(27), 11157–11162. https://doi.org/10.1073/pnas.1304080110

Stracy, M., Wollman, A. J. M., Kaja, E., Gapinski, J., Lee, J.-E., Leek, V. A., McKie, S. J., Mitchenall, L. A., Maxwell, A., Sherratt, D. J., Leake, M. C., & Zawadzki, P. (2019). Single-molecule imaging of DNA gyrase activity in living *Escherichia coli*. *Nucleic Acids Research*, *47*(1), 210–220. https://doi.org/10.1093/nar/gky1143

Strunnikov, A. V., Larionov, V. L., & Koshland, D. (1993). SMC1: An essential yeast gene encoding a putative head-rod-tail protein is required for nuclear division and defines a new ubiquitous protein family. *Journal of Cell Biology*, *123*(6), 1635–1648. https://doi.org/10.1083/jcb.123.6.1635

Suwanto, A., & Kaplan, S. (1989). Physical and genetic mapping of the Rhodobacter sphaeroides 2.4.1 genome: Presence of two unique circular chromosomes. *Journal of Bacteriology*, *171*(11), 5850–5859. https://doi.org/10.1128/jb.171.11.5850-5859.1989

Taylor, J. A., Seol, Y., Budhathoki, J., Neuman, K. C., & Mizuuchi, K. (2021). CTP and parS coordinate ParB partition complex dynamics and ParA-ATPase activation for ParABS-mediated DNA partitioning. *ELife*, *10*, e65651. https://doi.org/10.7554/eLife.65651

Tonthat, N. K., Arold, S. T., Pickering, B. F., Van Dyke, M. W., Liang, S., Lu, Y., Beuria, T. K., Margolin, W., & Schumacher, M. A. (2011). Molecular mechanism by which the nucleoid occlusion factor, SlmA, keeps cytokinesis in check: Mechanism of SlmA-mediated nucleoid occlusion. *The EMBO Journal*, *30*(1), 154–164. https://doi.org/10.1038/emboj.2010.288

Tran, N. T., Laub, M. T., & Le, T. B. K. (2017). SMC Progressively Aligns Chromosomal Arms in Caulobacter crescentus but Is Antagonized by Convergent Transcription. *Cell Reports*, *20*(9), 2057–2071. https://doi.org/10.1016/j.celrep.2017.08.026

Tupper, A. E., Owen-Hughes, T. A., Ussery, D. W., Santos, D. S., Ferguson, D. J., Sidebotham, J. M., Hinton, J. C., & Higgins, C. F. (1994). The chromatin-associated protein H-NS alters DNA topology in vitro. *The EMBO Journal*, *13*(1), 258–268.

Val, M.-E., Bouvier, M., Campos, J., Sherratt, D., Cornet, F., Mazel, D., & Barre, F.-X. (2005). The Single-Stranded Genome of Phage CTX Is the Form Used for Integration into the Genome of *Vibrio cholerae*. *Molecular Cell*, *19*(4), 559–566. https://doi.org/10.1016/j.molcel.2005.07.002

Val, M.-E., Kennedy, S. P., El Karoui, M., Bonné, L., Chevalier, F., & Barre, F.-X. (2008). FtsK-Dependent Dimer Resolution on Multiple Chromosomes in the Pathogen *Vibrio cholerae*. *PLoS Genetics*, *4*(9), e1000201. https://doi.org/10.1371/journal.pgen.1000201

Val, M.-E., Marbouty, M., de Lemos Martins, F., Kennedy, S. P., Kemble, H., Bland, M. J., Possoz, C., Koszul, R., Skovgaard, O., & Mazel, D. (2016). A checkpoint control orchestrates the replication of the two chromosomes of *Vibrio cholerae*. *Science Advances*, *2*(4), e1501914. https://doi.org/10.1126/sciadv.1501914

Val, M.-E., Skovgaard, O., Ducos-Galand, M., Bland, M. J., & Mazel, D. (2012). Genome Engineering in *Vibrio cholerae*: A Feasible Approach to Address Biological Issues. *PLoS Genetics*, *8*(1), e1002472. https://doi.org/10.1371/journal.pgen.1002472

Val, M.-E., Soler-Bistué, A., Bland, M. J., & Mazel, D. (2014). Management of multipartite genomes: The *Vibrio cholerae* model. *Current Opinion in Microbiology*, *22*, 120–126. https://doi.org/10.1016/j.mib.2014.10.003

Valens, M., Penaud, S., Rossignol, M., Cornet, F., & Boccard, F. (2004). Macrodomain organization of the Escherichia coli chromosome. *The EMBO Journal*, *23*(21), 4330–4341. https://doi.org/10.1038/sj.emboj.7600434

Varet, H., Brillet-Guéguen, L., Coppée, J.-Y., & Dillies, M.-A. (2016). SARTools: A DESeq2- and EdgeR-Based R Pipeline for Comprehensive Differential Analysis of RNA-Seq Data. *PLOS ONE*, *11*(6), e0157022. https://doi.org/10.1371/journal.pone.0157022

Vaughan, S., Wickstead, B., Gull, K., & Addinall, S. G. (2004). Molecular Evolution of FtsZ Protein Sequences Encoded Within the Genomes of Archaea, Bacteria, and Eukaryota. *Journal of Molecular Evolution*, *58*(1), 19–29. https://doi.org/10.1007/s00239-003-2523-5

Vecchiarelli, A. G., Han, Y.-W., Tan, X., Mizuuchi, M., Ghirlando, R., Biertümpfel, C., Funnell, B. E., & Mizuuchi, K. (2010). ATP control of dynamic P1 ParA-DNA interactions: A key role for the nucleoid in plasmid partition: ATP control of ParA in plasmid partition. *Molecular Microbiology*, no-no. https://doi.org/10.1111/j.1365-2958.2010.07314.x

Venkova-Canova, T., Saha, A., & Chattoraj, D. K. (2012). A 29-mer site regulates transcription of the initiator gene as well as function of the replication origin of *Vibrio cholerae* chromosome II. *Plasmid*, *67*(2), 102–110. https://doi.org/10.1016/j.plasmid.2011.12.009

Viollier, P. H., Thanbichler, M., McGrath, P. T., West, L., Meewan, M., McAdams, H. H., & Shapiro, L. (2004). From The Cover: Rapid and sequential movement of individual chromosomal loci to specific subcellular locations during bacterial DNA replication. *Proceedings of the National Academy of Sciences*, *101*(25), 9257–9262. https://doi.org/10.1073/pnas.0402606101

Vos, S. M., Stewart, N. K., Oakley, M. G., & Berger, J. M. (2013). Structural basis for the MukB-topoisomerase IV interaction and its functional implications in vivo. *The EMBO Journal*, *32*(22), 2950–2962. https://doi.org/10.1038/emboj.2013.218

Wang, H., Ayala, J. C., Benitez, J. A., & Silva, A. J. (2015). RNA-Seq Analysis Identifies New Genes Regulated by the Histone-Like Nucleoid Structuring Protein (H-NS) Affecting *Vibrio cholerae* Virulence, Stress Response and Chemotaxis. *PLOS ONE*, *10*(2), e0118295. https://doi.org/10.1371/journal.pone.0118295

Wang, Q., Mordukhova, E. A., Edwards, A. L., & Rybenkov, V. V. (2006). Chromosome Condensation in the Absence of the Non-SMC Subunits of MukBEF. *Journal of Bacteriology*, *188*(12), 4431–4441. https://doi.org/10.1128/JB.00313-06

Wang, X., Brandão, H. B., Le, T. B. K., Laub, M. T., & Rudner, D. Z. (2017). Bacillus subtilis SMC complexes juxtapose chromosome arms as they travel from origin to terminus. *Science*, *355*(6324), 524–527. https://doi.org/10.1126/science.aai8982

Wang, X., Le, T. B. K., Lajoie, B. R., Dekker, J., Laub, M. T., & Rudner, D. Z. (2015). Condensin promotes the juxtaposition of DNA flanking its loading site in Bacillus subtilis. *Genes & Development*, *29*(15), 1661–1675. https://doi.org/10.1101/gad.265876.115

Wang, X., Liu, X., Possoz, C., & Sherratt, D. J. (2006). The two Escherichia coli chromosome arms locate to separate cell halves. *Genes & Development*, *20*(13), 1727–1731. https://doi.org/10.1101/gad.388406

Wang, X., Reyes-Lamothe, R., & Sherratt, D. J. (2008). Modulation of Escherichia coli sister chromosome cohesion by topoisomerase IV. *Genes & Development*, *22*(17), 2426–2433. https://doi.org/10.1101/gad.487508

Wang, X., Tang, O. W., Riley, E. P., & Rudner, D. Z. (2014). The SMC Condensin Complex Is Required for Origin Segregation in Bacillus subtilis. *Current Biology*, *24*(3), 287–292. https://doi.org/10.1016/j.cub.2013.11.050

Watrin, E., & Prigent, C. (2012). Sister Chromatid Cohesion and Aneuploidy. In Z. Storchova (Ed.), *Aneuploidy in Health and Disease*. InTech. https://doi.org/10.5772/34114

Watrin, E., Schleiffer, A., Tanaka, K., Eisenhaber, F., Nasmyth, K., & Peters, J.-M. (2006). Human Scc4 Is Required for Cohesin Binding to Chromatin, Sister-Chromatid Cohesion, and Mitotic Progression. *Current Biology*, *16*(9), 863–874. https://doi.org/10.1016/j.cub.2006.03.049

Webb, C. D., Graumann, P. L., Kahana, J. A., Teleman, A. A., Silver, P. A., & Losick, R. (1998). Use of time-lapse microscopy to visualize rapid movement of the replication origin region of the chromosome during the cell cycle in Bacillus subtilis. *Molecular Microbiology*, *28*(5), 883–892. https://doi.org/10.1046/j.1365-2958.1998.00808.x

Wilhelm, L., Bürmann, F., Minnen, A., Shin, H.-C., Toseland, C. P., Oh, B.-H., & Gruber, S. (2015). SMC condensin entraps chromosomal DNA by an ATP hydrolysis dependent loading mechanism in Bacillus subtilis. *ELife*, *4*, e06659. https://doi.org/10.7554/eLife.06659

Witz, G., & Stasiak, A. (2010). DNA supercoiling and its role in DNA decatenation and unknotting. *Nucleic Acids Research*, *38*(7), 2119–2133. https://doi.org/10.1093/nar/gkp1161

Wolański, M., Donczew, R., Zawilak-Pawlik, A., & Zakrzewska-Czerwińska, J. (2015). OriC-encoded instructions for the initiation of bacterial chromosome replication. *Frontiers in Microbiology*, *5*. https://doi.org/10.3389/fmicb.2014.00735

Woo, J.-S., Lim, J.-H., Shin, H.-C., Suh, M.-K., Ku, B., Lee, K.-H., Joo, K., Robinson, H., Lee, J., Park, S.-Y., Ha, N.-C., & Oh, B.-H. (2009). Structural Studies of a Bacterial Condensin Complex Reveal ATP-Dependent Disruption of Intersubunit Interactions. *Cell*, *136*(1), 85–96. https://doi.org/10.1016/j.cell.2008.10.050

Yamaichi, Y., Bruckner, R., Ringgaard, S., Möll, A., Cameron, D. E., Briegel, A., Jensen, G. J., Davis, B. M., & Waldor, M. K. (2012). A multidomain hub anchors the chromosome segregation and chemotactic machinery to the bacterial pole. *Genes & Development*, *26*(20), 2348–2360. https://doi.org/10.1101/gad.199869.112

Yamaichi, Y., Fogel, M. A., McLeod, S. M., Hui, M. P., & Waldor, M. K. (2007). Distinct Centromere-Like parS Sites on the Two Chromosomes of Vibrio spp. *Journal of Bacteriology*, *189*(14), 5314–5324. https://doi.org/10.1128/JB.00416-07

Yamaichi, Y., Fogel, M. A., & Waldor, M. K. (2007). Par genes and the pathology of chromosome loss in *Vibrio cholerae*. *Proceedings of the National Academy of Sciences*, *104*(2), 630–635. https://doi.org/10.1073/pnas.0608341104

Yamaichi, Y., & Niki, H. (2000). Active segregation by the Bacillus subtilis partitioning system in Escherichia coli. *Proceedings of the National Academy of Sciences*, *97*(26), 14656–14661. https://doi.org/10.1073/pnas.97.26.14656

Yamanaka, K., Ogura, T., Niki, H., & Hiraga, S. (1996). Identification of two new genes,mukE andmukF, involved in chromosome partitioning inEscherichia coli. *Molecular and General Genetics MGG*, *250*(3), 241–251. https://doi.org/10.1007/BF02174381

Zechiedrich, E. L., Khodursky, A. B., & Cozzarelli, N. R. (1997). Topoisomerase IV, not gyrase, decatenates products of site-specific recombination in Escherichia coli. *Genes & Development*, *11*(19), 2580–2592. https://doi.org/10.1101/gad.11.19.2580